Improving Aerodynamic Performance of Wind Turbine by Adding Vortex Generators on the Blade Surface - A Case of Adama II Wind Turbine

Dagninet Terefe Kebie

A Thesis Submitted to the Department of Mechanical Engineering,

School of Mechanical, Chemical and Materials Engineering

Presented in Partial Fulfilment of the Requirement for the Degree of Master of Science in Thermal Engineering

Office of Graduate Studies

Adama Science and Technology University

May, 2024

Adama, Ethiopia

Improving Aerodynamic Performance of Wind Turbine by Adding Vortex Generators on the Blade Surface - A Case of Adama II Wind Turbine

Dagninet Terefe Kebie

Advisor: Dr. Addisu Bekele

Associate Professor of Thermal Engineering

A Thesis Submitted to the Department of Mechanical Engineering,

School of Mechanical, Chemical and Materials Engineering

Presented in Partial Fulfilment of the Requirement for the Degree of Master of Science in Thermal Engineering

Office of Graduate Studies

Adama Science and Technology University

May, 2024

Adama, Ethiopia

Declaration

I hereby declare that this Master Thesis entitled "Improving Aerodynamic Performance of Wind Turbine by Adding Vortex Generators on the Blade Surface - A Case of Adama II Wind Turbine" is my original work. That is, it has not been submitted for the award of any academic degree, diploma or certificate in any other university. All sources of materials that are used for this thesis have been duly acknowledged through citation.

Dagninet Terefe Kebie	________________________	________________
Name of student	Signature	Date

Recommendation of Advisor

I, the advisor of this thesis, hereby certify that I have read the revised version of the thesis entitled "Improving Aerodynamic Performance of Wind Turbine by Adding Vortex Generators on the Blade Surface - A Case of Adama II Wind Turbine" prepared under my guidance by Dagninet Terefe Kebie submitted in partial fulfillment of the requirements for the degree of Mater of Science in Thermal Engineering. Therefore, I recommend the submission of the thesis to the department following the applicable procedures

Dr. Addisu Bekele	________________________	________________
Advisor	Signature	Date

Approval Page

I, the advisor of the thesis entitled "Improving Aerodynamic Performance of Wind Turbine by Adding Vortex Generators on the Blade Surface - A Case of Adama II Wind Turbine" by Dagninet Terefe Kebie, hereby certify that the recommendation and suggestions made by the board of examiners are appropriately incorporated into the final version of the thesis.

Dr. Addisu Bekele	____________________	______________
Advisor	Signature	Date

We, the undersigned, members of the Board of Reviewers of the thesis by Dagninet Terefe Kebie have read and evaluated the thesis entitled "Improving Aerodynamic Performance of Wind Turbine by Adding Vortex Generators on the Blade Surface - A Case of Adama II Wind Turbine" and examined the candidate during open defense. This is, therefore, to certify that the thesis is accepted for partial fulfillment of the requirement of the degree of Master of Science in Thermal Engineering.

________________________	______________	______________
Chairperson	Signature	Date
________________________	______________	______________
Internal Examiner	Signature	Date
________________________	______________	______________
External Examiner	Signature	Date

Final approval and acceptance of the thesis is contingent upon submission of its final copy to the Office of Postgraduate Studies (OPGS) through the Department Graduate Council (DGC) and School Graduate Committee (SGC).

________________________	______________	______________
Department Head	Signature	Date
________________________	______________	______________
School Dean	Signature	Date
________________________	______________	______________
Office of Postgraduate Studies, Dean	Signature	Date

Acknowledgment

First and foremost, I want to express my sincere gratitude to the Almighty Holy Savior, who has never stopped showing me kindness and blessings. In addition to God, I would like to sincerely thank Dr. Addisu Bekele, my thesis advisor, for his unwavering encouragement, support, and direction during this project. His advice was helpful to me the entire time I was conducting research and writing my thesis. My profound gratitude also goes out to Adama Science and Technology University for providing me with the opportunity to pursue a Master of Science degree. Finally, but just as importantly, I want to thank my wife and my friends for their guidance and assistance throughout the study.

TABLE OF CONTENTS

LIST OF TABLES

LIST OF FIGURES

ACRONYMS

A	Amplitude
CFD	computational fluid dynamics
C_L	Coefficient of lift
C_{Lmax}	Maximum coefficient of lift
C_D	coefficient of Drag
C_{Dmin}	Minimum coefficient of drag
AoA	Angle of attack
EEP	Ethiopian electric power
D_F	Drag force
L_F	Lift Force
HAWT	Horizontal Axis wind turbine
NMSA	National Meteorological Services Agency
RANS	Reynolds-averaged Navier–Stokes
VGs	Vortex generators
VG1	Vortex generator 1
VG2	Vortex generator 2
VG3	Vortex generator 3
τ_{ij}	Stress tensor
AEP	Annual energy production
DNS	Direct numerical simulation
K-ω SST	Shear stress Turbulence model
WTG	Wind Turbine Generator

SYMBOLS

a	Wing span [m]
AoA	Angle of attack [◦]
c	Wing chord [m]
C_d	Two-dimensional drag coefficient
C_l	Two-dimensional lift coefficient
$C_{l,max}$	Maximum two-dimensional lift coefficient
Cl/Cd	Two-dimensional lift - drag ratio (airfoil efficiency)
H	Vortex generator height [m]
L	Chordwise length of vortex generator vanes [m]
Re	Reynolds number
S	Vortex generator span [m]
u,v,w	Velocity components [m/s]
x	Chord wise position on airfoil, x = 0 at the leading-edge [m]
y	Distance from airfoil surface [m]
Y_Γ	Average distance of the vortex centroids from the airfoil surface [m]
Z	Span wise position, z = 0 at mid-span [m]
Z	Span wise spacing between adjacent VGS [m]
β	Angle of incidence of VG vanes [◦]
δ	Boundary layer thickness [m]
ω_x	Stream wise vortices [1/s]
ω_{xmax}	Maximum stream wise vortices obtained for the respective configuration [1/s]

ABSTRACT

Wind energy stands as the fastest-growing renewable energy source today, crucial for combating climate change and achieving sustainability goals. Enhancing the efficiency of wind turbines is pivotal in maximizing energy capture. Conventionally, wind turbine blade roots employ thick airfoils to ensure structural integrity, albeit at the cost of increased drag and power loss during operation (Walelu, 2006). To mitigate this, vortex generators (VGs), small devices strategically placed at the onset of stall, are being studied intensively.

VGs serve as passive flow control devices, influencing the flow field near the turbine blade's suction surface. This research employs computational fluid dynamics (CFD) to investigate how the design and arrangement of VGs impact the aerodynamic performance of multi-megawatt wind turbine blades. By simulating Reynolds-averaged Navier–Stokes (RANS) steady-flow conditions and K-ω SST turbulence model, the study captures and analyzes the separated and vortex-induced flow behaviors on the blade surface equipped with VGs. The aerodynamic performance of the designed blade is examined using Computational Fluid Dynamic (CFD) analysis; due to its ability to capture flow separation and accuracy, the K-ω SST turbulence model transient model is preferred and implemented using ANSYS-FLUENT. Several vortex generator configurations were added on both the pressure and suction side of the blade surface and their corresponding effect on the aerodynamic performance is studied.

The primary objective in Adama-II Wind is to optimize the VG layout to minimize drag and maximize energy capture efficiency. This entails a detailed comparison and development of CFD models and simulations using tools like Simulink, aiming to refine the understanding of VG-induced aerodynamics and their practical application in wind turbine design. According to the findings of these investigations, the Adama II wind farm, with mean annual wind power densities between 634.6 w/m^2 and 462 w/m^2.Ultimately, these advancements of adding VG on blade surface promise to enhance the lift-to-drag ratio, overall performance and economic viability of wind energy systems, contributing significantly to their continued growth and adoption worldwide.

Keywords: - Vortex Generators, computational fluid dynamics, Wind power plant, Aerodynamic.

CHAPTER ONE

INTRODUCTION

1. Background

Ethiopia faces the third-highest electricity access deficit in Sub-Saharan Africa with an access rate of 51% in 2020; even as the Government and the utilities have made some concerted efforts to expand access (Endalamaw, 2023). Ethiopia has good wind resources with velocities ranging from 7 to 9 m/s**.** Its wind energy potential is estimated to be 10,000 MW (see Fig. 1.1). The Ethiopian National Meteorological Services Agency (NMSA) began work on wind data collection in 1971 using some 39 recording stations located in selected locations. Ever since the establishment of these stations, wind velocity has been measured and data made available to consumers. However, the number of stations established, the quality of data (in terms of comprehensiveness), and the distribution of the stations leave much to be desired.

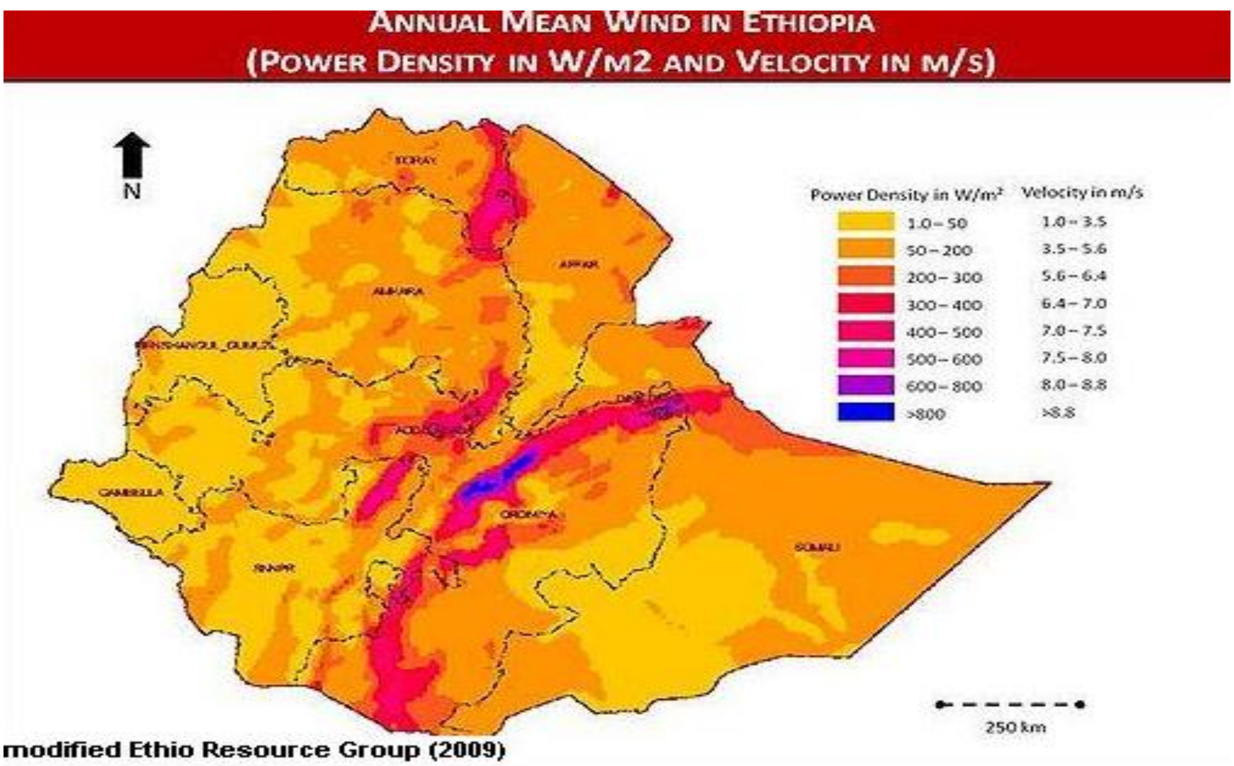

Figure 1-1 Annual Mean Wind Ethiopia

Ethiopia has substantial wind energy potential; the Ministry of Water estimates it is 5GW. Using this renewable resource can improve national electrification, lessen reliance on fossil fuels, and promote sustainable energy development. First, the development of modern energy infrastructure is required to increase electricity access for ordinary Ethiopians. Wind energy can complement the volatility of hydropower during the country's dry season (Frankton C, 2022).

Ethiopian Electric Power (EEP) harnessed 404 megawatts of electricity from wind power. The cumulative capacity of Ashegoda, Adama I and II, and Aysha II wind power plants now stands at 404 megawatts. Additionally, a feasibility study has been concluded for 18 wind power projects capable of generating 2,700 megawatts. These proposed projects are slated for locations such as ASsela, Gode, Kabribeyah, Tulu Guled, and Adigala.

Adama II wind power plant is one of the largest plants; located just outside Adama Town in Oromia Regional State in Ethiopia, produces 153 MW wind-energy infrastructure projects were developed by the Government of Ethiopia in collaboration with two Chinese contractors, HydroChina Corporation and China Geo-engineering Corporation Overseas Construction Group (CGCOC Group), using concessional loans from the Chinese Government (Frankton C, 2022).

Ethiopia is strategically prioritizing the advancement of renewable energy, particularly wind power, as a means to leverage its natural resources and decrease dependence on imported fossil fuels. It boasts the capacity to produce up to 1.3 Gigawatts of energy from wind, 45,000 megawatts from hydropower, and 10,000 megawatts from geothermal sources.

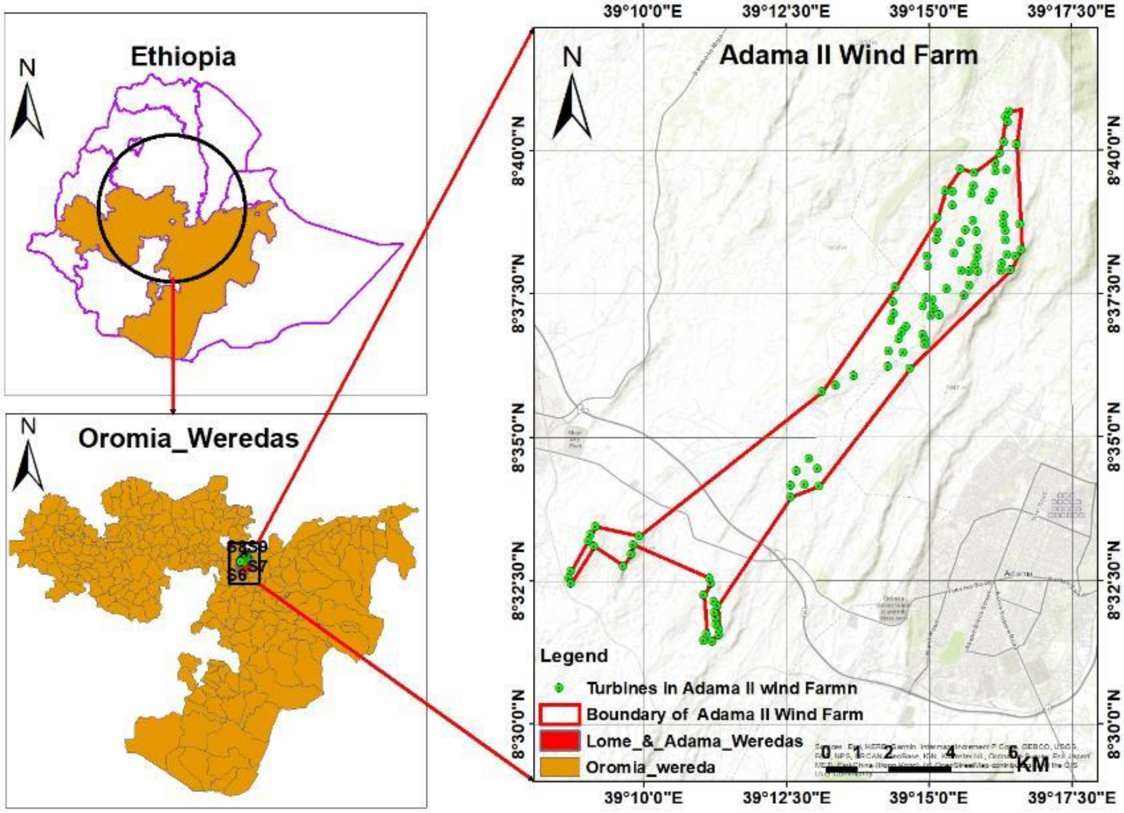

Figure 1-2 Location of Adama II Wind Farm (Abeba Debru ,2021)

To maximize efficiency and optimize energy output, however, a deeper comprehension of aerodynamic blade optimization and wind resource evaluation is needed. To maximize the efficiency of and to optimize energy there are many methods; one of to maximize the efficiencies and to get more production on HAWT is adding a vortex generator on the blade surfaces. Adama II wind power plant is located in the middle of Ethiopia, about 7km from Adama, at the elevations 0f 1741-2173m. The install capacity of the wind power is 153MW, with 102 wind turbine generators,1500KW each and a total energy output of 476.665GWh. Adama II wind power plant produces maximum power in clear blades (without a vortex generator), but I want to add the best design vortex generator type on the blade surfaces and see the impact of aerodynamic performances.

Vortex generators (VGs) are passive flow control devices that are commonly employed on airfoils to prevent flow separation. There is a rich variety of different designs, but all of them rely on generating stream-wise vortices that transfer high-momentum fluid from the free stream to the slower-moving boundary layer (Ashill et al., 2001). By energizing the retarded fluid, VGs help overcome the adverse pressure gradients experienced at increasing angles of attack (Ashill et al., 2001; Lin, 2002). As the use of vortex generators inevitably results in a drag penalty, some research was recently directed at examining smaller, less intrusive designs, so-called sub-boundary-layer VGs. However, their use is limited to applications where the flow-separation locations are relatively fixed (Permatasari & Widyawati, 2023), which is not the case on wind turbine blades. Thus, it is not feasible to employ such devices on wind turbines, even though they may have some merit for improving the stall behavior. Nevertheless, minimizing the parasitic drag associated with VGs is a crucial objective

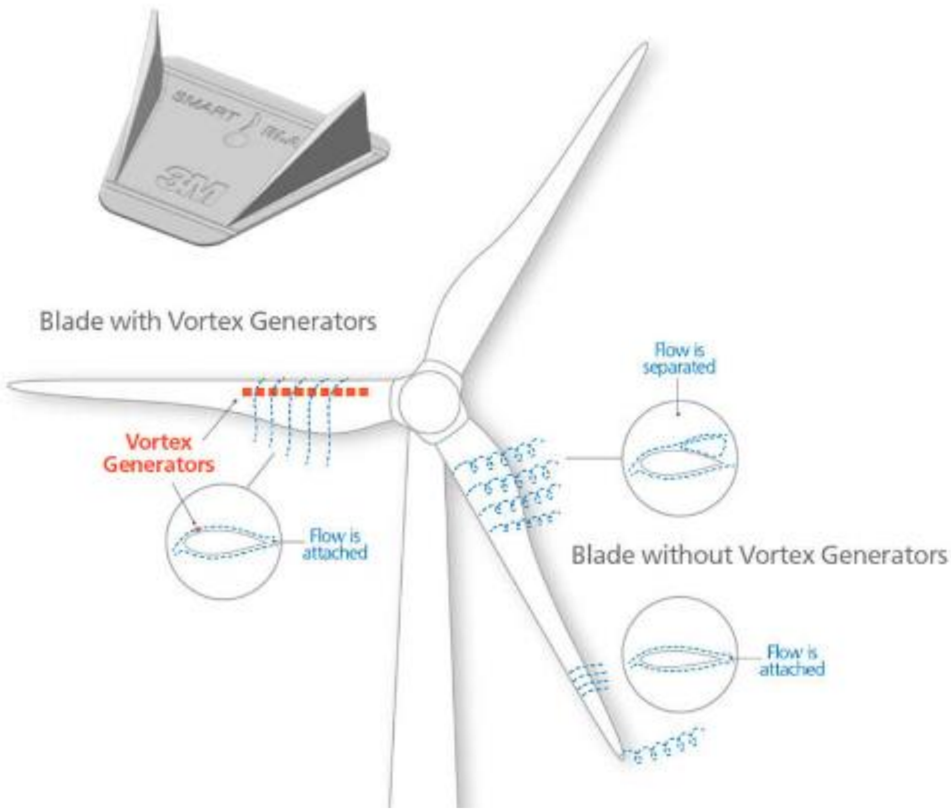

Figure 1-3: How vortex generators improve wind turbine performance (Permatasari & Widyawati, 2023)

1.1 Statements of problem

According to Ethiopian Electric Power (EEP), Ethiopia has the potential to generate almost 1.3 million megawatts (MW) of wind power, making it one of Africa's most promising wind energy markets.

A wind turbine's maximum energy extraction from wind is 59.3% of the kinetic energy that comes in, according to Betz's analysis. But most wind turbines aren't able to reach this level of efficiency.

Optimizing energy extraction while adhering to constraints is a common difficulty faced by wind turbine designers.

Airfoils are stacked throughout the blade span to create wind turbine rotor blades. The lift force produced by pressure differential in the airfoil flow over is the primary driving force behind blade rotation. According to a recent study, vortex generators on the surface of aircraft airfoils improve the aircraft's mobility and aerodynamic efficiency by reducing stall. Despite the obvious differences between an aircraft's and a wind turbine's airfoil, it is reasonable to infer from these findings that a vortex generator can improve the wind turbine's power extraction coefficient.

The root section of modern wind turbine blades performs poorly aerodynamically worldwide. The causes are the operating constraints and blade manufacturing Wind energy is a promising renewable energy source, but its efficiency is limited by aerodynamic problems with wind turbine blades. Blade stall and flow separation cause the turbine to produce noticeably less power and inflict more stress on it.

The Adama II Wind Power Plant's particular site features are the cause of these issues. On 5 years of data from 2017-2022, G.C annual Energy produces less than that expected of full capacity (476 GWhr). So due to the above critical problems, selecting the best type and adding vortex generators is studied on the blade surface of a horizontal wind turbine, and also on this thesis improves the suitability of vortex generators for wind turbine blades and to get a better production than what it produces every year.

1.2 General and specific objectives

1.2.1 General objectives

To develop and test a workable method for using vortex generators at Adama II Wind Power Plant to significantly improve the wind turbines' aerodynamic performance. This will increase lift-to- drag coefficient or energy generation and assist Ethiopia in achieving its renewable energy goals.

1.2.2 Specific objective

The general objective will be demonstrated via the achievement of the following specific objectives

- Examine wind turbine blade data (power output, wind speed, etc.) to pinpoint specific aerodynamic problems that can impair efficiency, such as flow separation and stall on the site.
- Numerical modeling of blades with and without vortex generator in different types of parameters in CFD.
- Analyze CFD and wind tunnel data; evaluate how optimized vortex generators affect the lift, drag, and stall characteristics of wind turbine blades.
- Determine the best design for wind turbine blades by developing and testing a variety of vortex generator configurations using CFD simulations
- Compare installing vortex generators on the site (wind turbine blades) will affect the economy (more electricity output, lower running costs) than without vortex generators.

1.3 Significance of the Study

These studies improved aerodynamic efficiency through vortex generators will lead to higher power output from Adama II, contributing to Ethiopia's energy security and reducing reliance on fossil fuels. With more energy produced by vortex generators, Adama II's power production may rise, improving revenue generation and allowing the power plant's operator to profit from more electricity sales as well as a reduction in reliance on fossil fuels. By lowering its dependency on conventional power sources, Ethiopia may meet its clean energy targets with the support of increased wind energy generation. Thus, constant and enhanced power generation from Adama II may contribute to a more stable national grid.

1.4 Scope of the study

The principal aim of this thesis is to enhance aerodynamic performance by adding a vortex generator and using well-established CFD techniques. Based on wind and Adama II blade geometry, construct and optimize vortex generators. One of the study's limitations is that the system is not implemented.

CHAPTER TWO

LITERATURE REVIEW

2. Potential Energy Assessment of Wind

The next part examines previous research on the process of assessing wind energy potential in addition to the evaluation findings of both national and international investigations

The industrialized world is reevaluating its energy mix and developing a variety of clean, renewable energy sources due to rising energy prices, supply uncertainty, and environmental concerns. The majority of developed nations are attempting to increase the amount of energy they produce from affordable, domestic resources that can be "renewed" or replaced without having a significant negative impact on the environment or contributing to climate change. Fossil fuel alternatives are seeing a 30% annual growth rate in wind power, with installed capacity rising from 196,653 MW in 2010 to 239,000MW at the end of 2011. 2011 saw enough production to meet 3% of the global power demand. Europe, Asia, and the US all use a lot of wind power. India, China, Germany, Spain, and the United States (Mulugeta et al., 2017)

To reduce reliance on hydropower, the Ethiopian government has made plans to increase and diversify the mix of renewable energy sources. As a result, the emphasis has switched to renewable energy sources to meet demand. In addition to recommending 51 wind projects with a combined planned capacity of 5,280 MW, the Ethiopian government has prepared a Master Plan for Wind and Solar Energy to investigate the available wind and solar energy resources and suggest major policy options to be developed for wind and solar energy expansion. (MOFAOD, 2016).

Shu *et al*., (2015) have completed a statistical examination of Hong Kong's wind potential and characteristics. The Weibull distribution is without a doubt one of the most often used models for the statistical analysis of wind characteristics and wind energy potential evaluation among all the known probability distribution functions. Hennessey (1977) did a good job of outlining the benefits of the Weibull distribution function. According to Hennessey (1977), the Weibull distribution model makes it easier to estimate the mean and standard deviation of total wind power density in addition to providing a good depiction of the wind speed distribution. This paper concludes with a discussion of the final findings from the techniques and the computation of the necessary parameters, such as wind power density.

Bharani *et al.,* (2019) generates a collection of wind datasets using a vast volume of wind data to determine the potential for wind energy in the chosen region throughout India. Data on wind energy potential were gathered between 2014 and 2016 at a height of 100 meters above mean sea level (MSL). The features of wind energy and the best location for installing wind turbines were analyzed using the wind speed and direction. Four distinct monitoring sites recorded the maximum wind power density. Based on the results the research concludes that altitude of the monitoring station and geomorphology of the site significantly controls the wind power density.

Abdoulkader *et al.,* (2019) analyze potential for wind power energy in the city of Djibouti for the first-time using wind speed data gathered over 5 years (2014–2018) at a height of 10 meters using Weibull criteria. Before, there was little data available in this urban region, making such a study impractical. The final findings demonstrated the potential for Djibouti City's urban wind energy industry to be developed and implemented for residential uses. The power density, wind rise, and statistical wind speed were calculated. Based on the analysis of wind power production, Djibouti City must erect wind turbines with a hub height larger than 80.5 meters to gather wind energy efficiently.

2.1 Blade Design of Wind Turbine

Peter et al., (2012) studies Optimizing aerodynamic performance is essential for designing efficient rotors. Since aerodynamic lift is the force that drives the turbine's power generation, it is crucial to optimize this force through sensible design. Friction creates a resistive drag force that opposes the blade's motion and needs to be reduced. It follows that when designing rotor blades, an airfoil section with a high lift-to-drag ratio typically more than 30 should be used.

Although it is challenging to calculate analytically, freely available software, like XFOIL, can properly forecast the coefficient for lift and drag of airfoils, except post-stall, extreme angles of attack, and airfoil thickness situations. Traditionally, airfoils are examined experimentally using tables that relate lift and drag at various Reynolds numbers and angles of attack. Historically, airplane technologies with comparable Reynolds numbers and section thicknesses appropriate for the conditions at the blade tip have been the source of inspiration for wind turbine airfoil designs.

However, due to the variations in operating conditions and mechanical loads, particular considerations should be given to the design of airfoil profiles specific to wind turbines.

2.2 Concept of Vortex Generator

Hanns et al., (2012) studies Vortex generators (VGs) are passive flow control devices typically deployed to prevent flow separation on wind turbine blades. They boost lift and hence reduce the destructive fatigue loads caused by stall, which increases rotor torque. This paper is the culmination of a research endeavor that used VGs to optimize both the sectional and the whole rotor-blade aerodynamics. VG size, chord wise position, and span wise spacing were all examined using force balance measurements of a two-dimensional wing section. The static stall angle and maximum lift increased significantly when the distance between neighboring VGs was reduced, however, there was also a noticeable rise in drag and severe lift excursions at angles higher than the static stall angle. It was discovered that the range of x/c = 15%–20% was the ideal chord wise position for the vortex generators since this resulted in a smooth post-stall lift curve and relatively minimal parasitic drag. Measurements of particle image velocimetry were made at different chord wise points to shed light on the interactions between neighboring stream wise vortices. Their impact on the aerodynamics of wind turbine blades was projected using the optimal VG configuration's experimental aerodynamic performance curves. Blade Element Momentum (BEM) code (QBlade) created by Smart Blade GmbH was used to simulate multiple stalls and pitch-regulated wind turbine models and to construct three distinct rotor blades. A simulation was conducted to evaluate the impact of variable guides (VGs) on the aerodynamic performance and loads of the rotor blades. Lastly, the adverse effect of surface roughness on the performance of the previously described rotor blades was simulated using previously obtained steady-state performance curves under high-roughness conditions. This makes it possible to evaluate how well the VGs could work as retrofit components to restore the performance of blades with polluted surfaces.

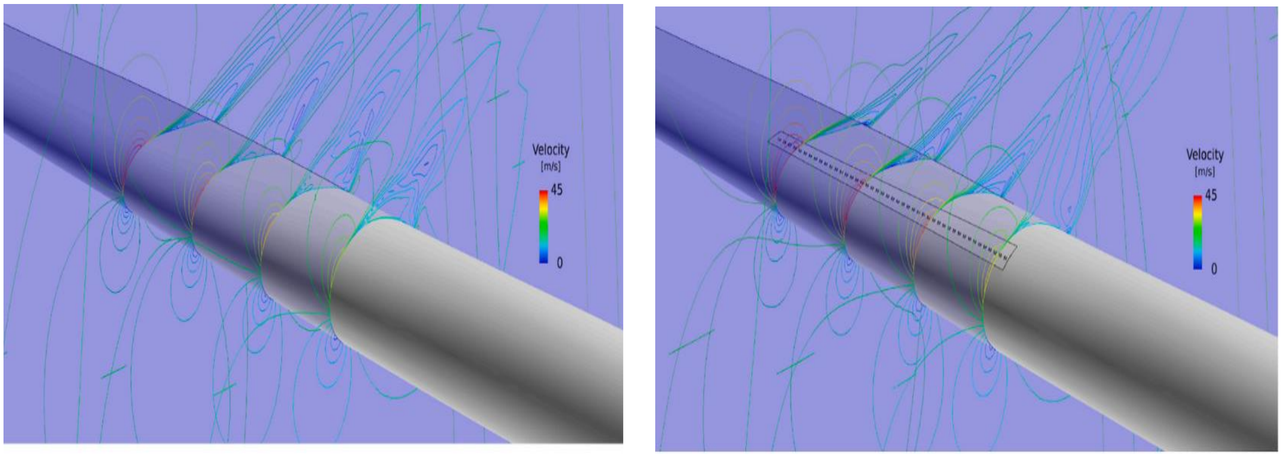

Figure 2-1 Blade Without vortex Generator and Blade with Vortex Generator (Moon et al., 2023)

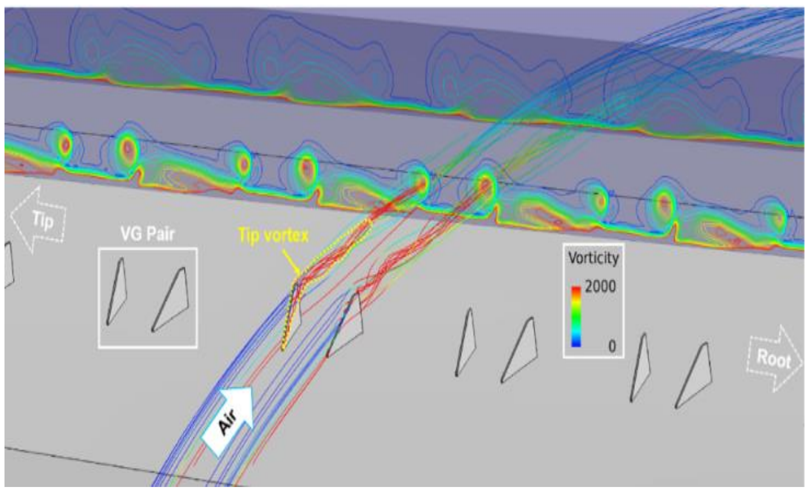

Figure 2-2 Analysis of vortex behavior near VG through CFD analysis (Moon et al., 2023)

Vortex generator on Aircraft

Fouatih et al., (2019) explored how placing vortex generators at specific positions on the NACA 4415 airfoil affects its aerodynamic performance. They found that these generators improve lift at high angles of attack by keeping the airflow attached to the airfoil longer, preventing flow separation. At lower angles of attack, the airfoil performs better naturally without the need for additional devices like vortex generators. The researchers also determined the optimal placement of these vortex generators along the chord of the airfoil to achieve the best results.

Booma et al., (2016) colleagues released a work in the International Journal of Mechanical, Aerospace, Industrial, Mechatronic and Manufacturing Engineering titled Computational Analysis of Cavity Consequence over Aircraft Wing. The wing was modelled in CATIA V5R20 for their study, and ANSYS CFX was used for the exams. Vortex in square and triangle forms were considered. They demonstrate that increasing the maximum lift coefficient or decreasing the drag coefficient can both lead to increased efficiency. Their computational results show an increase in lift. A strong controlling technique to increase the angle of stall and lift coefficient is the presentation of a vortex generator.

Vortex Generator on HAWT

Fouatih et al., (2019) investigates the use of vortex generators in passive flow control for improving the aerodynamic performance of the NACA 4415 airfoil. Results show that vortex generators enhance the lift coefficient of the profile for high attack angles, while low attack angles yield better aerodynamic performance. The optimal position relative to the profile chord (XVG) was found.

Permatasari & Widyawati, (2023) studies use Computational Fluid Dynamics (CFD) simulations to analyze the impact of adding vortex generators on the aerodynamic characteristics of the NACA 632-415 airfoil. Results show that adding vortex generators can delay flow separation, increase lift force coefficient by 24.9%, drag force coefficient by 2.7%, and gliding ratio by 9.1%.

Moon et al., (2023) studies explore the impact of vortex generator configurations on rotor performance in horizontal axis wind turbines. Counter-rotating vortex generators improve power by 1.04% at rated wind speed. Optimizing span-wise separation distance and location along the chord improves aerodynamic performance at low attack angles.

Hares et al., (2019) investigates the impact of a new VG configuration on a curved profile, predicts flow patterns, and investigates flow control using "V" shape VGs. Gothic-shaped vortex generators were found to improve aerodynamic performance, reduce drag force, and increase lift coefficient for high attack angles. Optimal dimensions and positions of vortex generators were determined.

Zhu et al., (2020) investigates deep dynamic stalls of wind turbine airfoils with VGs. Single-row and double-row VGs delay the onset of deep dynamic stall. Single-row VGs reduce aerodynamic pitch damping; double-row VGs restore efficiency. Double-row VGs are better than single-row VGs in controlling deep dynamic stalls. VGs can improve wind turbine performance without external energy expenditure. The effect of VGs on dynamic stalls is little known, which is one of the study's limitations. Prior research was limited to light dynamic stalls that were VG-controlled.

Ashill et al., (2001) studies Vortex generators (VGs) are passive flow control devices that are commonly employed on airfoils to prevent flow separation. There is a rich variety of different designs, but all of them rely on generating stream-wise vortices that transfer high-momentum fluid from the free stream to the slower-moving boundary layer

Yan et al., (2019) Studies the effectiveness of vortex generators (VGs) in reducing drag in wind turbines and aerospace vehicles. It highlights the need for more research on VGs' performance at higher Reynolds numbers, supercritical and trans cortical Reynolds numbers. VGs are compact and lightweight, making them easy to install on existing turbine towers. They also suppress vortex-induced vibrations and shorten lock-in regions. The paper concludes that further research is needed to understand the impact of VGs on various geometries and structures.

By energizing the retarded fluid, VGs help overcome the adverse pressure gradients experienced at increasing angles of attack (Ashill et al., 2001; Lin, 2002). As the use of vortex generators inevitably results in a drag penalty, some research was recently directed at examining smaller, less intrusive designs, so-called sub-boundary-layer VGs. However, their use is limited to applications where the flow-separation locations are relatively fixed (Permatasari & Widyawati, 2023), which is not the case on wind turbine blades. Thus, it is not feasible to employ such devices on wind turbines, even though they may have some merit for improving the stall behavior. Nevertheless, minimizing the parasitic drag associated with VGs is a crucial objective.

The above literature reviews could be summarized as follow. In order to harness energy potential proper design of wind turbine blade is a necessity, among different methods of designing HAWT blade element momentum (BEM) is the most widely and preferred method in previous works. The literature review has also showed that vortex generator on the surface of aircraft wing and wind turbine blades have also exhibit enhancing lift force by delaying flow separation.

In this thesis based on the reviewed literature’s method and research gap found the aerodynamic effect of surface vortex generator is examined with HAWT blade design using BEM is done.

CHAPTER THREE

MATERIALS AND METHODS

3. Introduction

Adama II wind power plant has 1.5MW wind turbine generator system (WTGS). Technical parameters of Adama II wind power plant WTGS is shown below in table. The hydro china SE7715 1.5MW WTGS adopts the overall design scheme on synchronization of horizontal axis, three blades, upwind, pitch adjustment, direct drive and double feed induction generator. It adopts the pitch-controlled system to control the power of the turbine. When the wind speed exceeds wind speed rate, the output of WTGS will be controlled within 1.5MW through the pitch angle changing so as to prevent the overload of generator and converter system.

Table 1 Technical parameters of the 1.5MW of SE7715 series WTGS

Parameter	Parameter value / Description
WTGS model	SE7715
Wind turbine class	IEC II
Rated power	1500Kw
Inverter output voltage	690V
Diameter of rotor	77.6
Swept area	4736m^2
Hub height	70
Rated rotation speed of rotor	19 rpm
Rated wind speed Cut-in wind speed	11.5 m/s 3.5 m/s

Cut-out wind speed	25m/s
Maximum survival wind speed (3 seconds)	59.5m/s
Maximum allowable maintenance wind speed	11.5
Operating temperature	$21C^0$
Survival temperature of WTGS	$-40C^0 \pm 50C^0$
Design service life	≥20 years
Lightning protection design standard	IEC61400-24; IEC62305

3.1 Blade Design

The number of blades, type of airfoil section, blade chord, twist distributions, and design tip-speed ratio (TSR=rotational speed x rotor radius/design wind speed at hub height) are all factors in the aerodynamic design of a wind turbine rotor. In terms of blade number (NB), a single-bladed rotor can be more affordable and simpler to install, but it is not as common and produces excessive noise. Although it is easier to assemble and erect, the two-bladed rotor generates less power than the three-bladed one. The latter is more aesthetically pleasing and yields a smoother power output with balanced gyroscopic stresses. The average wind speed at a given location and the amount of energy required for a particular application are the primary determinants of blade length (or rotor size). One of the most important aspects of creating an effective wind rotor is deciding on the type of airfoil section to use. (Hartfield and Burger, 2006).

In this study, the energy density of the location is determined to be 612 w/m^2, and a HAWT blade is designed using Blade Momentum Theory (BEM) based on the analysis of wind data. BEM is used to determine which blade constituent composition has the highest lift-to-drag ratio. The chord and twist distribution at a selected tip speed ratio are obtained, and these values are used to define the aerodynamic form of the blade in each segment and the maximum available power coefficient. The power coefficient, angle of attack, drag, and lift coefficients are the design parameters.

Selecting Airfoils

An appropriate airfoil selection is required for wind turbine design. Using site condition as an input, two distinct types of wind turbine airfoils are chosen, and their related aerodynamic performance is compared. The airfoils for the location were NACA63-XXX and DU-XXX of HAWT. So NACA63-218 airfoil is selected for this site.

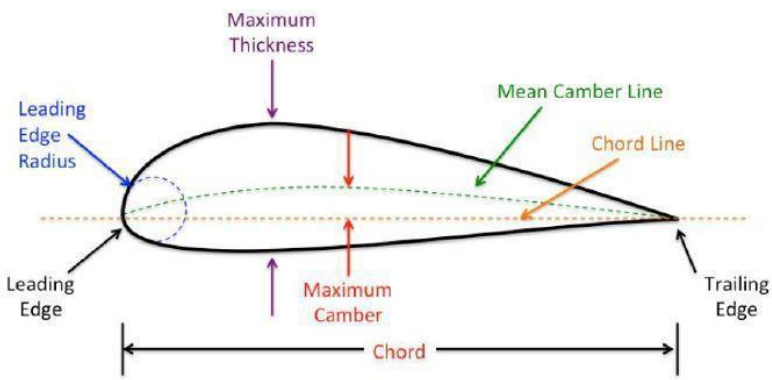

Figure 3-1 Airfoil Terminology (Gedion Fikade et.al; 2019)

The aerodynamic data (Re) numbers of the chosen airfoil at the associated flow conditions are crucial for the design and study of wind turbine blades.

$$R_e = \frac{U_{rel}C}{\upsilon} \ldots\ldots\ldots\ldots\ldots\ldots\ldots\ldots\ldots\ldots\ldots\ldots\ldots\ldots\ldots \text{(3.1)}$$

Where: U_{rel} is the relative wind speed (m/s).

C is chord length (m).

Ʋ= is kinematic viscosity of air (ν = 14 × 10-6 m^2/s)

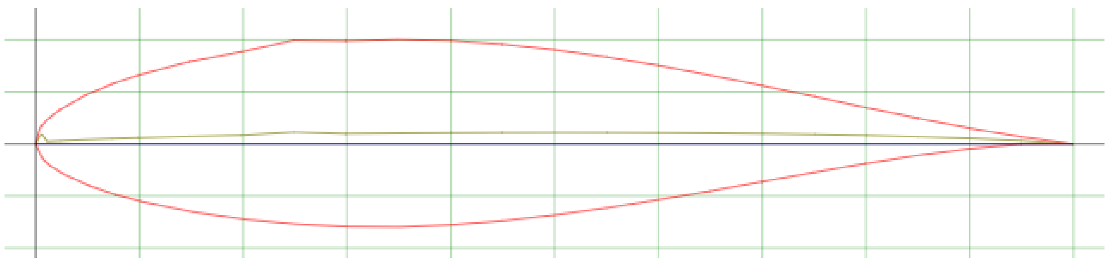

Figure 3-2 NACA63 (3)-218 Wind Turbine Airfoil (Aerofoiltools.Com, 2024)

Table 2 ADAMA II Wind power plant NACA 63-218 blade profile Specification data

Radius(m)	0	1	7.9	10.47	15	23.1	30	38
Chord length(mm)C_{opt}	1890	1895	3182	2934	2295	1546	1180	150
Twist Angle (^{0}**)**	10	13.06	13.8	9.7	5.73	2.29	0.52	-0.791
Profile type	Cylinder	Cylinder	GUP-40	GUP-35	GUP-30	GUP-25	GUP-21	GUP-18

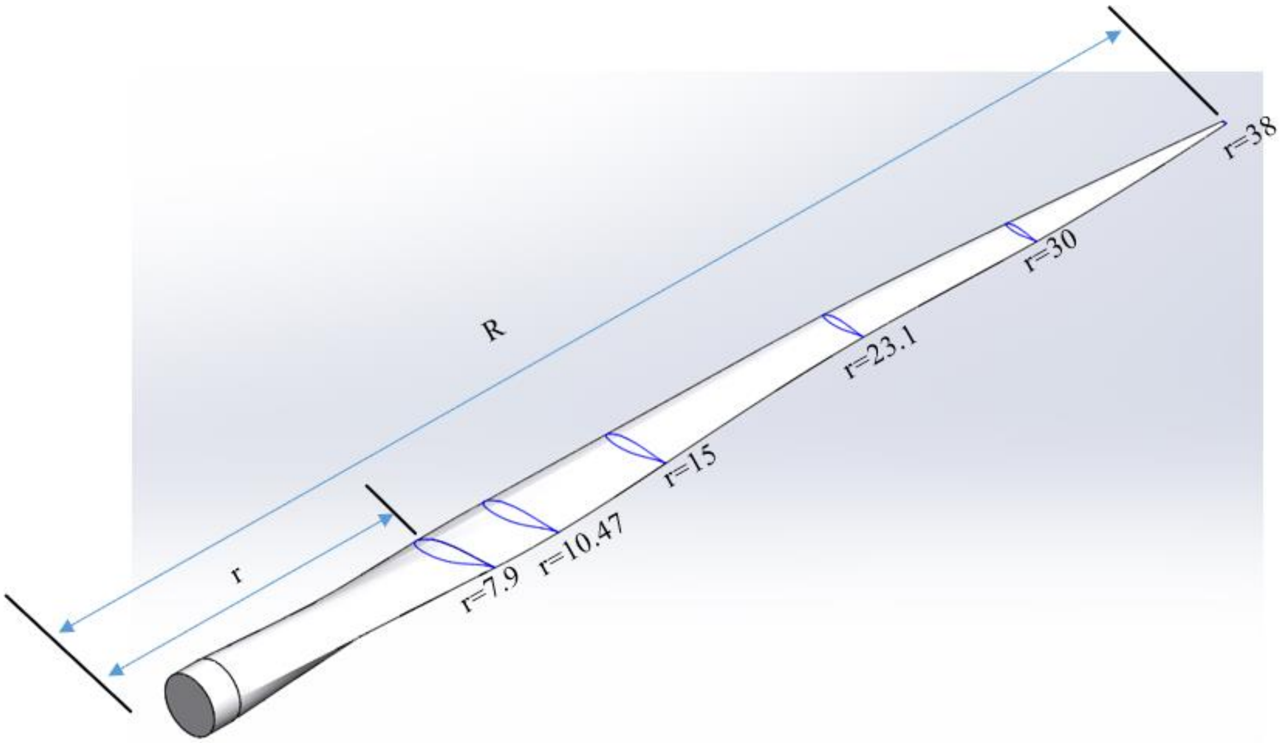

Figure 3-3 Isometric drawing of Baseline blade

3.1.1 **Distribution of Chords and Twist Angle**

Tip Speed Ratio: - The relationship between the rotor blade velocity and the relative wind velocity is known as the tip speed ratio. The primary design parameter, from which all other ideal rotor dimensions are derived, is Equation 3.2: Hansen and others (1993)

$$\lambda = \frac{\Omega_r}{V_w} \ldots\ldots\ldots\ldots\ldots\ldots\ldots\ldots\ldots\ldots \text{(3.2)}$$

Where: λ= Tip speed ratio

Ω_r= Rotational velocity (rad/s),

r = blade radius,

V_w = Wind speed.

Blade dimension and type of plan: - Using BEM approach, the chord length of a HAWT rotor blade is determined based on the Betz limit, local air velocities, and airfoil lift, defining the best plan form. Several complicated theories can be used to determine the ideal chord length (Hansen et al., 1993). The most basic theory is based on the Betz optimization. Betz's momentum theory provides a good approximation for blades with tip speed ratios of six to nine that use airfoil sections with little drag and tip losses. (Peter and Associates, 2012).

This approach may be deemed imprecise in situations involving low tip speeds, high-drag airfoil sections, and blade sections surrounding the hub. Wake and drag losses need to be taken into consideration in these circumstances (Hansen et al., 1993). The basic form of a modern wind turbine blade can be found using the Betz method (Hansen and others (1993)

$$\boldsymbol{C_{opt} = \frac{2\Pi\Gamma\ 8\ U_{wd}}{n9C_{L\lambda V_r}}} \ldots\ldots\ldots\ldots\ldots\ldots\ldots\ldots\ldots\ldots \textbf{(3.3)}$$

Where; $V_r = \sqrt{V^2{}_w + U^2}$

r = radius (m), n = Blade quantity, C_L = Lift coefficient, λ = Local tip speed ratio, V_r = Local resultant air velocity (m/s), U= Wind speed (m/s), U_{wd} = Design wind speed (m/s), C_{opt} = Optimum Chord length

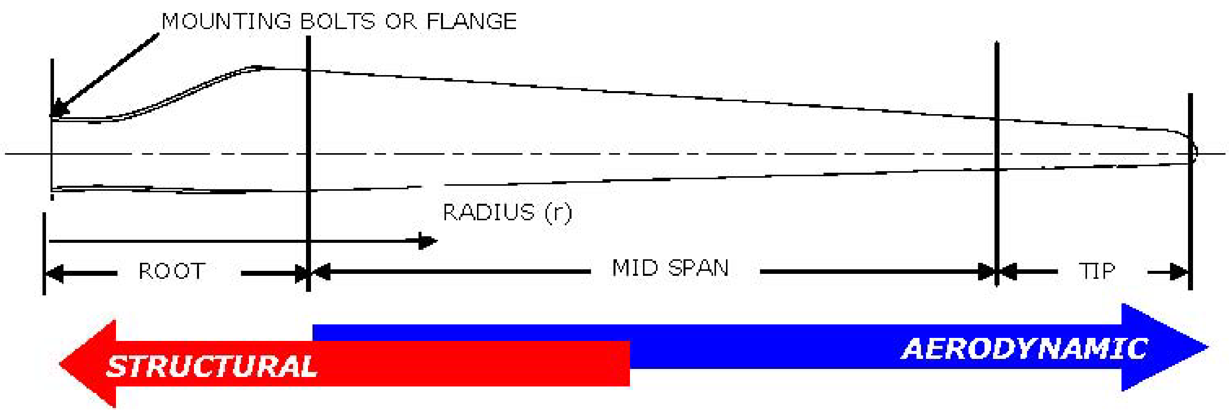

Figure 3-4 The three-blade region (Peter, 2012)

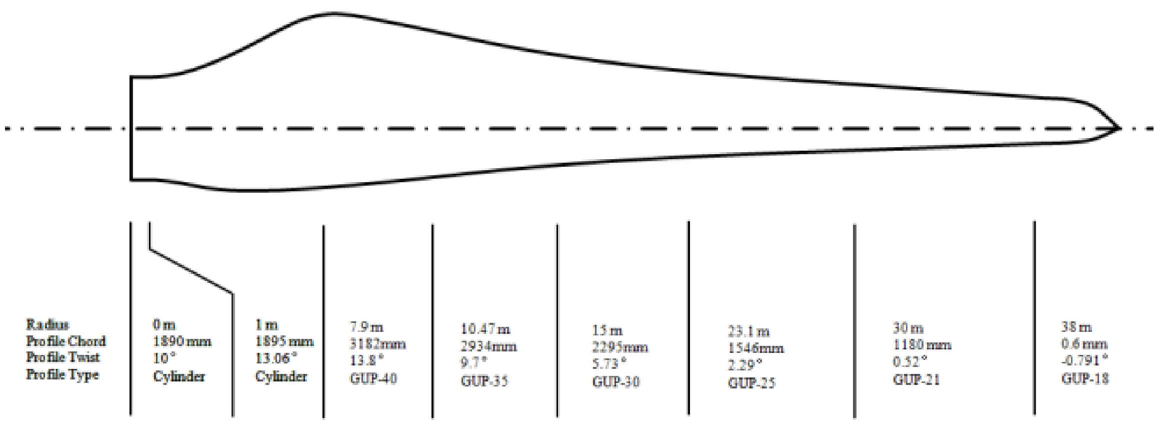

Figure 3-5 Adama II Wind turbine Blade Aerodynamic profile (SANY; 2017)

The wind speed range in which Adama II turbines are intended to function is specified. Cut-off wind speeds of 25 m/s, rated wind speeds of 11.5 m/s, and cut-in wind speeds of 3 m/s are chosen based on the chosen site. The blade's tangential speed varies over its span, as does the amount of lift it produces. From root to tip, the chord distribution blade varies in order to have a uniform lift coefficient. On below chart plots chord distribution result along the span using the BEM approach.

Twist Angle

The angle at which an airfoil segment attacks the incoming air stream determines how much lift it produces. The rotating speed and wind speed velocity at a certain radius determine the air stream's inflow angle. The required airfoil angle of attack and tip speed ratio determine the necessary twist angle. The hub's airfoil section is often inclined towards the wind because of the high wind-to-blade radial velocity ratio. The blade tip, however, is probably going to be nearly normal about the wind. Equation 3.4 is used by the BEM technique to get the blade twist angle. Hansen and others (1993)

$$\varphi = \frac{2}{3}\tan^{-1}\frac{1}{\lambda_r} \qquad (3.4)$$

Where, λ_r =local speed ratio, φ= is the blade twist angle.

The purpose of the twist is to create a consistent lift from the hub to the tip. The actual speeds of the different parts of the blade vary as the blade turns. Because the blade tip covers a larger distance in a comparable amount of time than the hub, it moves quicker than the area close to the hub. On the above Table 2 shows the angle of the twist's conclusion based on the mathematical correlation used earlier.

The maximum chord length of 3.182m at a span radius of 7.9m and the minimum chord length of 0.15 m at a span radius of 38.5 m are the analytical results of the BEM model. This figure displays the chord distribution and twist angle of the planned blade utilizing the NACA63-218 airfoil, both schematically and through a surface drawing.

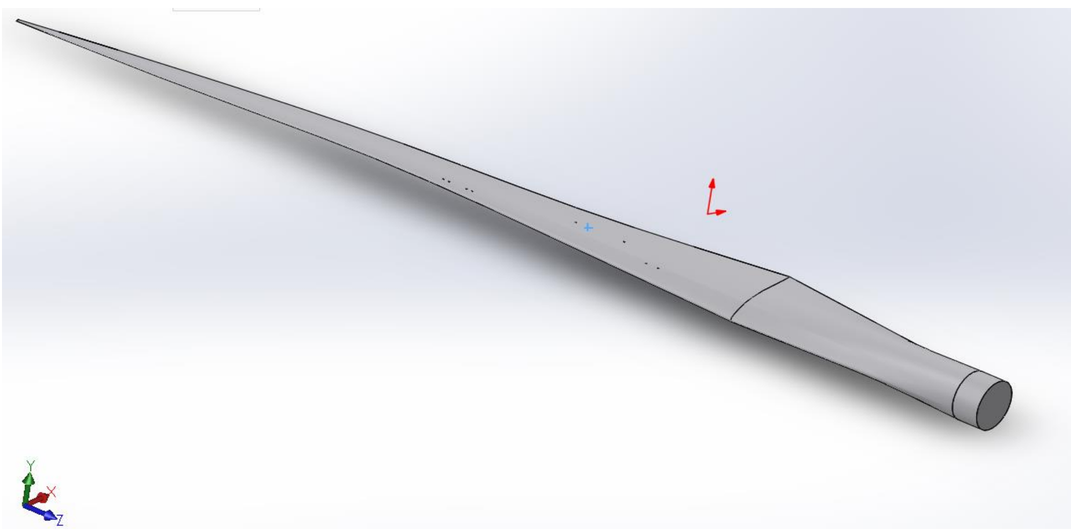

Figure 3-6 Designed wind Turbine Blade

Vortex Generator Design:

Vortex generators (VGs) are passive flow control devices typically deployed to prevent flow separation on wind turbine blades. They boost lift and hence reduce the destructive fatigue loads caused by stall, which increases rotor torque. This paper is the culmination of a research endeavor that used VGs to optimize both the sectional and the whole rotor-blade aerodynamics. VG size, chord wise position, and span wise spacing were all examined using force balance measurements of a two-dimensional wing section. The static stall angle and maximum lift increased significantly when the distance between neighboring VGs was reduced, however, there was also a noticeable rise in drag and severe lift excursions at angles higher than the static stall angle. It was discovered that the range of x/c = 15%–20% was the ideal chord wise position for the vortex generators since this resulted in a smooth post-stall lift curve and relatively minimal parasitic drag. Measurements of particle image velocimetry were made at different chord wise points to shed light on the interactions between neighboring stream wise vortices. Their impact on the aerodynamics of wind turbine blades was projected using the optimal VG configuration's experimental aerodynamic performance curves. Blade Element Momentum (BEM) code (QBlade) created by Smart Blade GmbH was used to simulate multiple stalls and pitch-regulated wind turbine models and to construct three distinct rotor blades. A simulation was conducted to evaluate the impact of variable guides (VGs) on the aerodynamic performance and loads of the rotor blades. Lastly, the adverse effect of surface roughness on the performance of the previously described rotor blades was simulated using previously obtained steady-state performance curves under high-roughness conditions. This makes it possible to evaluate how well the VGs could work as retrofit components to restore the performance of blades with polluted surfaces.

So, on this thesis Triangular vortex generators is selected rather than other flow control methods. Triangular vortex generators strike an optimal balance between effective boundary layer control, minimal drag impact, ease of installation, and robustness. This makes them a superior choice for enhancing the aerodynamic performance of wind turbine blades compared to other shapes. Their ability to generate strong, coherent vortices while maintaining low drag and compatibility with various blade designs solidifies their preference in the industry. The most researchers VG sizing selection that have good performed parameters are Height (H) =10mm, Length(L)=20mm, the distance between two vertex(S)=40mm, the gap between arrangements(Z)=180mm and Angle of incidence of VG vanes(β)=200. After select the design and modeling of vortex generator it will mount on the blade surfaces at a given specified places.

Mounting vortex generators (VGs) are strategically placed on blade surfaces to improve aerodynamic performance by controlling airflow separation. They can be attached using adhesive bonding, riveting, or embedding, and oriented parallel to the airflow direction. The size and shape of VGs depend on blade geometry, airfoil characteristics, and flow conditions. Tests and optimizations are done using computational fluid dynamics simulations. Regular inspection and maintenance are crucial to ensure VGs remain functional and secure over time.

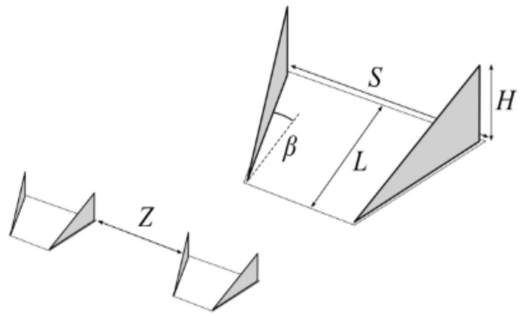

Figure 3-7 Schematic of vortex generator geometry

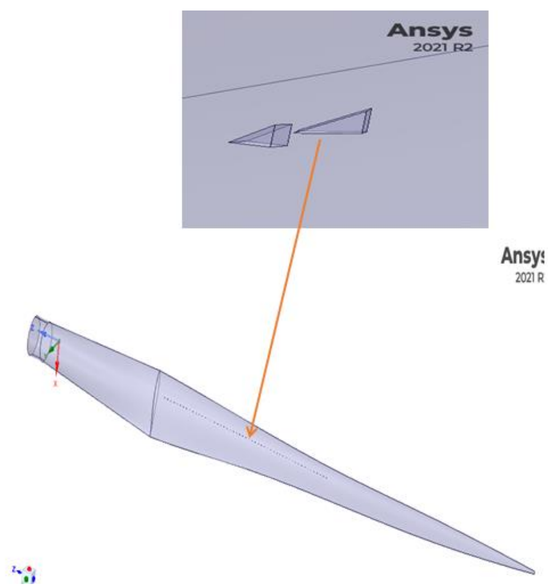

Figure 3-8 Schematic of blade with VG

3.2 A Numerical Study of Aerodynamic Performance

The aerodynamic behavior of wind turbines, the specific flow field characteristics surrounding a spinning wind turbine rotor or blade, and the power performance may all be studied and modeled using the computational fluid dynamics (CFD) technique and methodology. Turbulence models and mesh topology are the key interests in solving CFD problems. As computing power increases, the CFD technique is becoming a practical tool to model and simulate wind turbine aerodynamic performance in three-dimensional spaces and instantaneous time domains. An expansion of fluid mechanics, computational fluid dynamics (CFD) uses computer-based numerical methods to explain fluid motion. It deals with the solution of the pressure field for a given set of fluid parameters (such as velocity fields like surface tension, viscosity, and density).

Viscosity and geometry are the two main barriers to a viable theory in fluid mechanics. Viscosity can be disregarded in a limited set of idealized circumstances, making the stream fields inviscid. On the other hand, the majority of the time viscosity is present and can even vary, which makes it harder to create and apply the fundamental equations (White, 2008). Additionally, it may destabilize the previously described stream field, resulting in an unpredictable, disordered event known as turbulence.

Problems with complex geometry that exhibit abrupt changes in the fluid's geometrical boundaries make it challenging to identify "closed-formed analytical solutions. Numerical methods can be applied to address difficult geometry and viscosity problems on a Computational fluid dynamics (CFD) is the general term for this type of computer.

The three basic conservation equations of

- Mass (continuity) is among the conservation principles that CFD applies.
- Momentum, or the second law of Newton
- Energy (thermodynamics' first law)

The Navier-Stokes (N-S) Equations, which come in several versions, can be defined by utilizing conservation principles in fluid motion. They are provided in incompressible vector form by equations 4.1 and 4.2. Any Newtonian fluid's motion can be described using these equations.

$$\nabla \vec{V} = 0 \quad \text{……………………………………………………………………(4.1)}$$

$$\rho\left(\frac{\partial \vec{V}}{\partial t} + \vec{V}.\nabla \vec{V}\right) = -\nabla P + \mu \nabla^2 \vec{V} + \vec{S} \quad \text{………….…………………….. (4.2)}$$

Where;

$\vec{V}$ = the velocity vector t= time, ρ= density p= pressure, μ= the viscosity, $\vec{S}$ =a source term and ∇^2= Laplacian operator

The eddy-viscosity idea is used in several models but to varying degrees. Algebraic models, one equation model, and two-equation models.

Two equation model: The most basic complete system used in CFD modeling, two-equation models is complete and offer a closed system. They compute two equations: one for the particular kinetic energy of turbulence and another for the turbulence length scale. The second equation and the computed variable, such as the turbulence length scale (l), specific dissipation (ε), or specific dissipation rate (ω), are the key differences across the numerous models. The k-τ model was the first two-equation model created by Kolmogorov in 1942. Closure coefficients are the property of both equation models, and they have been used to substitute algebraic expressions containing known attributes for double and triple correlation terms. If turbulence theory was accurate these coefficients would be set from first principles but it is not and the models are developed based on dimensional analysis and observations. While there are several models, the k-ε, k-ω, and k-ω shear stress transport (k-ω SST) models which are covered in greater detail are the primary models used in practice today.

k-ω shear transport (K-ω SST) Model: Menter devised the two-equation eddy-viscosity model known as the k-ω SST turbulence model. It employs the k-ω model in the near wall region and the k-ε model in the far field within the free streams. The k-ε model is transformed into a k-ω formulation to accomplish this. Because of this arrangement, k-ω SST is more accurate than k-ω and k-ε combined. Compared to previous k-ω models, k-ω SST is more accurate and dependable for flows such as airfoils, transonic shock waves, and unfavorable pressure gradient flows (ANSYS, 2021).

The turbulent viscosity change to the turbulent shear stress transfer is considered when naming the k-ω SST model. Without the need for an additional damping function, the k-ω SST model is applied for low Reynolds turbulence and deep down to the wall borders viscous sublayer. In addition, the k-ω SST overcomes the usual k-ω issue of the model being overly sensitive to the inlet free-stream turbulence qualities by switching to a k-ε behavior in the free-stream. To guarantee that the model equations behave suitably in both the near-wall and far-field zones, additional modifications include the insertion of a blending function and a cross-diffusion term in the ω equation (Karim et al., 2011).

3.3 ANSYS-FLUENT

A commercially available general-purpose finite volume code with multiple discretization types and solvers, ANSYS Fluent is used to predict reactions, heat transfer, and turbulence. Applying it to wind turbine research with single blades (Mahu, 2011; Qunfeng et al., 2011), complete rotors (WuBow et al., 2007), and actuator discs (Makridis, 2009; Makridis, 2013) has been documented. The simulation setup (Geometry Development, Computational Domain & Scaling) and parameters used (Turbine Specifications, Turbulence Modeling, Boundary Conditions, Numerical Methods & Post-Processing) based on the provided information the ANSYS-FLUENT is done.

3.3.1 **Description of the Model**

Using Solid Works, the geometry of the reference turbine was built according to the requirements listed in the Blade design section and potential evaluation for rated conditions. The domain geometry was then generated by exporting this geometry into ANSYS Design-Modeler. The dimensions of the domain were as follows: 20 meters were measured upstream, 40 meters downstream of the first turbine, and 20 meters span wise on both sides of the turbines. The domain's overall height was established at 35 meters. The model and flow tunnel were eventually reduced to a ratio of one to a hundred.

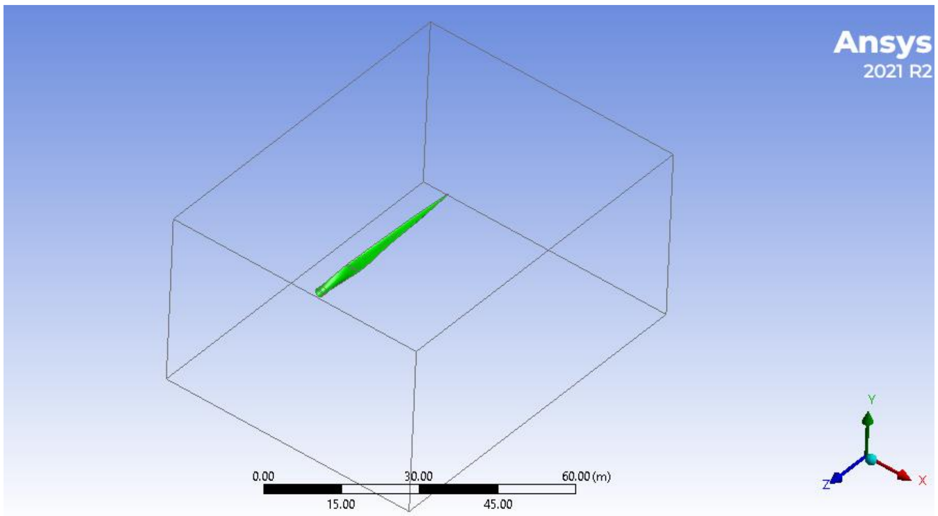

Figure 3-9 Baseline model in flow tunnel

The baseline blade model and three additional vortex generator orientations imprinted on the baseline model are featured in the following figures that depict HAWT blades. These models are imported into ANSYS-DESIGN MODELER and a corresponding virtual wind tunnel is generated to simulate the fluid mechanics processes.

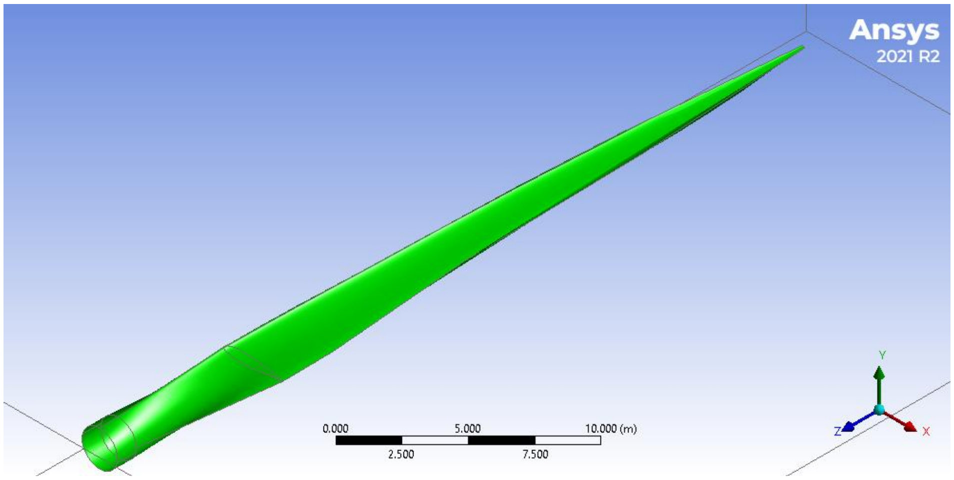

Figure 3-10 Blade Baseline Models

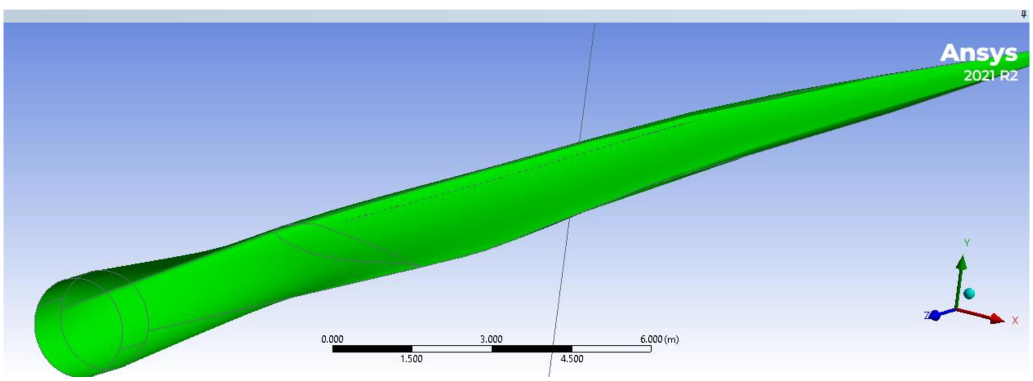

Figure 3-11 Blade with vortex generator Orientation one

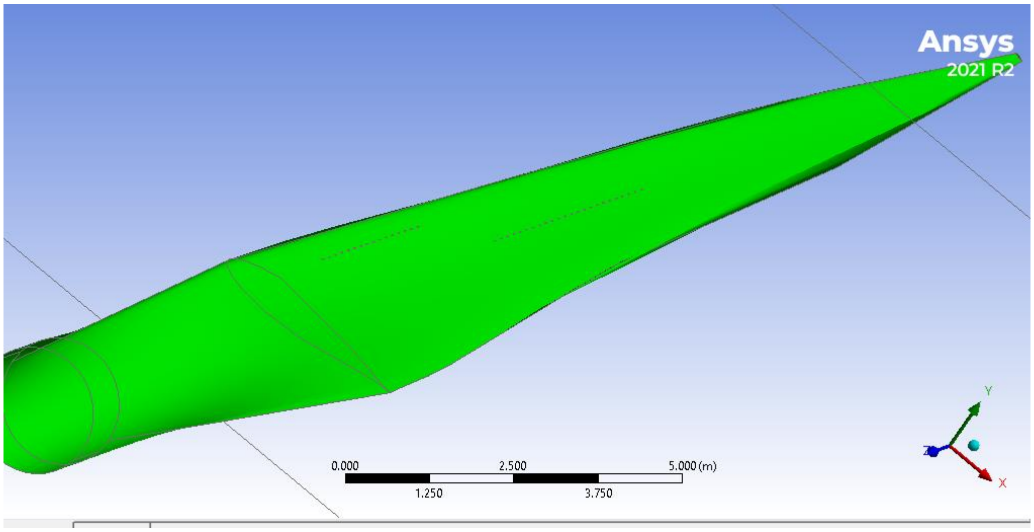

Figure 3-12 Blade with vortex generator Orientation Two

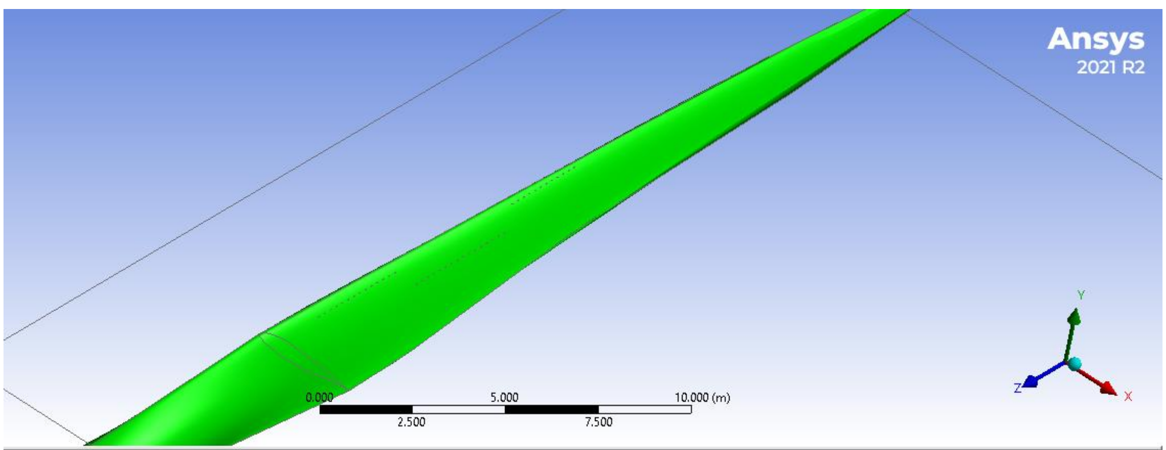

Figure 3-13 Blade with vortex generator Orientation Three

3.3.2 **Meshing**

In CFD, the computational domain is divided into smaller discrete elements or cells, collectively known as a grid or mesh. In ANSYS Meshing, an unstructured tetrahedral mesh is used for meshing. On the blade faces, cell sizes were fixed to one millimetre, and on the blade tips, to 0.5 millimetres. The maximum size of a cell was limited to one millimetre in both the vertical and horizontal dimensions. For every solid surface, inflation layers with a maximum growth rate of 1.2 were applied. There were almost two million cells in each of the stationary reference turbine blade meshes.

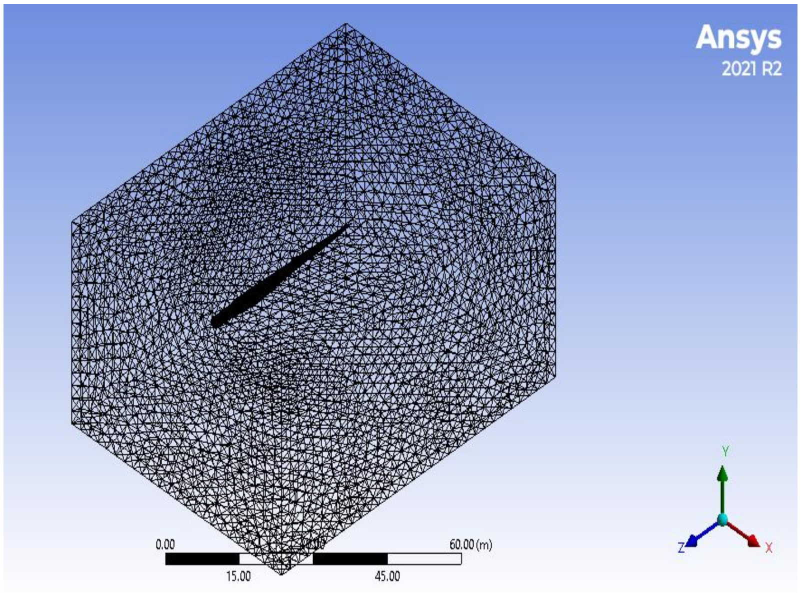

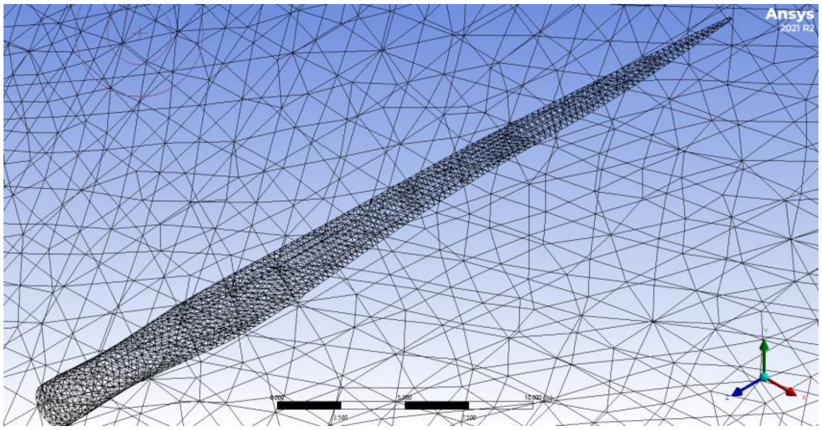

Figure 3-14 Blade mesh

3.3.3 Grid Independence Test

The fineness of the mesh is the main issue while simulating any system in ANSYS Fluent. Insufficient mesh fineness could result in a discrepancy in values. Therefore, the research model's surface mesh ought to be precise enough to remove all errors. The mesh size is reorganized from coarse to fine mesh until an estimated value is determined to assess its impact. Mesh independence test was performed using simulation on baseline blade at 0^{o} angle of attack (the angle considered at maximum chord length). The main worry was the solution on the blade surface, so tested the mesh there starting with a coarser mesh size and working way up to a finer mesh.

Table 3 Grid independent test of element size and number of elements

Mesh number	Mesh Element size	Number of Element
Mesh 1	0.3m	296475
Mesh 2	0.2m	416840
Mesh 3	0.1m	984417
Mesh 4	0.08m	1390087
Mesh 5	0.07m	1735078
Mesh 6	0.06m	2232240

So, by this element size the ratio of lift force to drag force is used to assess the aerodynamic performance of any device or component, including wind turbines, cars, aircraft, and other objects. Using k-ω shear shear transport (K-$\boldsymbol{\omega}$ SST)., the lift and drag coefficients of the planned blade at various angles of attack are computed. Everybody The simulation's CFD results are shown in the Appendix, from which the following graphs are created. The lift coefficient, drag coefficient, and aerodynamic performance of the baseline blade are depicted in below tables with graphs.

Table 4 Mesh independent test of different mesh size of Element size, Cl, Cd and Cl/Cd

Mesh size	Element size	Cl	Cd	Cl/Cd
Mesh 0.3	296475	19.580796	8.1828851	2.392896364
Mesh 0.2	416840	18.223925	8.7395722	2.085219343
Mesh 0.1	984417	17.590412	11.373534	1.546609172
Mesh 0.08	1390087	17.791947	13.057133	1.36262279
Mesh 0.07	1735078	18.362403	14.14108	1.298514894
Mesh 0.06	2232240	18.78689	15.728421	1.19445493

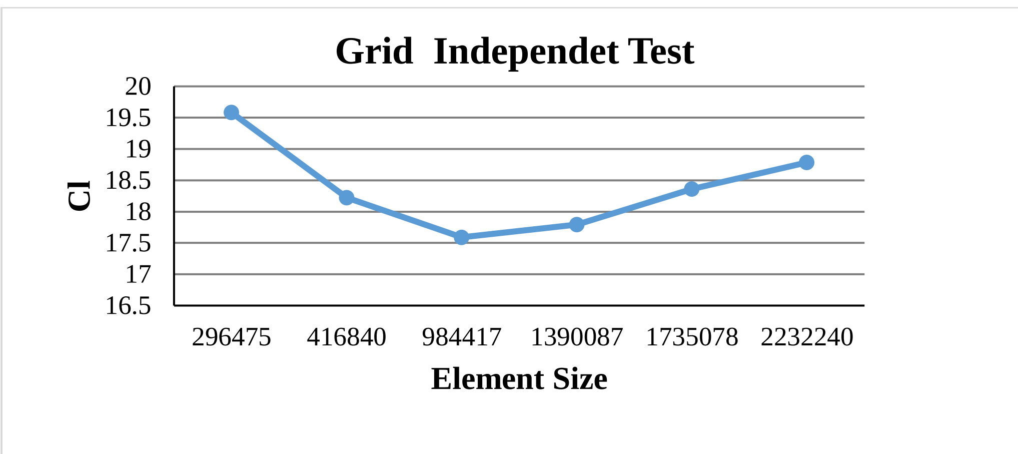

Figure 3-15 Grid independent Test result for Cl vs Element size

3.3.4 **Solution Scheme**

Because of its quick convergence and correctness, the Semi-Implicit Method for Pressure-Linked Equations (SIMPLE) approach was chosen in this thesis. Velocity and pressure are separated using the Semi-Implicit Method for Pressure-Linked Equations (SIMPLE) algorithm (Muiruri et al., 2019). The pressure variable was initially calculated using the pressure correction equation in this method, which also implicitly used the continuity and momentum equations. The velocity variables were then explicitly derived from the momentum equations. The turbulent kinetic energy and specific dissipation rate were calculated using a first-order upwind approach for their quick convergence, whereas the pressure was calculated using a second-order method and momentum was in a second-order upwind method.

In this research, the parallel technique was used in all simulations and the three-dimensional configuration of the ANSYS Fluent finite volume method was utilized with double precision. For the flow model, a pressure-based type solver with an absolute velocity formation steady state flow condition was used. A mixture of both k-ω and k-ε was used in the k-ω SST turbulence model. For free streams, k-ω operates, and k-ω operates close to the blade surface.

CHAPTER FOUR

RESULTS AND DISCUSSIONS

4. Introduction

This section displays the results of numerical research on wind energy potential evaluation, wind turbine blade design, and vortex generator effect. The outcome and discussion also are based on the baseline blade and blade with vortex generator data from ANSYS Fluent. This study was done to demonstrate the vortex generator's aerodynamic effect on the fluid flow phenomena across the blades. Then compare the vortex generator's aerodynamic impact on the blade surface to that of the baseline blade. ANSYS Fluent will provide many graphs and plots to support this aerodynamic finding.

4.1 Aerodynamic Characteristics of Baseline Blade

It is important to talk about the aerodynamic properties of a blade to understand how fluid flow phenomena impact the blade's aerodynamic efficiency, particularly its lift-to-drag coefficient. Based on the data taken from ANSYS Fluent, the study's flow characteristics for the baseline blade are examined in this section. The Adama II wind turbine's designed wind average velocity of 11.5 m/s was used in the simulation.

4.1.1 Pressure contour and velocity stream line

Different flow phenomena are experienced by wind turbine blades under various flow conditions. The main factors influencing aerodynamic forces and flow behavior are angle of attack and velocity. This thesis investigates the planned blade flow phenomenon by changing the angle of attack at a constant Reynolds number from -5^0 0^0,5^0,10^0,15^0,20^0 and 25^0. The pressure contour and velocity streamline are presented in the following charts along the planned blade at particular AOAs. The fluid will have a variable flow pattern along the blade span of a wind turbine due to the blade's angle of twist, as shown in the below figure, which shows three separate contour-capturing positions (i.e., 12.5m, 18m and 23.5m because the most vortex arrangements are get on this section of blade surfaces).

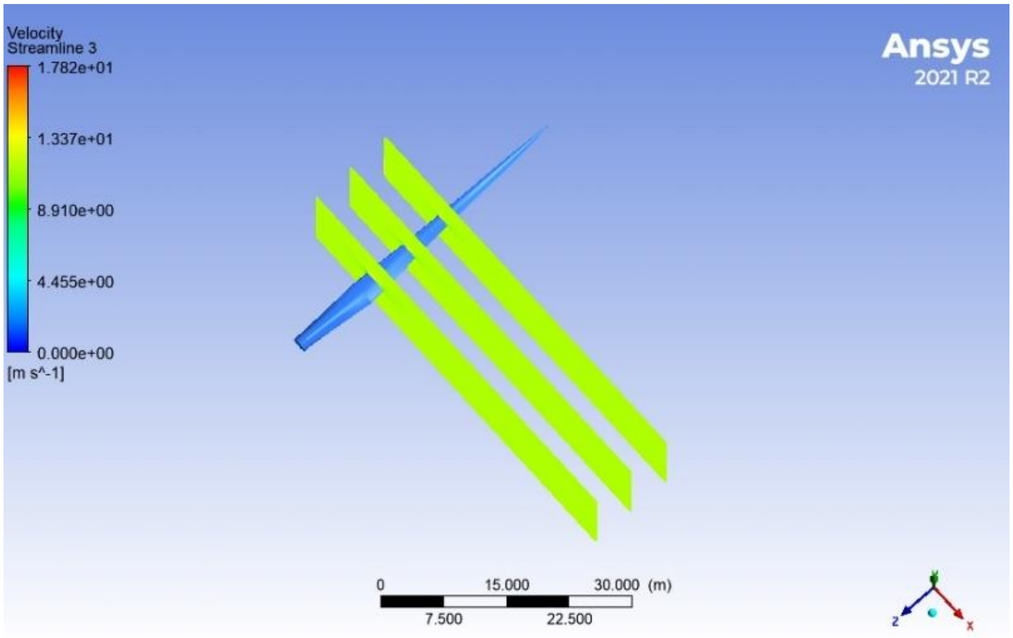

Figure 4-1 Testing plane section location from root of blade at 12.5m, 18m and 23.5m

4.1.1.1 At an Angle of Attack (AoA) of (-5^0)

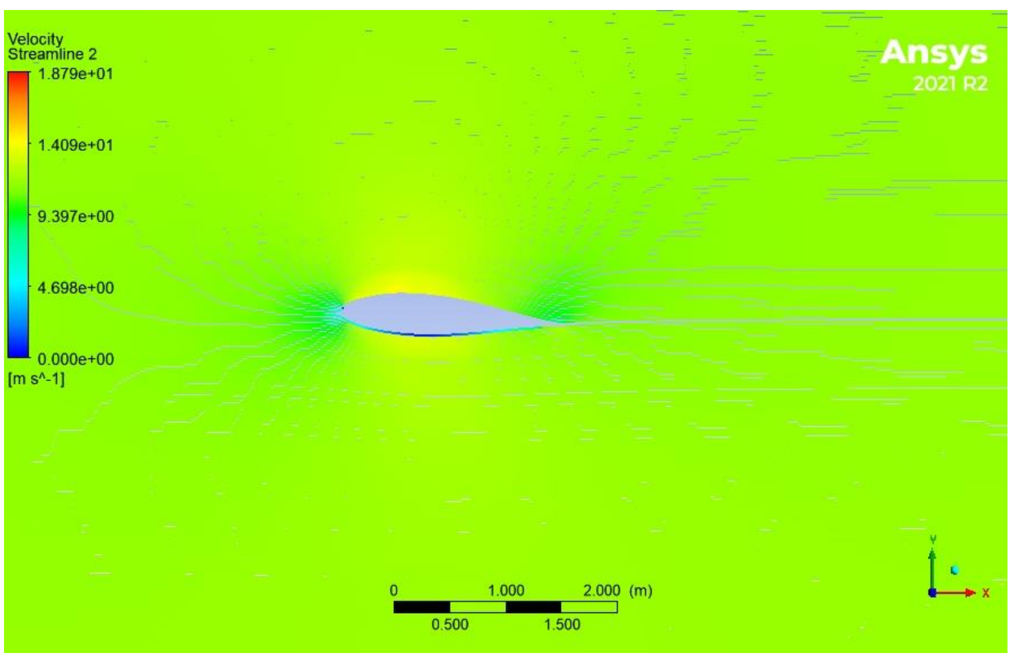

Figure 4-2 Baseline Velocity Streamline At $\alpha = -5^0$

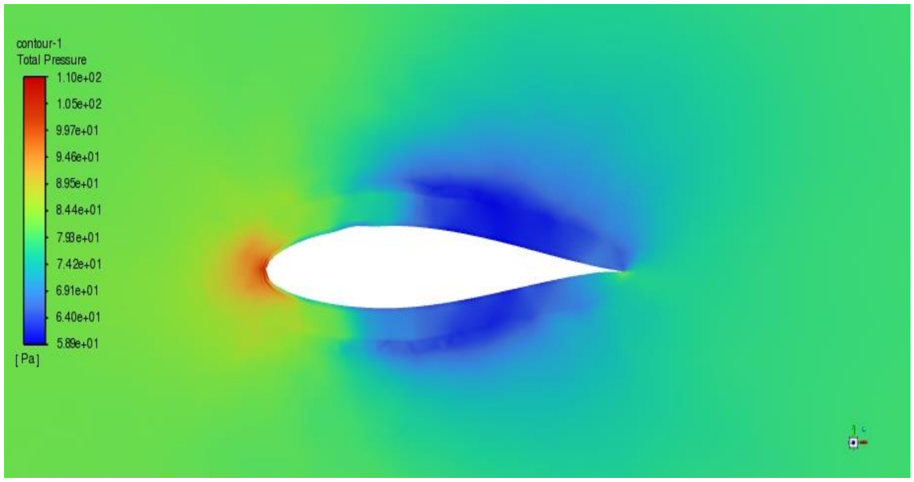

Figure 4-3 Baseline pressure contour at α = -5^0

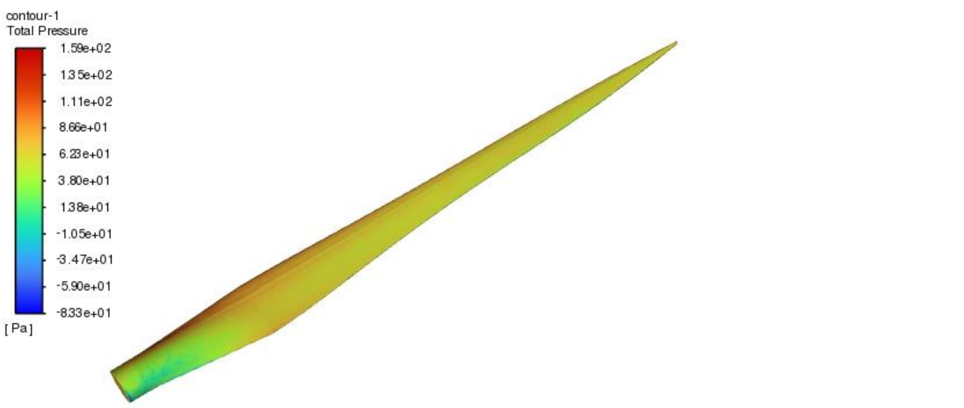

Figure 4-4 Baseline Suction Side Pressure Contour At α= -5^0

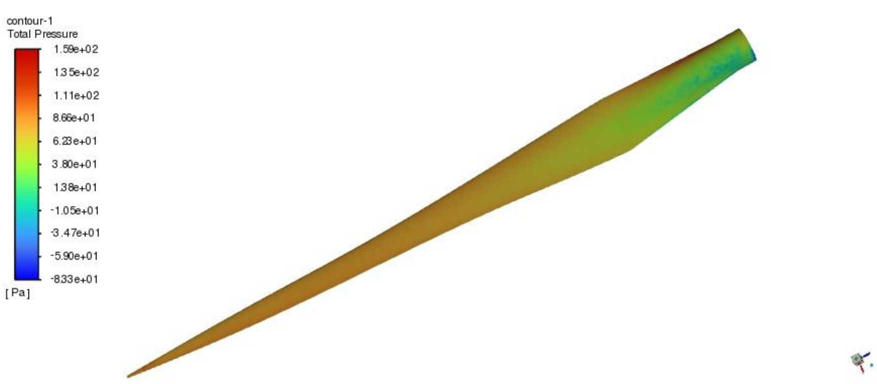

Figure 4-5 Baseline Pressure Side Pressure Contour At α= -5^0

As shown in the above figures the velocity at leading edge near the suction side is almost zero, so it is the reason to experience high-pressure around the leading edge and pressure at leading edge or pressure side develops a small Pressures.

4.1.1.2 At an Angle of Attack (AoA) of (-0^0)

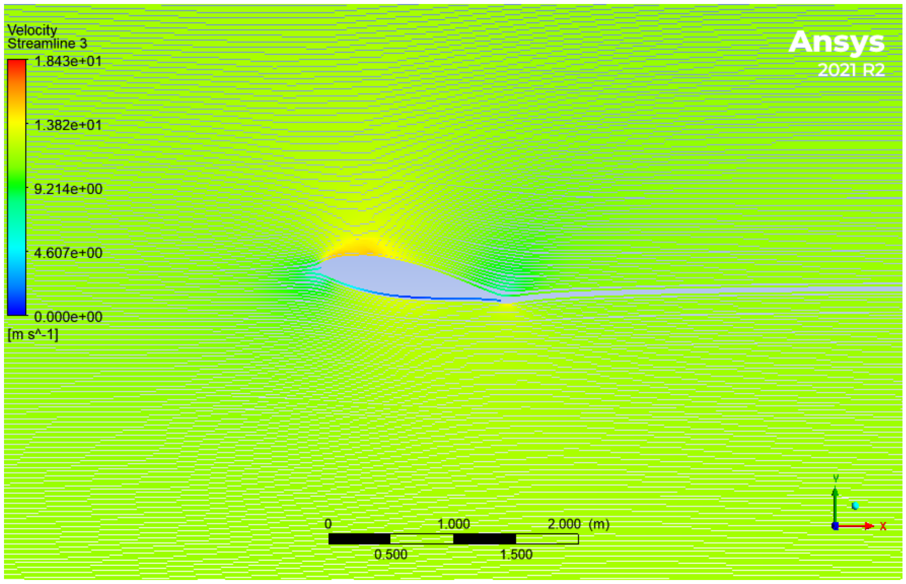

Figure 4-6 Baseline Velocity Streamline At α = 0^0

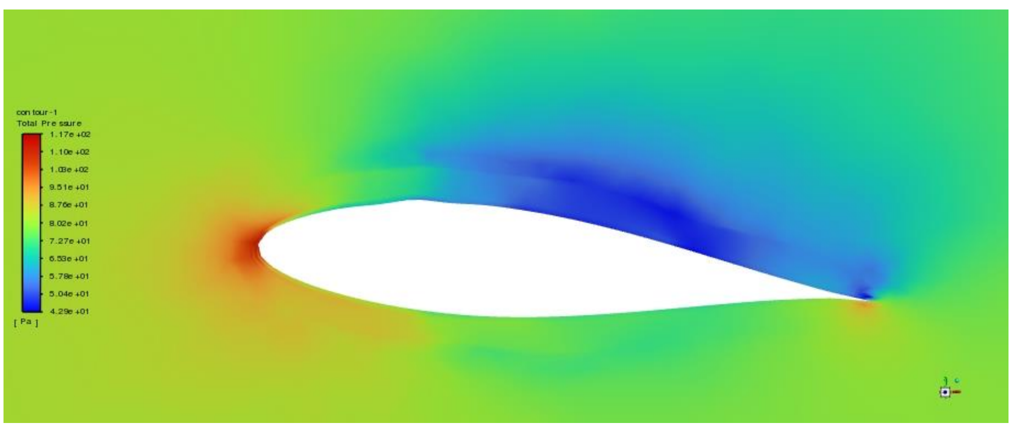

Figure 4-7 Baseline pressure contour at α = 0^0

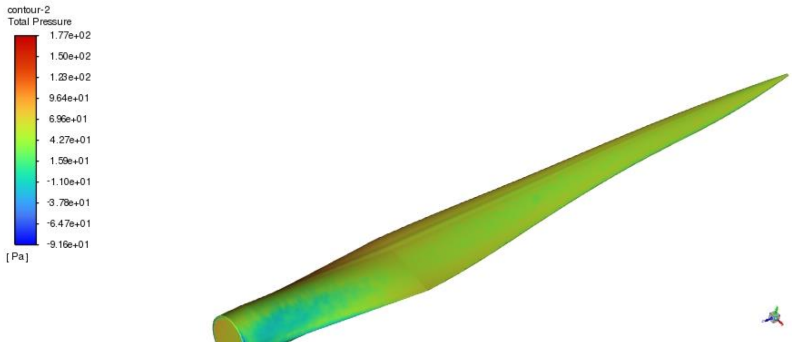

Figure 4-8 Baseline Suction Side Pressure Contour At α= 0^0

Figure 4-9 Baseline Pressure Side Pressure Contour At α= 0^0

On the above figures at AoA 0^0 results the velocity at leading edge near the suction side is better than AoA 5^0, so it is the reason to experience high-pressure around the leading edge.

4.1.1.3 At an Angle of Attack (AoA) of (5^0)

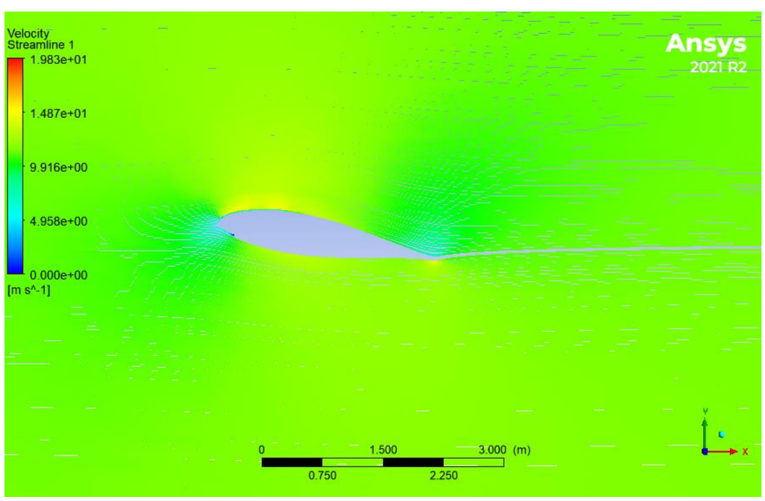

Figure 4-10 Baseline Velocity Streamline At α = 5^0

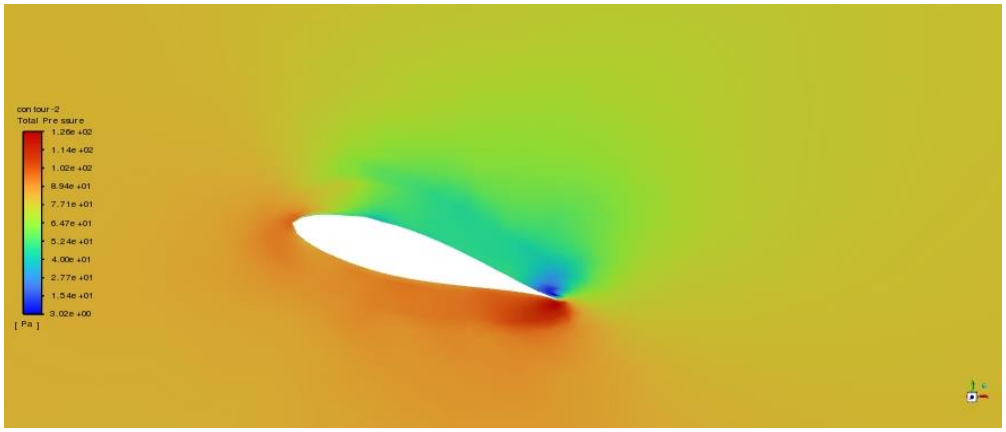

Figure 4-11 Baseline pressure contour at α = 5^0

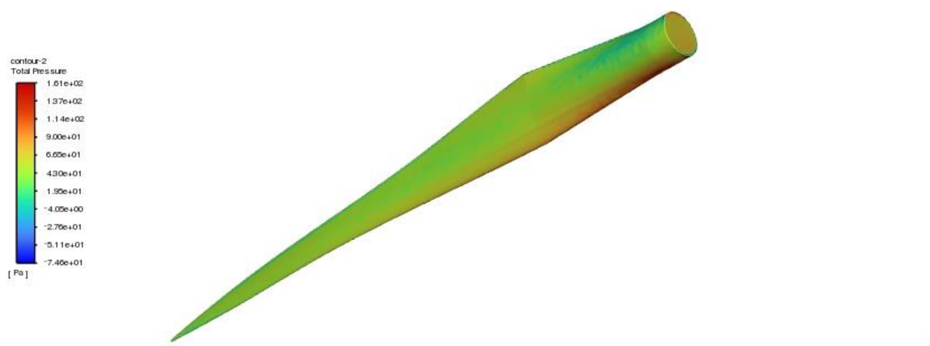

Figure 4-12 Baseline Suction Side Pressure Contour At α= 5^0

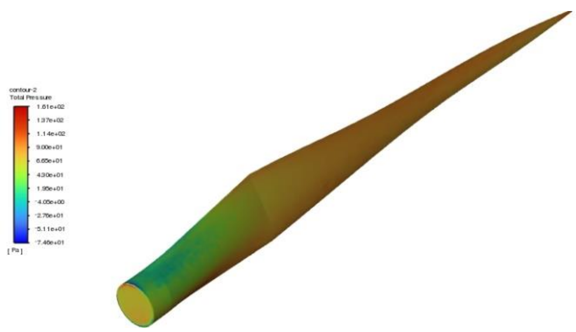

Figure 4-13 Baseline Pressure Side Pressure Contour At α= 5^0

On the above figures at AoA 5^0 results the velocity at leading edge near the suction side is better than AoA 0^0, so it is the reason to experience high-pressure around the leading edge.

4.1.1.4 At an Angle of Attack (AoA) of (10^0)

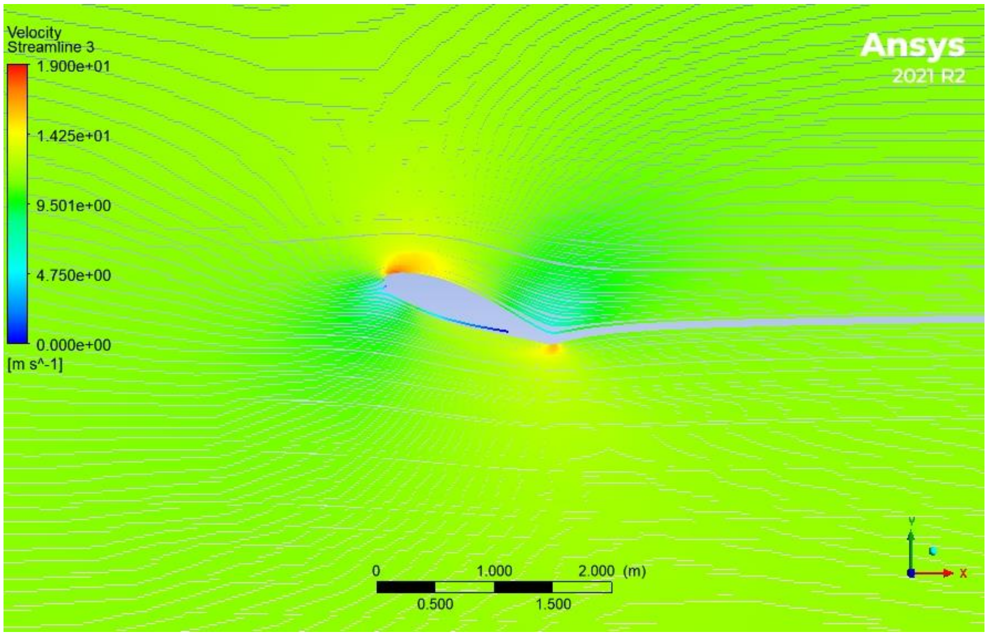

Figure 4-14 Baseline Velocity Streamline At α = 10^0

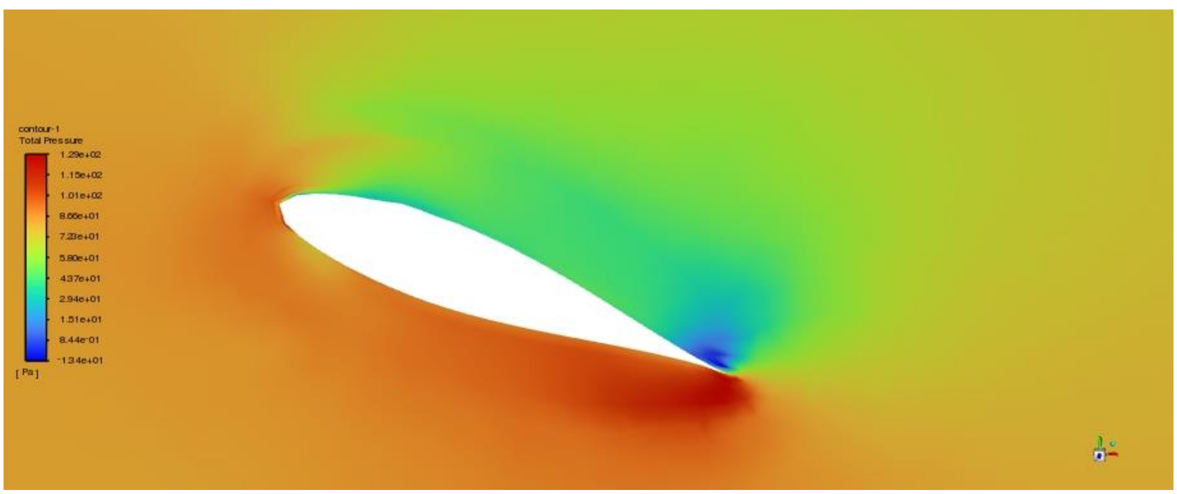

Figure 4-15 Baseline pressure contour at α = 10^0

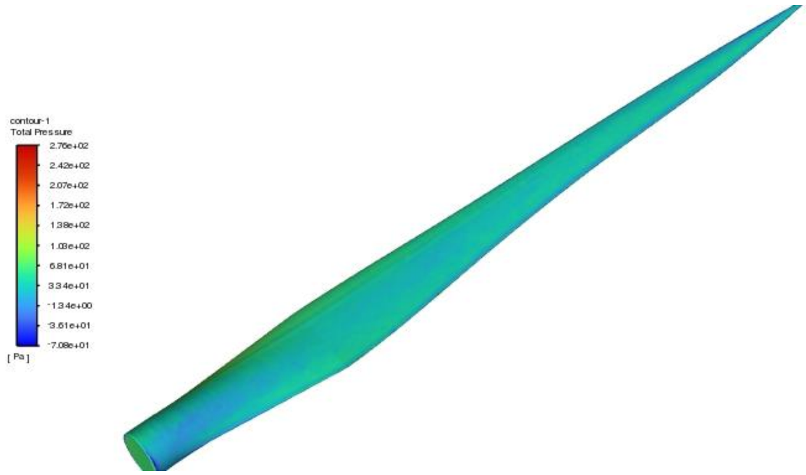

Figure 4-16 Baseline Suction Side Pressure Contour At α= 10^0

Figure 4-17 Baseline Pressure Side Pressure Contour At α= 10^0

4.1.1.5 At an Angle of Attack (AoA) of (15^0)

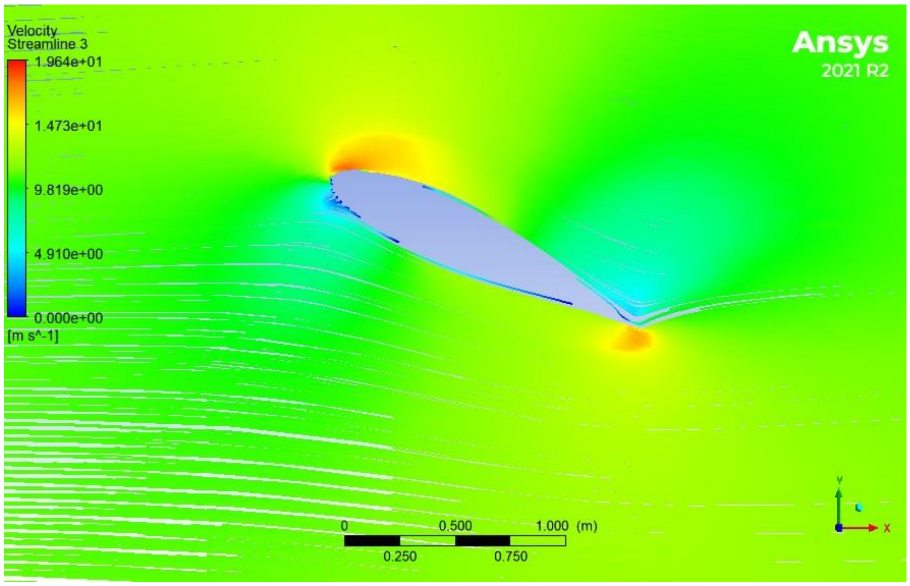

Figure 4-18 Baseline Velocity Streamline At α = 15^0

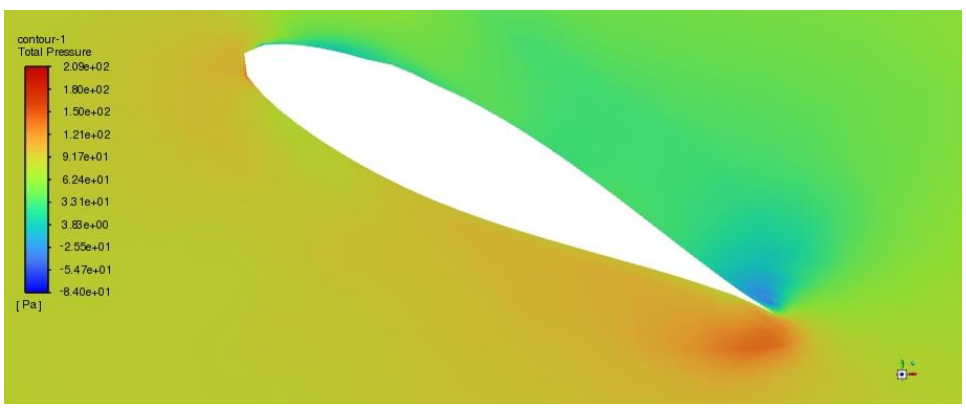

Figure 4-19 Baseline pressure contour at α = 15^0

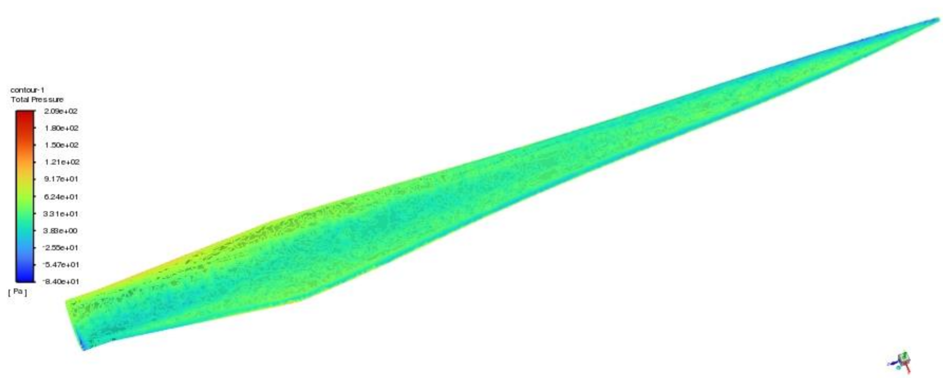

Figure 4-20 Baseline Suction Side Pressure Contour At α= 15^0

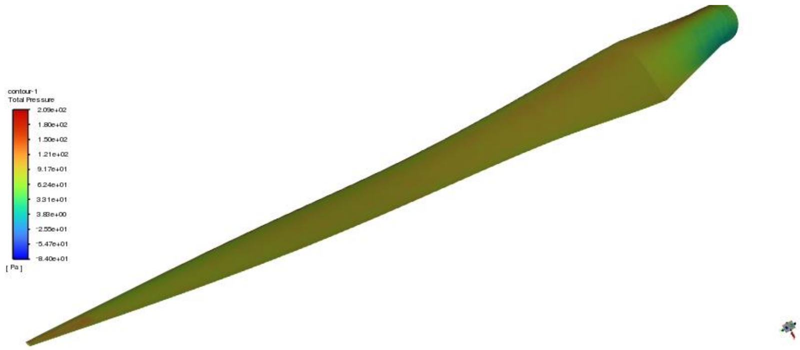

Figure 4-21 Baseline Pressure Side Pressure Contour At α= 15^0

4.1.1.6 At an Angle of Attack (AoA) of (20^0)

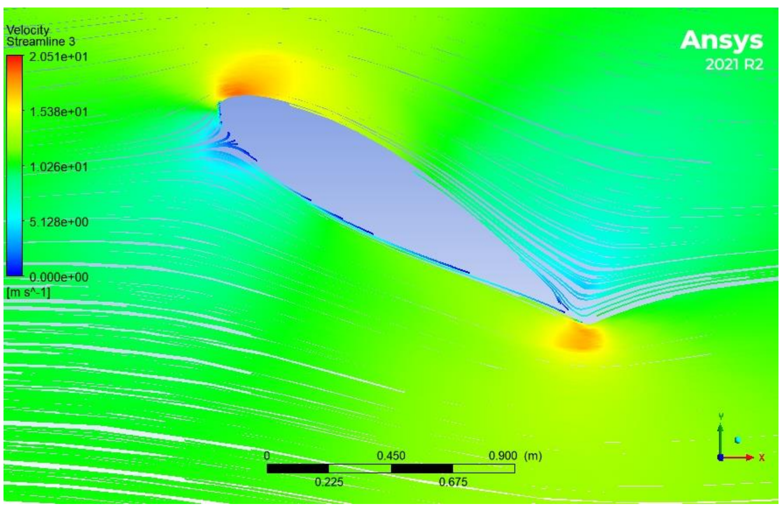

Figure 4-22 Baseline Velocity Streamline At α = 20^0

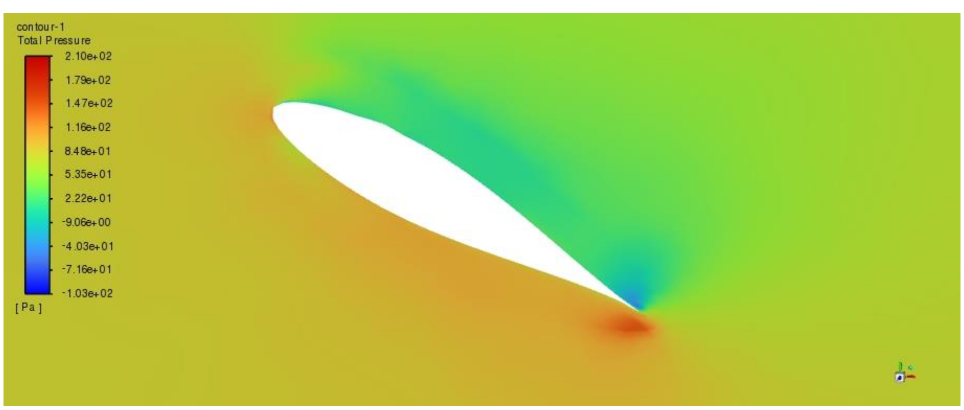

Figure 4-23 Baseline pressure contour at α = 20^0

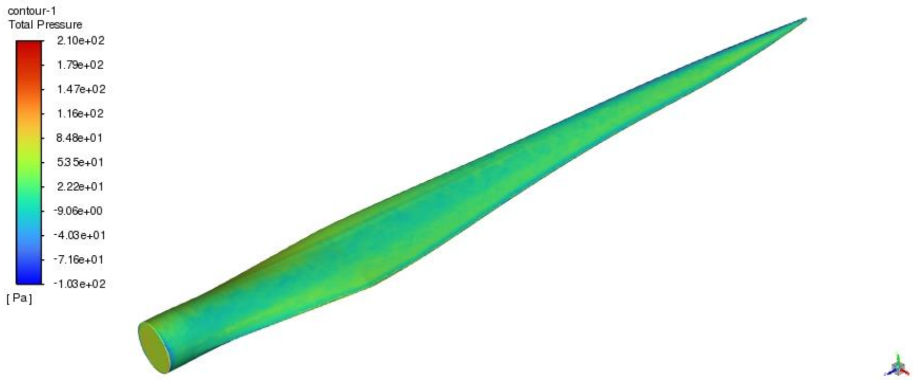

Figure 4-24 Baseline Suction Side Pressure Contour At α= 20^0

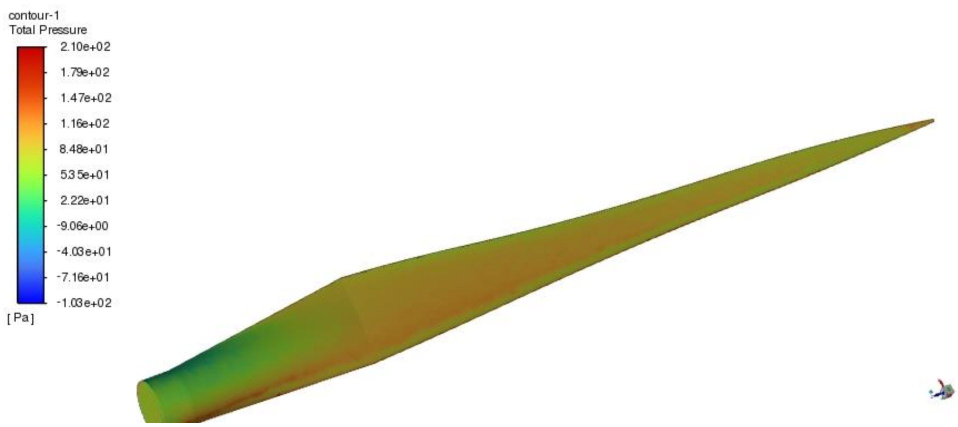

Figure 4-25 Baseline Pressure Side Pressure Contour At α= 20^0

4.1.1.7 At an Angle of Attack (AoA) of (25^0)

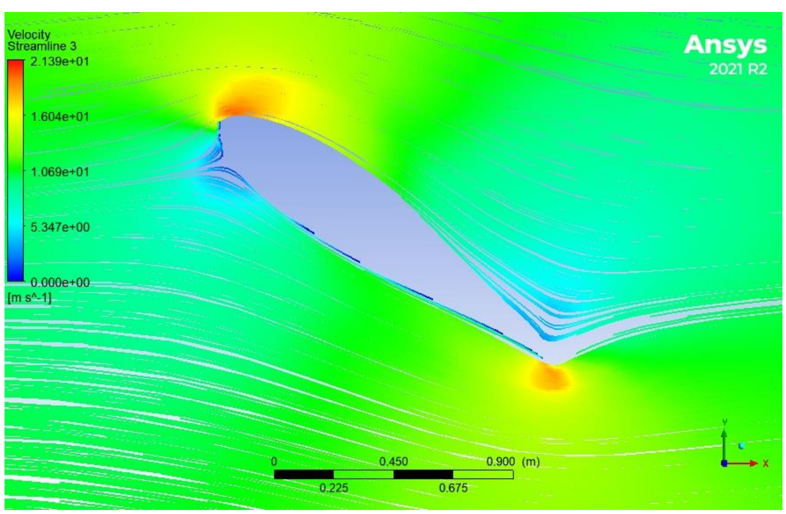

Figure 4-26 Baseline Velocity Streamline At α = 25^0

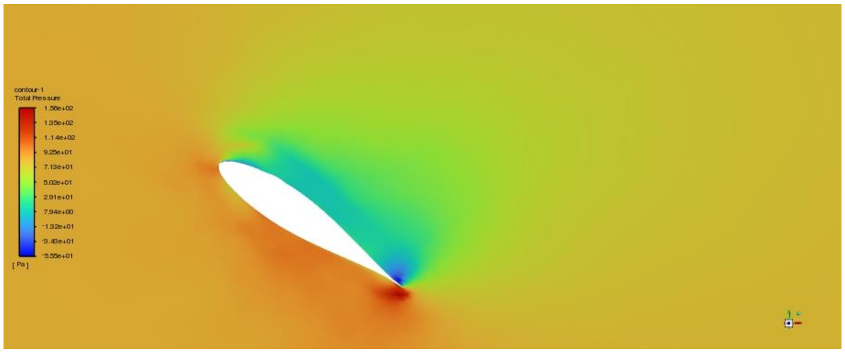

Figure 4-27 Baseline pressure contour at α = 25^0

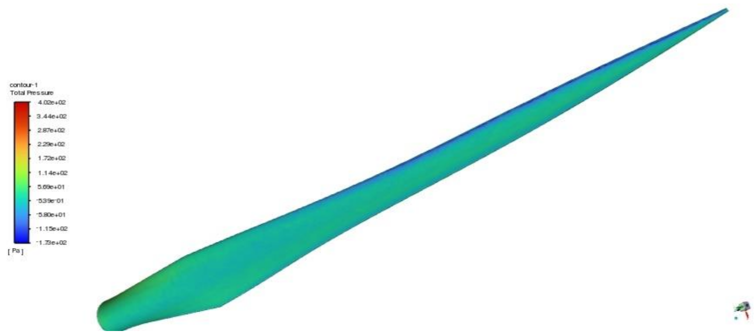

Figure 4-28 Baseline Suction Side Pressure Contour At α=25^0

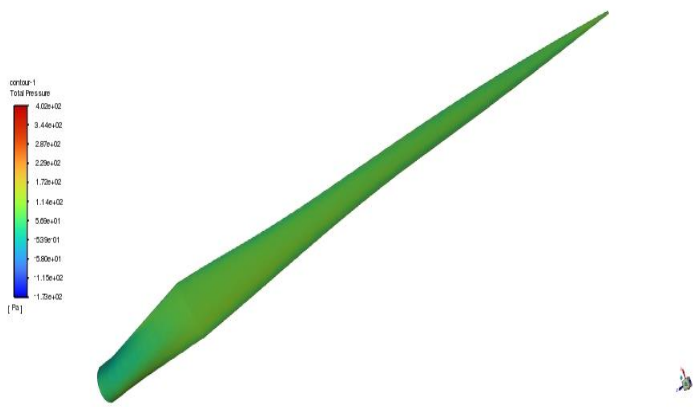

Figure 4-29 Baseline Pressure Side Pressure Contour At α= 25^0

In the above figures at AoA 25^0 the maximum velocity streams 21.36m/s occurs and the minimum velocity stream is 18.43 m/s at 0^0. When a baseline blade is at an angle of attack (AOA), several aerodynamic effects come into play. At low angles of attack, increasing the angle typically increases the velocity of the airflow over the blade. This increase in velocity is due to the airflow being redirected around the blade, which creates a pressure difference, increasing velocity to compensate.

However, as the angle of attack continues to increase from 0^0 to 10^0, there comes a point where the airflow over the blade starts to detach from the surface. This detachment causes a sudden drop in pressure on the surface of the blade at AOA 15^0, leading to a decrease in lift and an increase in drag. This phenomenon is often referred to as stall. Stall occurs because the airflow cannot follow the curvature of the blade surface at high angles of attack, leading to separation and a significant decrease in lift generation. The sudden drop in pressure and increase in drag can have adverse effects on the performance and stability of the blade or airfoil.

As a result, the baseline at 10^0 AoA was chosen. Ultimately, the test of fluent results at 25^0 can obtain maximum velocity and high pressures in comparison to other AoA, but at 10^0 AoA already receive maximum lift-to-drag coefficient.

Table 5 pressure contour and velocity streams

AOA (^{0})	velocity stream m/s	Pressure(pa)
-5	18.79	159
0	18.43	117
5	19.82	120
10	19	129
15	19.64	209
20	20.5	210
25	21.36	150

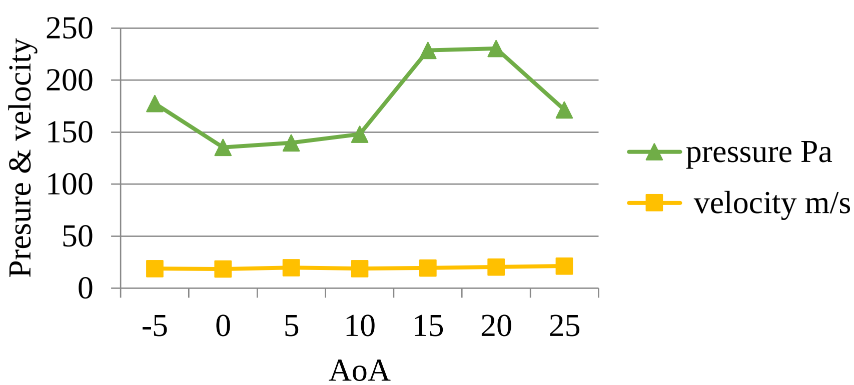

Figure 4-30 Pressure contour & Velocity stream of Baseline

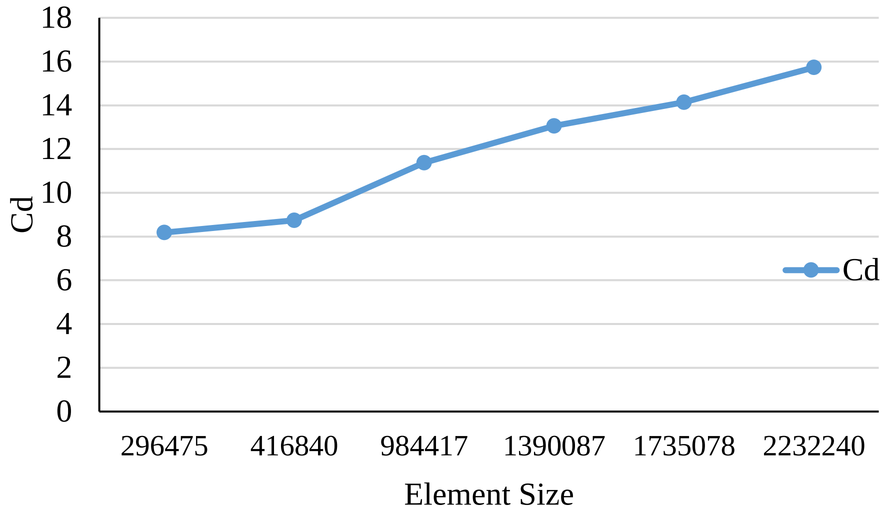

Figure 4-31 Grid independent Test result for Cd vs Element size

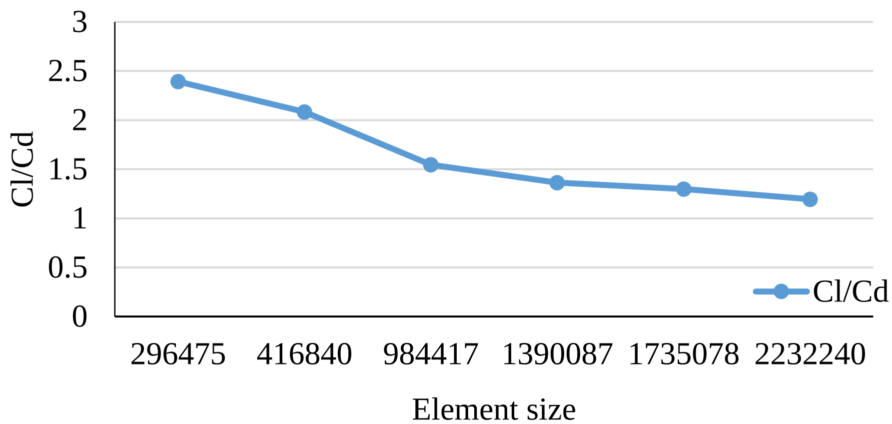

Figure 4-32 Grid independent Test result for Cl/cd vs Element size

Table 6 Cl and Cd of baseline, VG1, VG2 and VG3 blade profile at-5^0, 0^0, 5^0, 10^o, 150, 20^0 & 25^0

Baseline blade				VG1orientation one			VG2 orientation Two			VG3orientation Three		
AOA	Cl	Cd	Cl/Cd	Cl	Cd	Cl/Cd	Cl	Cd	Cl/Cd	Cl	Cd	Cl/Cd
-5	6.19731	12.656081	0.48967	7.14276	3.49004	2.04661	7.1086	3.47113	2.04792	7.14943	3.54936	2.01429
0	18.7869	15.728421	1.19445	15.9496	4.45316	3.58163	16.0498	4.43886	3.61575	16.0764	4.45453	3.609
5	30.545	16.032627	1.90518	24.3474	6.72882	3.61838	24.3444	6.73802	3.61299	24.1333	6.7016	3.60113
10	41.8195	20.042545	2.08654	33.5367	10.877	3.08328	33.4646	10.7037	3.12646	33.3977	10.7256	3.11383
15	52.1441	25.522422	2.04307	43.3563	16.5267	2.6234	43.5893	16.6816	2.61302	43.2439	16.4366	2.63094
20	61.264	32.450182	1.88794	52.9261	23.7811	2.22555	52.9121	23.7842	2.22468	53.007	23.8303	2.22435
25	65.3511	36.918937	1.77013	61.9827	32.9304	1.88223	60.9695	31.8389	1.91494	59.9284	30.5965	1.95867

The lift and drag coefficients in wind turbine blade design are influenced by a range of factors, including the shape of the blade, its angle of attack, surface roughness, and operational conditions. While increasing lift is generally desirable for energy extraction, managing drag is critical to maintaining efficiency and minimizing energy losses. So on this research uses by the use of AoA;it compares Cl and Cd.it means that the lift coefficient increases with the angle of attack up to a certain point. As the angle of attack increases, the airflow over the blade generates more lift, which is crucial for the blade to extract energy from the wind and the drag coefficient also rises with the angle of attack, especially beyond the optimal range. As the angle increases, the airflow separation becomes more pronounced, increasing pressure drag. So, in the above tables grid independent test at baseline the maximum lift to drag coefficient gets at AOA 10^0, but on blades with VG1, VG2 and VG3 better than baseline blades and to compares blades with VG's at VG1 gets highest lift to drag coefficient and graphically compare as below.

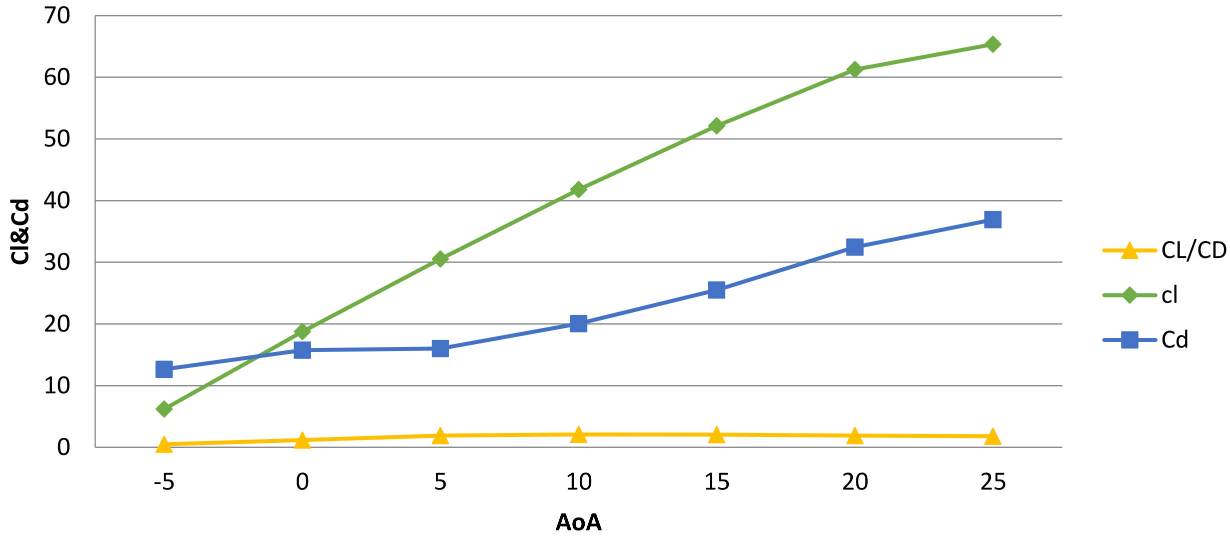

Figure 4-33 Grid independent test of Cl and Cd of baseline blade profile

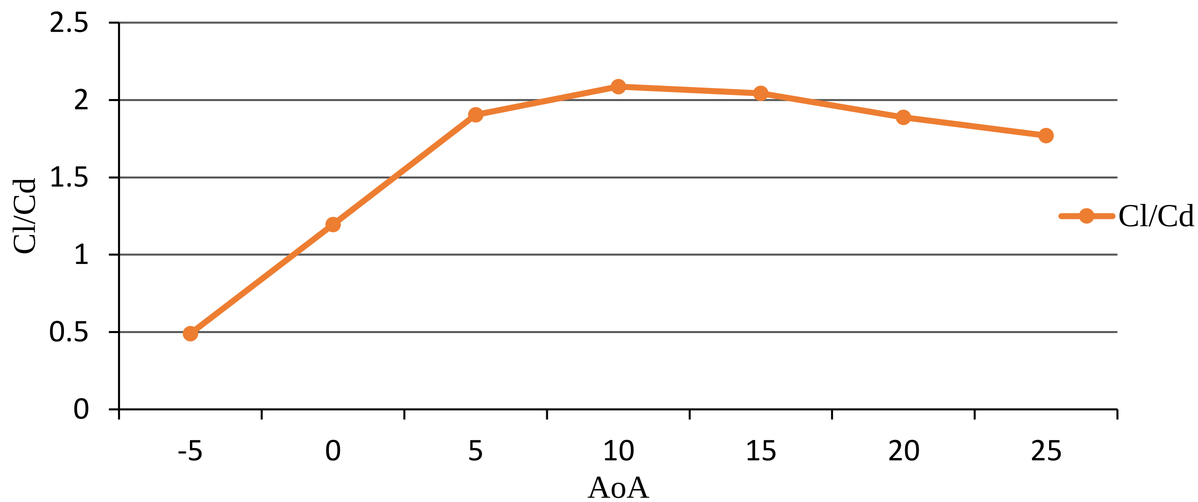

Figure 4-34 Grid independent test Cl/Cd of baseline

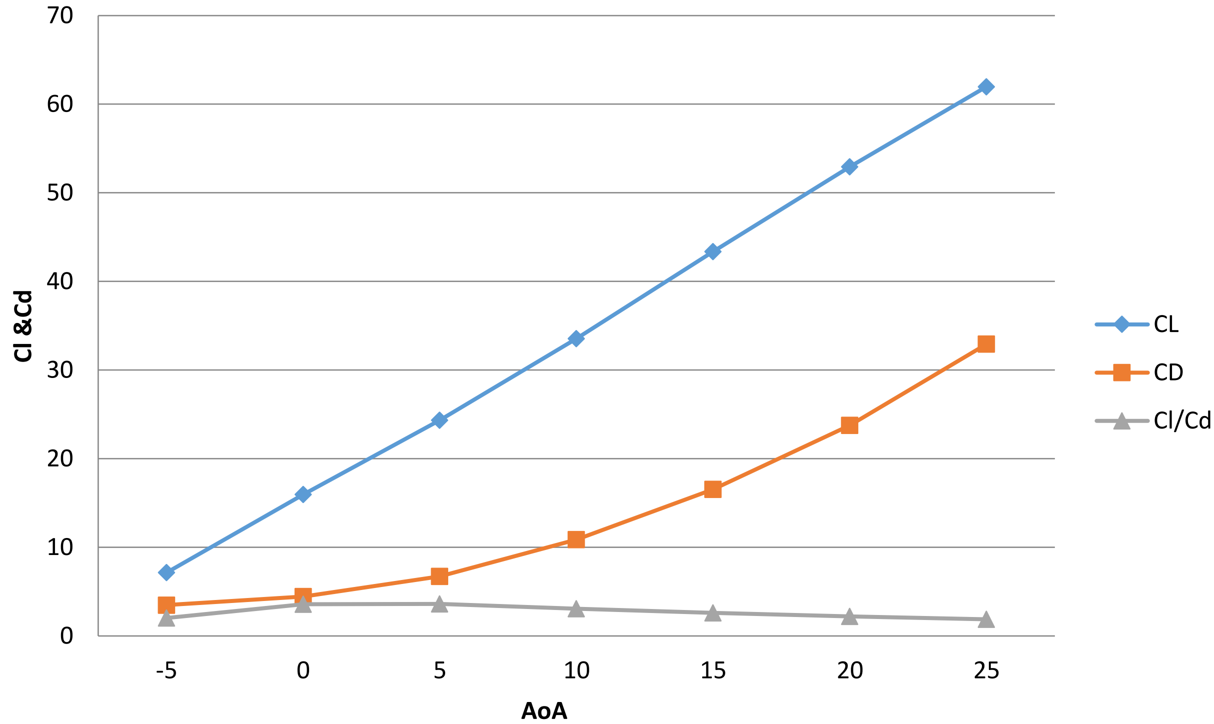

Figure 4-35 Blade with VG1

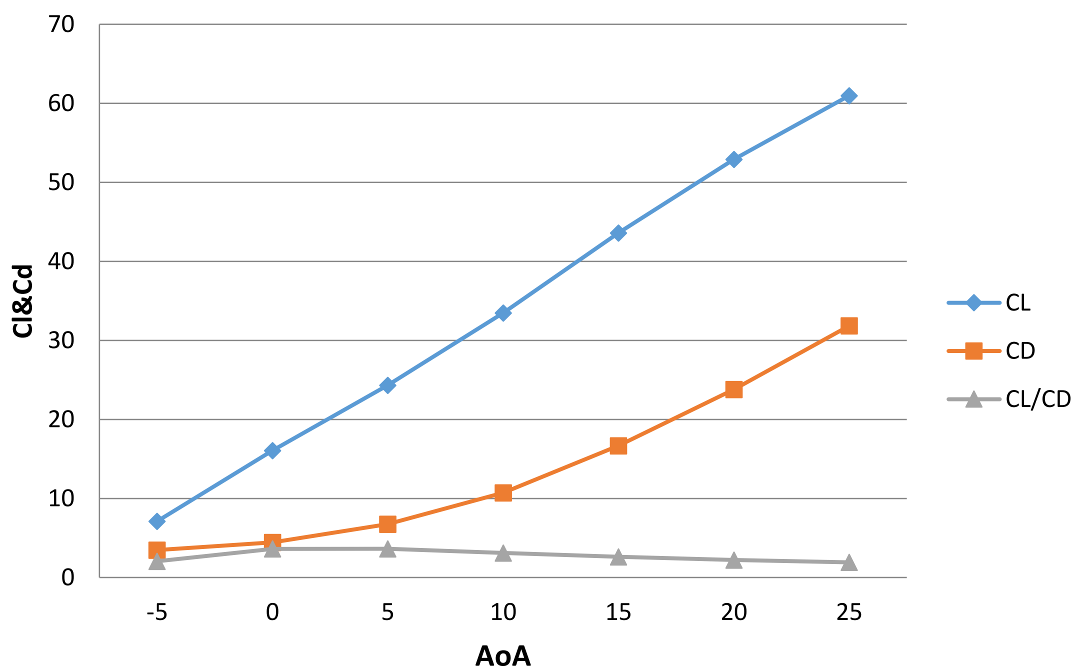

Figure 4-36 Blade with VG2

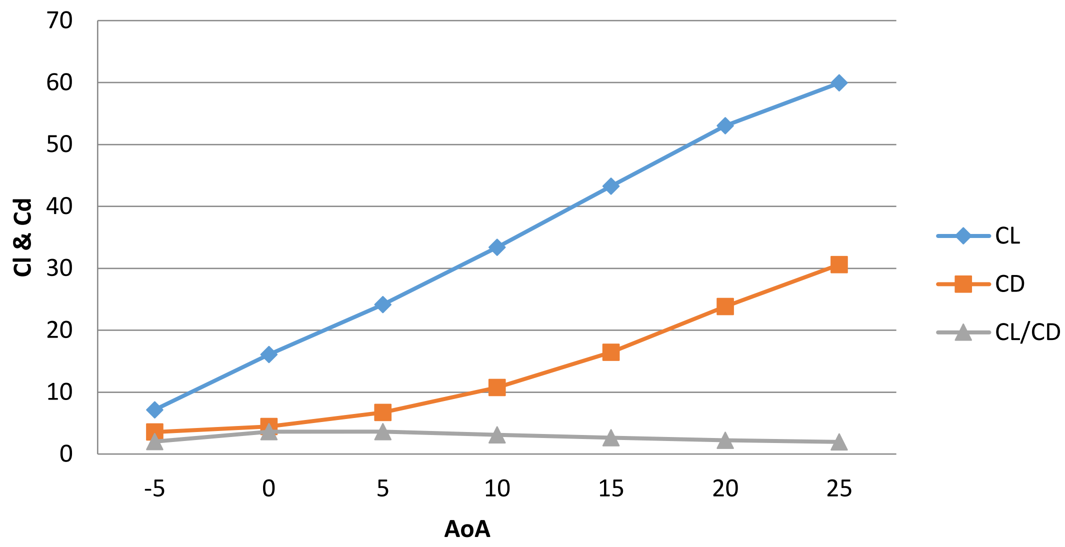

Figure 4-37 Blade with VG3

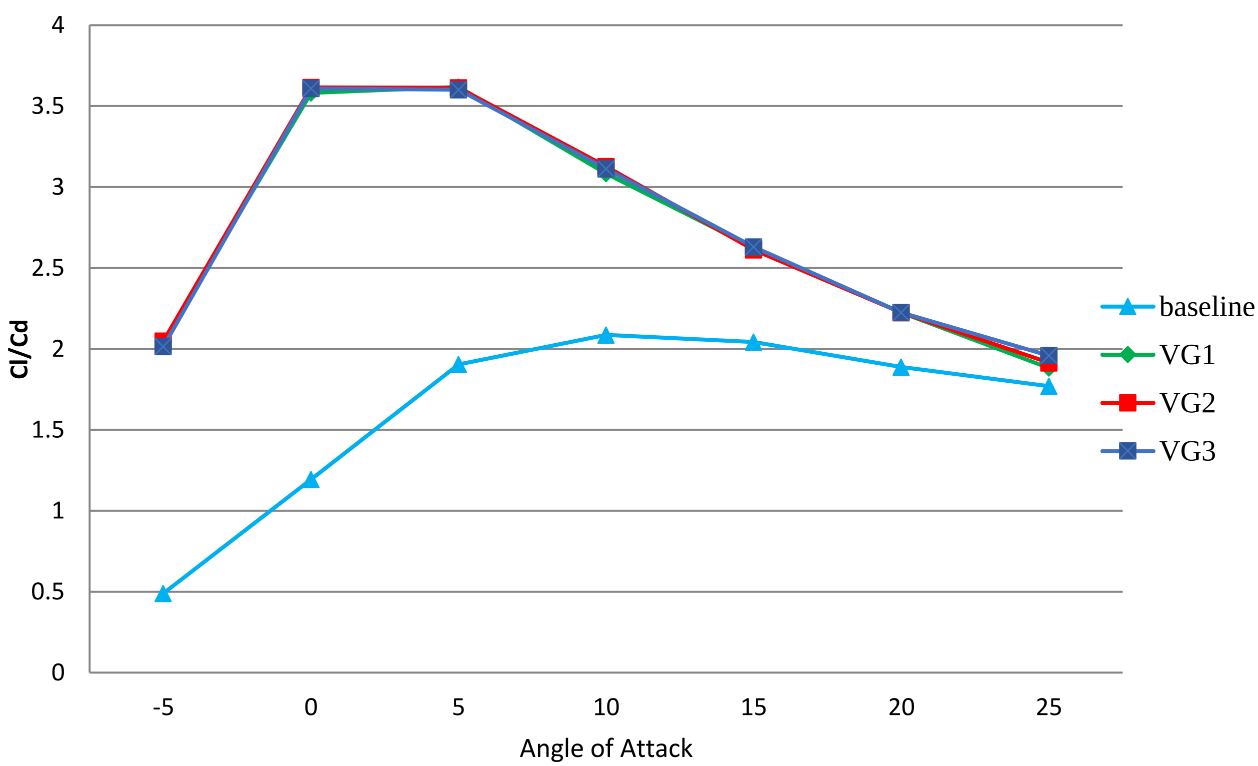

Figure 4-38 Comparisons of baseline blade and blade with Vortex generators Cl/Cd

4.2 Aerodynamic Characteristics of Blade with Vortex Generator

The vortex generator blade's aerodynamic performance was tested in six different positions with the same blade profiles at angles of attack of -5^0, 0^o, 5^o, 10^0, 15^o, 20^0, and 25^0. The flow conditions were the same as those of the baseline blade.

Based on the ratio of lift to drag coefficient, the baseline blade and the blade equipped with the vortex generator's aerodynamic performance were compared. From ANSYS, the blade with vortex generators' lift and drag coefficient numbers were taken. The appendix A.2 contains fluid results such as the baseline blade and the graphs.

4.2.1.1 At an Angle of Attack (AoA) of (-5^0)

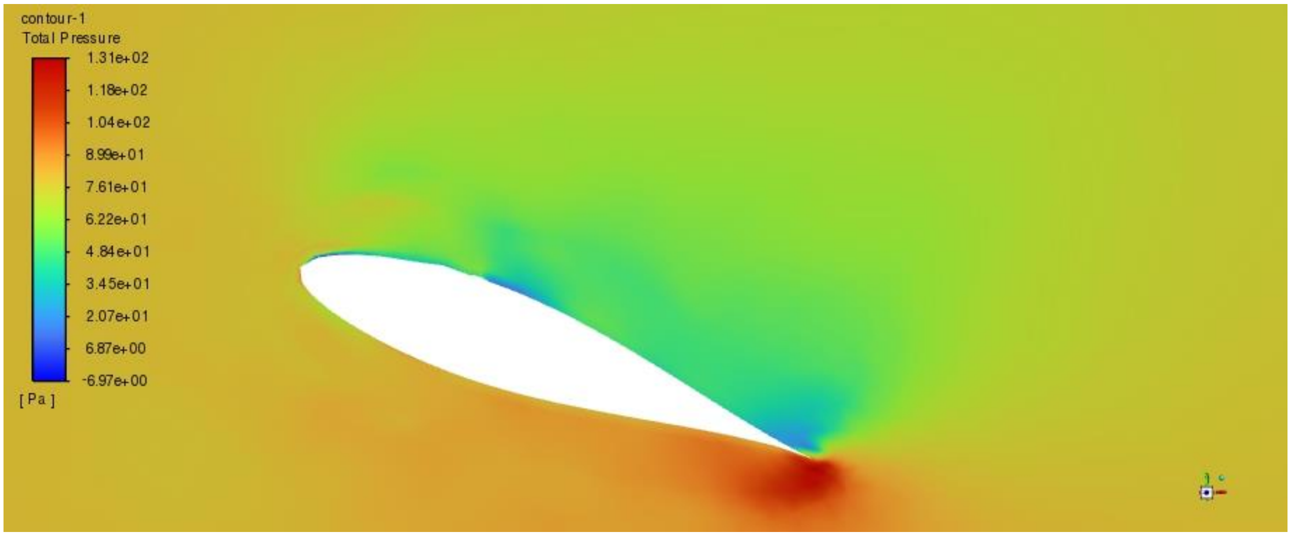

Figure 4-39 Suction Side and Pressure side Contour At α=-5^0

4.2.1.2 At an Angle of Attack (AoA) of (0^0)

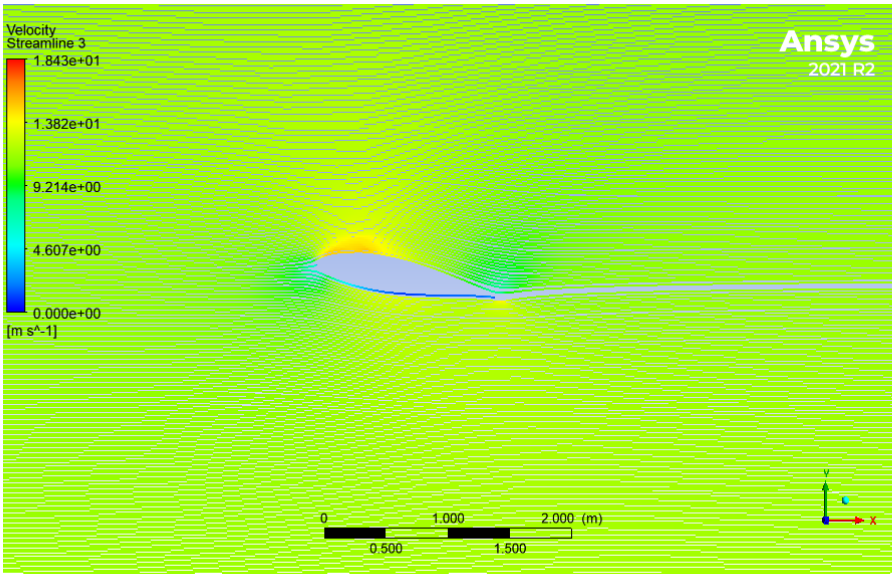

Figure 4-40 Blade with vortex generator At Velocity Streamline At $\alpha = 0^0$

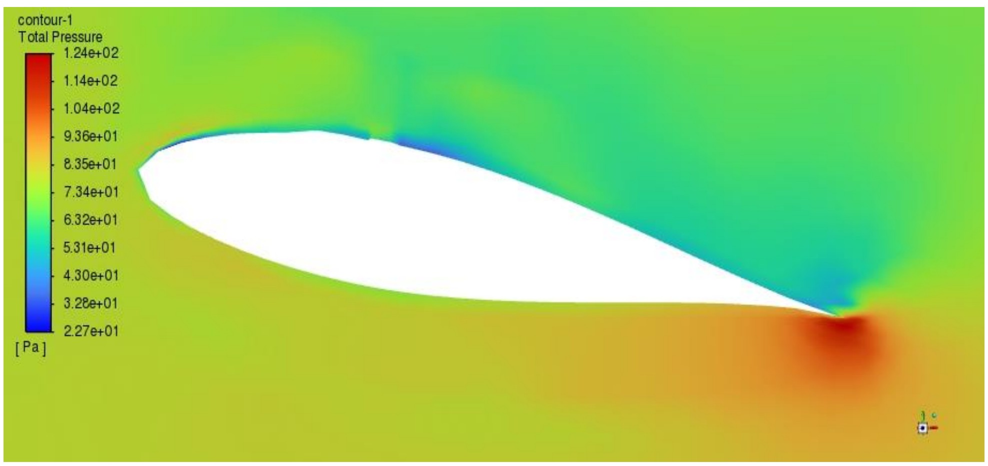

Figure 4-41 Suction Side and Pressure side Contour At $\alpha=0^0$

4.2.1.3 At an Angle of Attack (AoA) of (5^0)

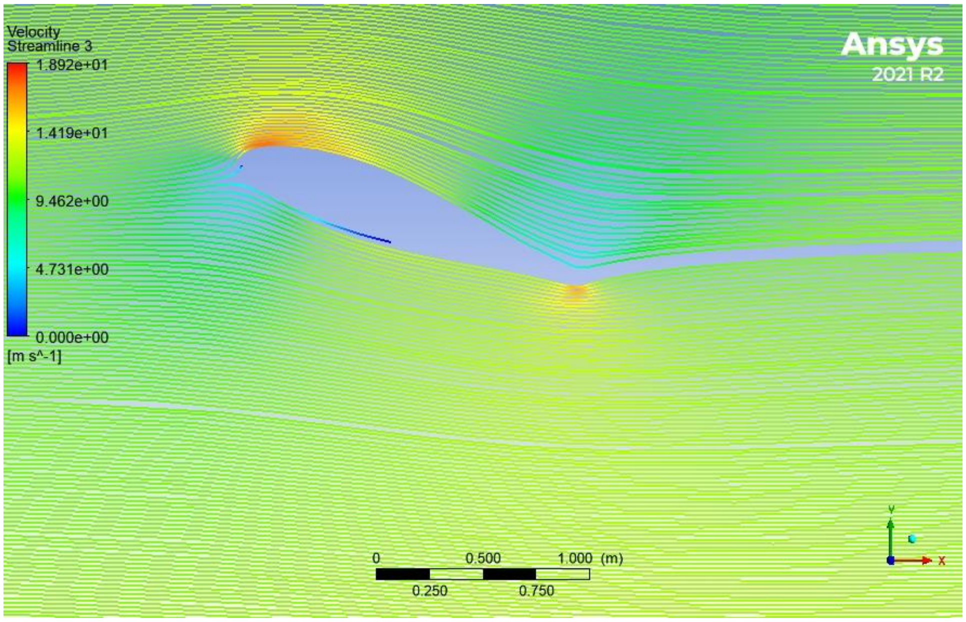

Figure 4-42 Velocity Streamline At $\alpha = 5^0$

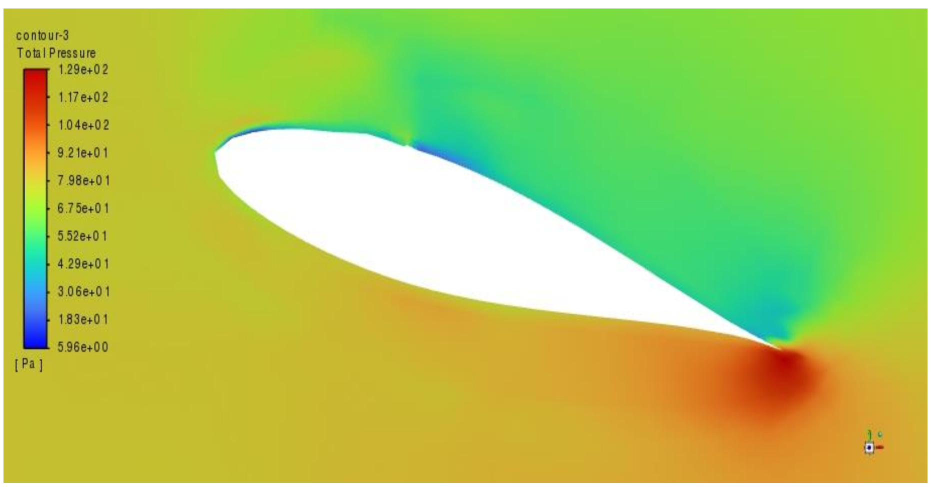

Figure 4-43 Pressure contour at $\alpha = 5^0$

4.2.1.4 At an Angle of Attack (AoA) of (10^0)

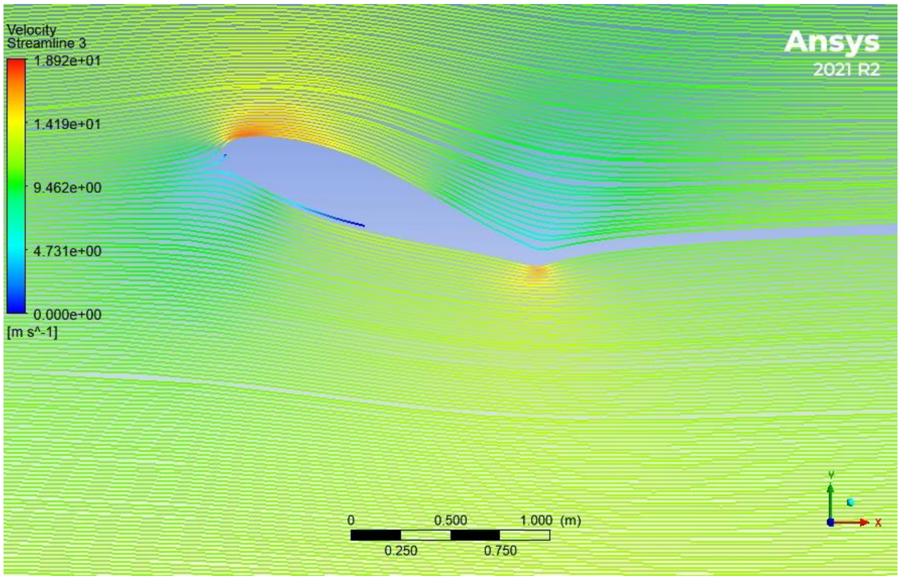

Figure 4-44 Velocity Streamline At $\alpha = 10^0$

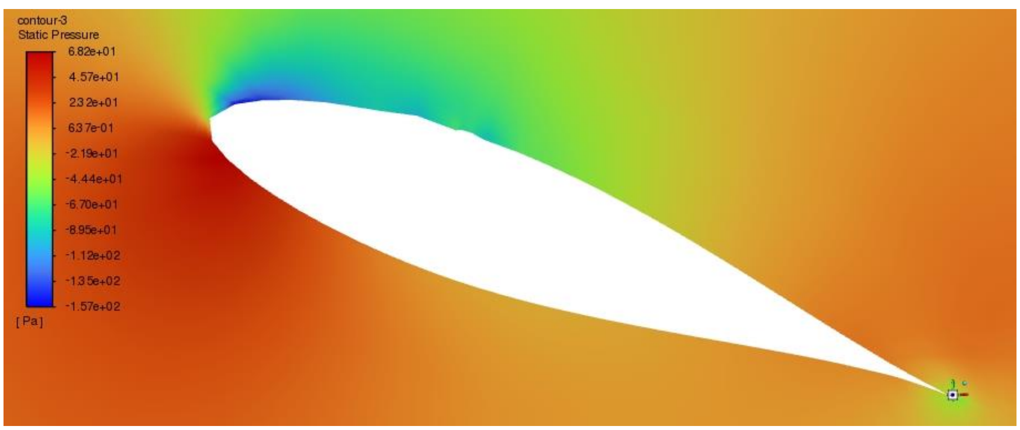

Figure 4-45 Pressure contour at $\alpha = 10^0$

4.2.1.5 At an Angle of Attack (AoA) of (15^0)

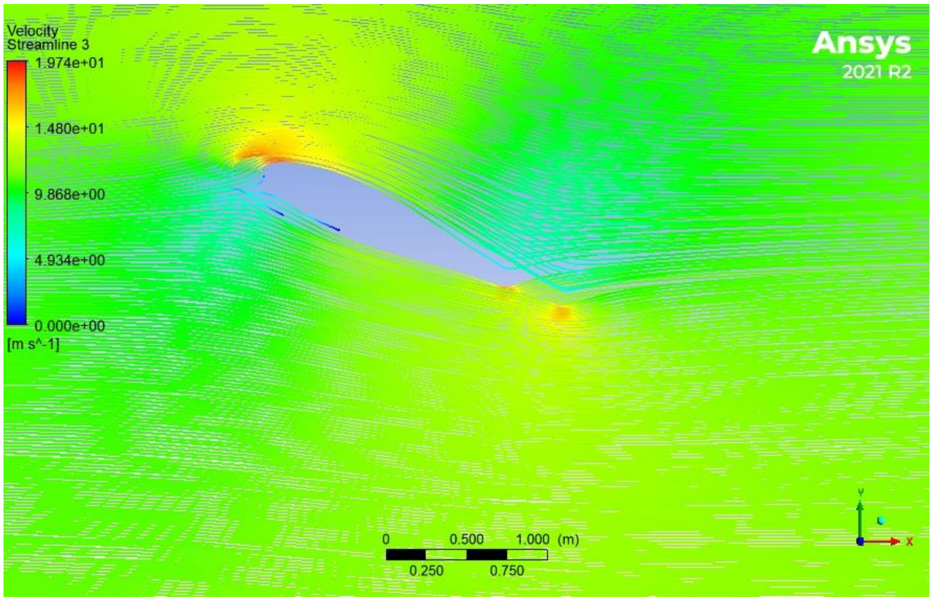

Figure 4-46 Velocity Streamline At α =15^0

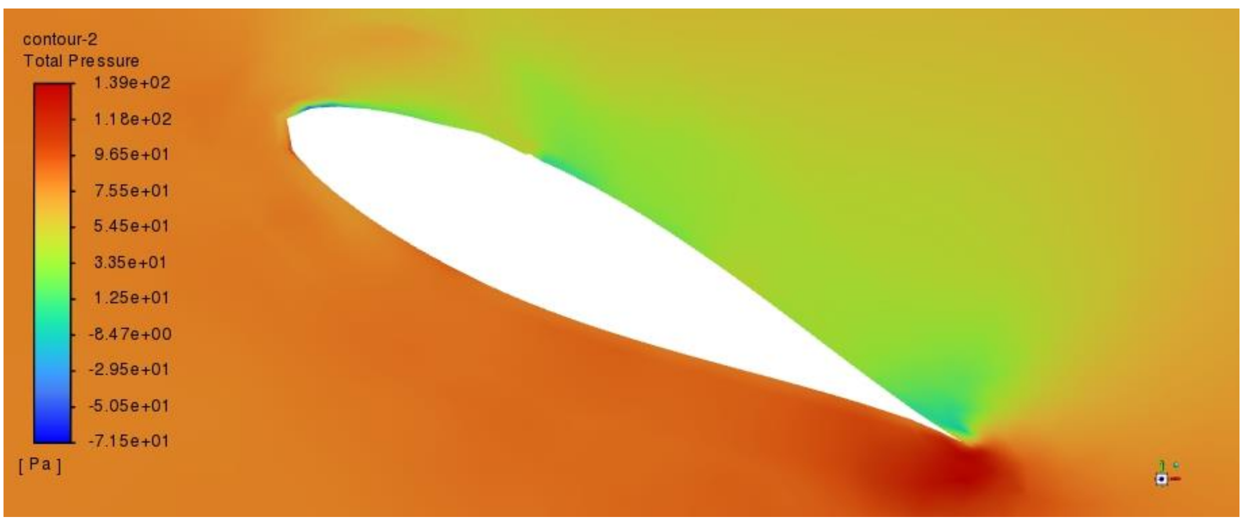

Figure 4-47 Pressure contour at α =15^0

Figure 4-48 Pressure contour at α =15^0

4.2.1.6 At an Angle of Attack (AoA) of (20^0)

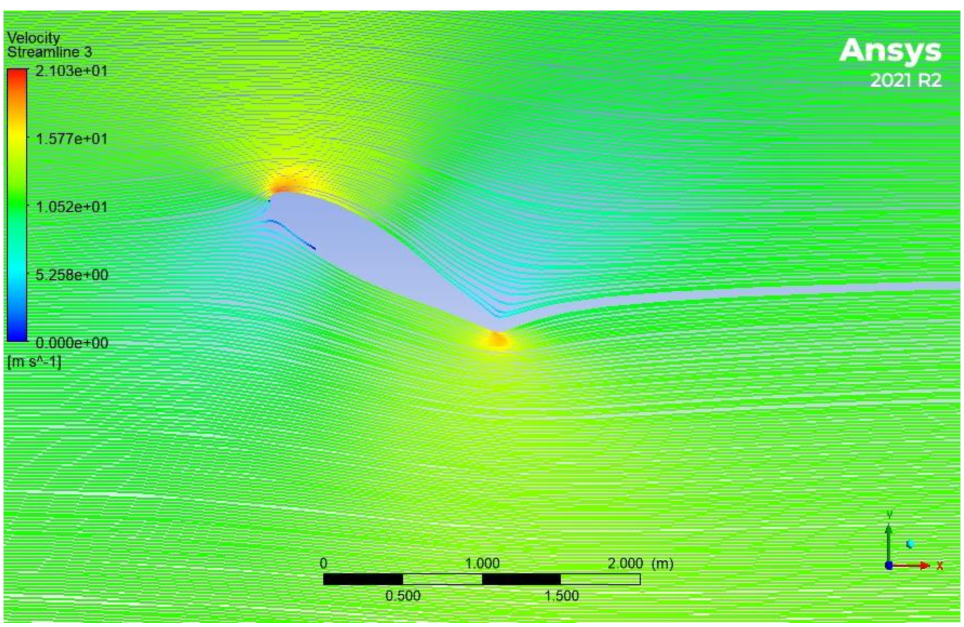

Figure 4-49 Velocity Streamline At α = 20^0

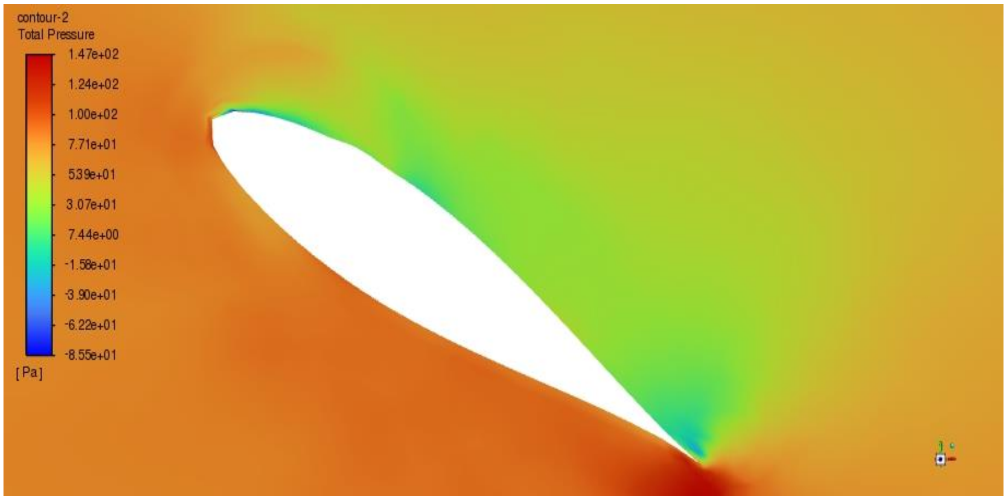

Figure 4-50 Pressure contour at α $=20^0$

4.2.1.7 At an Angle of Attack (AoA) of (25^0)

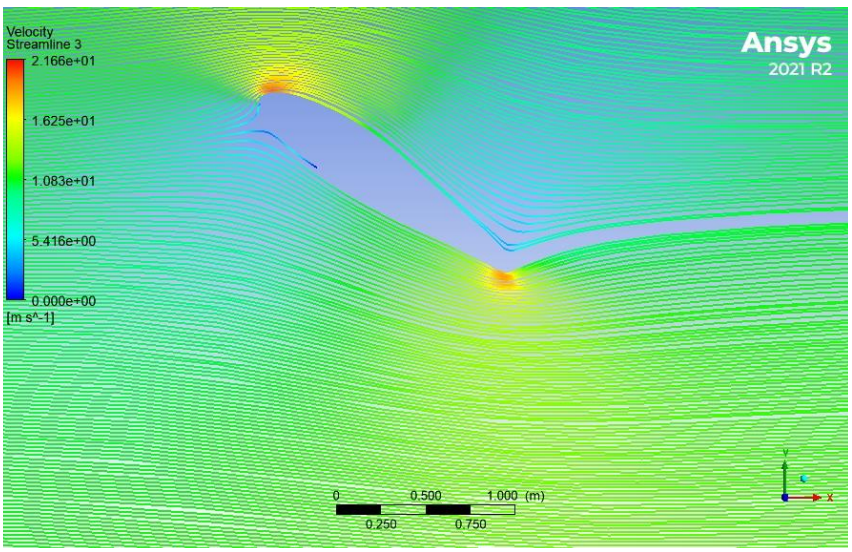

Figure 4-51 Velocity Streamline At α $=15^0$

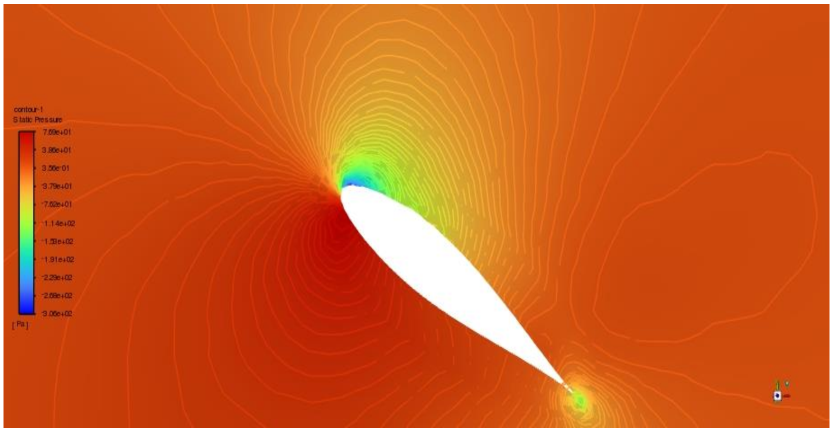

Figure 4-52 Pressure contour at $\alpha = 25^0$

In the above figures one possible cause of the behavior you see in ANSYS simulation results is a phenomenon known as flow separation. The airflow over the surface of an object, such as an airfoil, can alter when it encounters various angles of attack. The airflow may diverge from the surface at specific angles of attack, creating a low-pressure area behind the item. Variations in the pressure distribution across the object's surface may result from this flow separation.

The pressure distribution on the blade surface is changed with vortex generators, which can produce vortices. Usually, they can aid in postponing the boundary layer's separation, which lowers drag and may even increase lift. Pressure contours would display changes in the blade's surface pressure distribution, possibly resulting in fewer low-pressure areas behind the vortex generators and more uniform pressure gradients all around.so the above figures adding on VG on blade surfaces pressure contour. Because of the delayed flow separation and more even pressure distribution across the blade surface, the pressure suction side peaks are less noticeable. Therefore, adding to the vortex generators' blade surfaces aids in preserving the connected flow and lessening the intensity of the divided flow areas.in the above figures fluid or air flows on blade with VG velocity stream can be mixed and altered with vortex generators. There areas of greater turbulence behind the vortex generators, which postponing flow separation. When compared to the absence of vortex generators, the velocity streamlines were exhibit less separation and smoother flow patterns overall. Less separation and smoother flow patterns were seen in the velocity A blade surface's aerodynamic performance may be enhanced by the addition of a vortex generator, such as a winglet or vortex generator tab, especially at greater angles of attack. By energizing the boundary layer and delaying separation, these devices are intended to decrease drag and increase the lift-to-drag ratio. A blade with a vortex generator is likely to stall later than a blade without one at an angle of attack of 5^0. This implies that the blade equipped with the vortex generator can sustain elevated lift coefficients before stalling, which could lead to an increase in lift-to-drag ratios. In comparison to a blade with a vortex generator, a blade without one may reach its maximum lift coefficient earlier, resulting in an earlier stall and a poorer lift-to-drag ratio. Streamlines, especially close to the leading edge and over the suction side of the blade.

Table 7 Pressure contour and Velocity stream of blade with VG

AOA (^{0})	velocity stream m/s	Pressure(pa)
-5	18	131
0	16.22	124
5	17.99	129
10	18.92	68.2
15	19.74	139
20	21.03	147
25	21.66	76.9

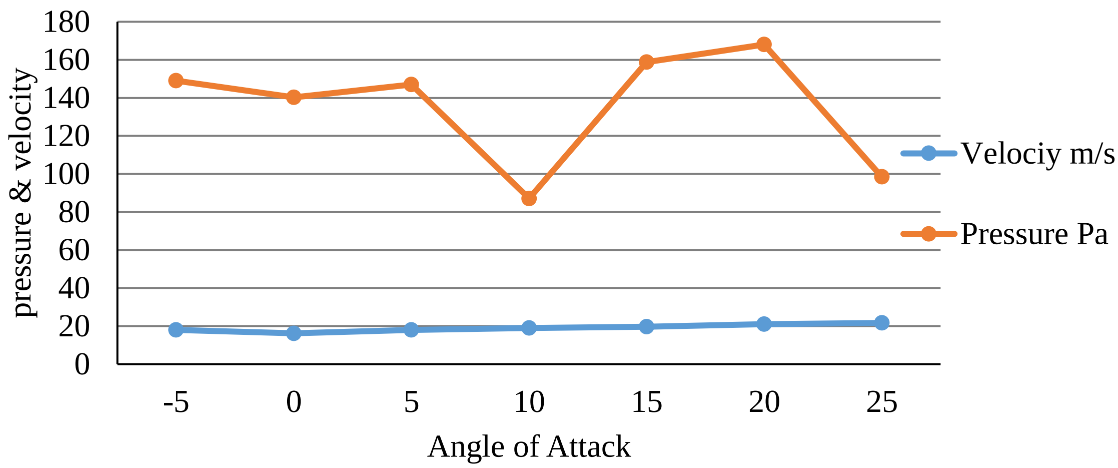

Figure 4-53 Velocity stream and pressure contour of VG with Blade

4.3 Performance Improvement on the Wind Turbine baseline blade with VG

The previous section covered an aerodynamic performance analysis and comparison based on the angle of attack to determine which blade with VG1 performed better than the baseline blade. This section compares the baseline blade based on varying wind speeds with the best-performing blade with vortex generator orientation 1 (blade with VG1). The test was run at 5m/s, 8m/s, 11.5m/s,15m/s and 19m/s at a 5^0 AoA. The results showed that the blade with VG1 performed best at 5^0 AoA. As wind speed increases, the lift-to-drag coefficient ratio rises for both the baseline and VG1 blades. Additionally, at all wind velocities, the blade with VG1 has a greater lift-to-drag coefficient ratio than the baseline blade. So, on average wind speed at 11.5m/s the maximum lift-to-drag ratio on base line at AoA 10^0 is 2.08654, but on VG1 at 5^0 the maximum lift-to-drag ratio is 3. 61838.It means adding vortex generator on blade surface enhance performance due to Cl/Cd ratio increment.

4.4 Numerical Validation

There are two methods often used to delay the flow separation over an aerofoil which are the active and the passive method, to enhance the overall efficiency of an aerofoil. The methods for active flow control require energy expenditure and may consist of one or more moving parts mounted on the body of the aerofoil. So basically, to validate vortex generator with dimple adding on the blade surfaces.

On this thesis the CFD work the aerodynamic effect of vortex generator on wind turbine surface of NACA63-218 wind turbine airfoil. On average wind speed at 11.5m/s the maximum lift-to-drag ratio on base line at AoA 10^0 is 2.08654, but on VG1 at 5^0 the maximum lift-to-drag ratio is 3. 61838.It means adding vortex generator on blade surface enhance performance due to Cl/Cd ratio increment.

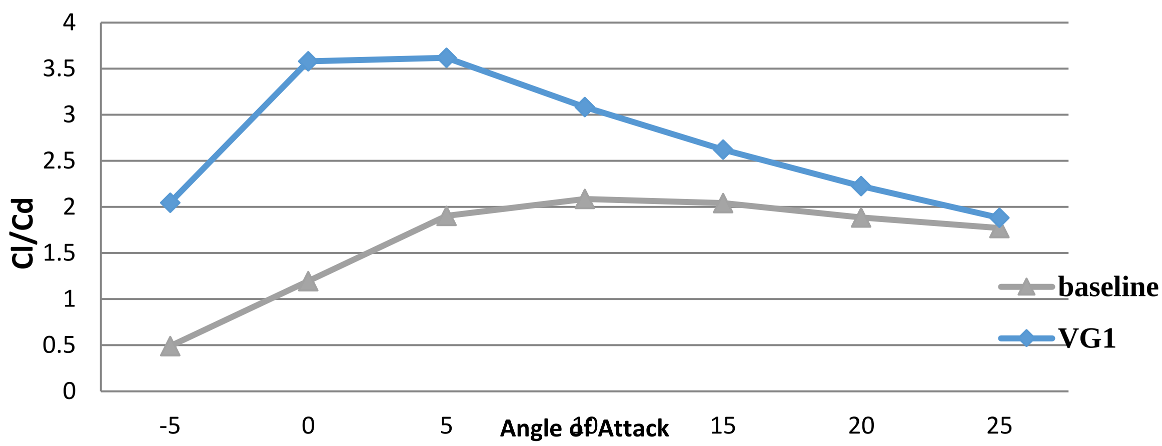

Figure 4-54 Cl, Cd &Cl/Cd of baseline and Vortex generator

Likewise, the aerodynamic effect of dimple on wind turbine surface of S830 wind turbine airfoil. Different experiment by varying the wind speed is carried and the results were also increase lift to drag force as shown below graphs. (Gedion Fikade et.al; 2019)

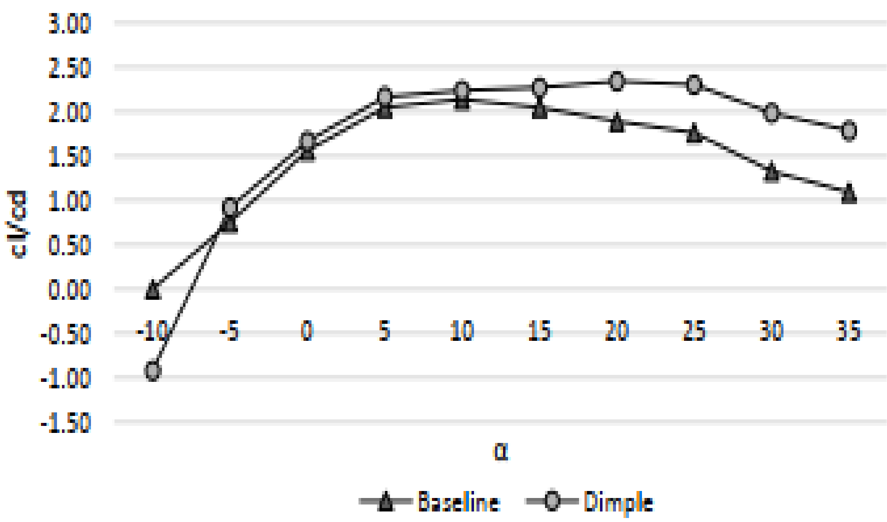

Figure 4-55 Aerodynamic performance comparison of Baseline &Dimpled S830. (Gedion Fikade et.al; 2019)

Eventually hence all flow separation control methods reveal that surface vortex or dimple enhance the aerodynamic performance it’s possible to say the computational fluid dynamics analysis results which claims vortex generator enhance aerodynamic performance is valid.

CHAPTER FIVE

CONCLUSIONS AND RECOMMENDATIONS

5.1. Conclusions

This thesis concentrated on investigating the aerodynamic effect of vortex generators on wind turbine blades, and enhancing the aerodynamic performance of wind turbines at Adama II Wind Turbine Oromia, Ethiopia.

In order to assess the aerodynamic performance impact of adding a triangular vortex generator to the surface of turbine blades, tests were conducted on Adama II wind turbine blades profiles both with and without the vortex generator. These tests were carried out with the understanding that lowering blade vortex separation a source of drag is one method of enhancing a wind turbine's aerodynamic performance.

The following conclusions can be drawn from the results of this investigation.

K-ω SST turbulence model was used to assess the planned blade's aerodynamic performance. The blade with VG performs at its best aerodynamically at an AOA of 5°. Assuming that 1.5 MW of power can be extracted, the wind turbine blade design must achieve the principle of Betz limit. At an angle of attack greater than 10^0, flow separation happens on the baseline blade's pressure side. This unfavorable phenomenon will reduce the turbine's efficiency. But when VG's add on blade surface has better enhance aerodynamic performance than baseline because the lift-to-drag ratio is better on VG's add on blade surface than baseline. So ADAMA II wind turbine get better and enhance aerodynamic performance adding VG's on blade surface at AoA 5^0 by the vortex generator arrangement (VG1).

5.2. Recommendation

- Wind turbine blades include numerous add-on devices to improve their aerodynamic performance. It is advised that future research examine if the add-on devices are appropriate for wind turbine blades.
- Aero acoustics and aero elastic effects of vortex generators on wind turbines are being investigated.
- There are many methods or approaches but, on this research, it is enough to uses the RANS (k-ω SST turbulence model) approach used to carry out the investigation; however, for more accuracy,
- Only one kind of aerofoil profile for a vortex generator was studied in this study. Investigate the impact of an increased vortex generator's aerofoil profile in the next research.

References

Ashill, P., Fulker, J., & Hackett, K. (2001, January 8). Research at DERA on sub boundary layer vortex generators (SBVGs). 39th Aerospace Sciences Meeting and Exhibit. https://doi.org/10.2514/6.2001-887

Endalamaw, R. S. (2023). Identifying and Analyzing the Technical Challenges of Grid Tide Inverters for PV System: A Case Study of Ethiopia and Zambia. Journal of Energy Research and Reviews, 14(3), 9–39. https://doi.org/10.9734/jenrr/2023/v14i3284

Fouatih, O. M., Imine, B., & Medale, M. (2019). Numerical/experimental investigations on reducing drag penalty of passive vortex generators on a NACA 4415 airfoil. Wind Energy, 22(7), 1003–1017. https://doi.org/10.1002/we.2330

Frankton C. (2022). Adama I and Adama II Wind Power Projects.

Hares, H., Mebarki, G., Brioua, M., & Naoun, M. (2019). Aerodynamic performance improvement of NACA 4415 profile by passive flow control using vortex generators. Journal of the Serbian Society for Computational Mechanics, 13(1), 17–38. https://doi.org/10.24874/jsscm.2019.13.01.02

Lin, J. C. (2002). Review of research on low-profile vortex generators to control boundary-layer separation. Progress in Aerospace Sciences, 38(4–5), 389–420. https://doi.org/10.1016/S0376-0421(02)00010-6

Moon, H., Jeong, J., Park, S., Ha, K., & Jeong, J.-H. (2023). Numerical and experimental validation of vortex generator effect on power performance improvement in MW-class wind turbine blade. Renewable Energy, 212, 443–454. https://doi.org/10.1016/j.renene.2023.04.104

Permatasari, R., & Widyawati, G. (2023). Effect of Vortex Generators on Airfoil NACA 632-415 to Aerodynamic Characteristics Using CFD. International Journal of Electrical, Energy and Power System Engineering, 6(1), 133–137. https://doi.org/10.31258/ijeepse.6.1.133-137

Yan, Y., Avital, E., Williams, J., & Cui, J. (2019). CFD analysis for the performance of micro-vortex generator on aerofoil and vertical axis turbine. Journal of Renewable and Sustainable Energy, 11(4). https://doi.org/10.1063/1.5110422

Zhu, C., Wang, T., Chen, J., & Zhong, W. (2020). Effect of Single-Row and Double-Row Passive Vortex Generators on the Deep Dynamic Stall of a Wind Turbine Airfoil. Energies, 13(10), 2535. https://doi.org/10.3390/en13102535

Lamnaouer, M. (2010). Numerical modeling of the shock tube flow fields before and during ignition delay time experiments at practical conditions. University of Central Florida.

Kemenov, K. A., & Pope, S. B. (2011). Molecular diffusion effects in LES of a piloted methane–air flame. Combustion and Flame, 158(2), 240-254.

APPENDIX

A-1 Aerodynamic Properties of NACA 63(3)-218 airfoils

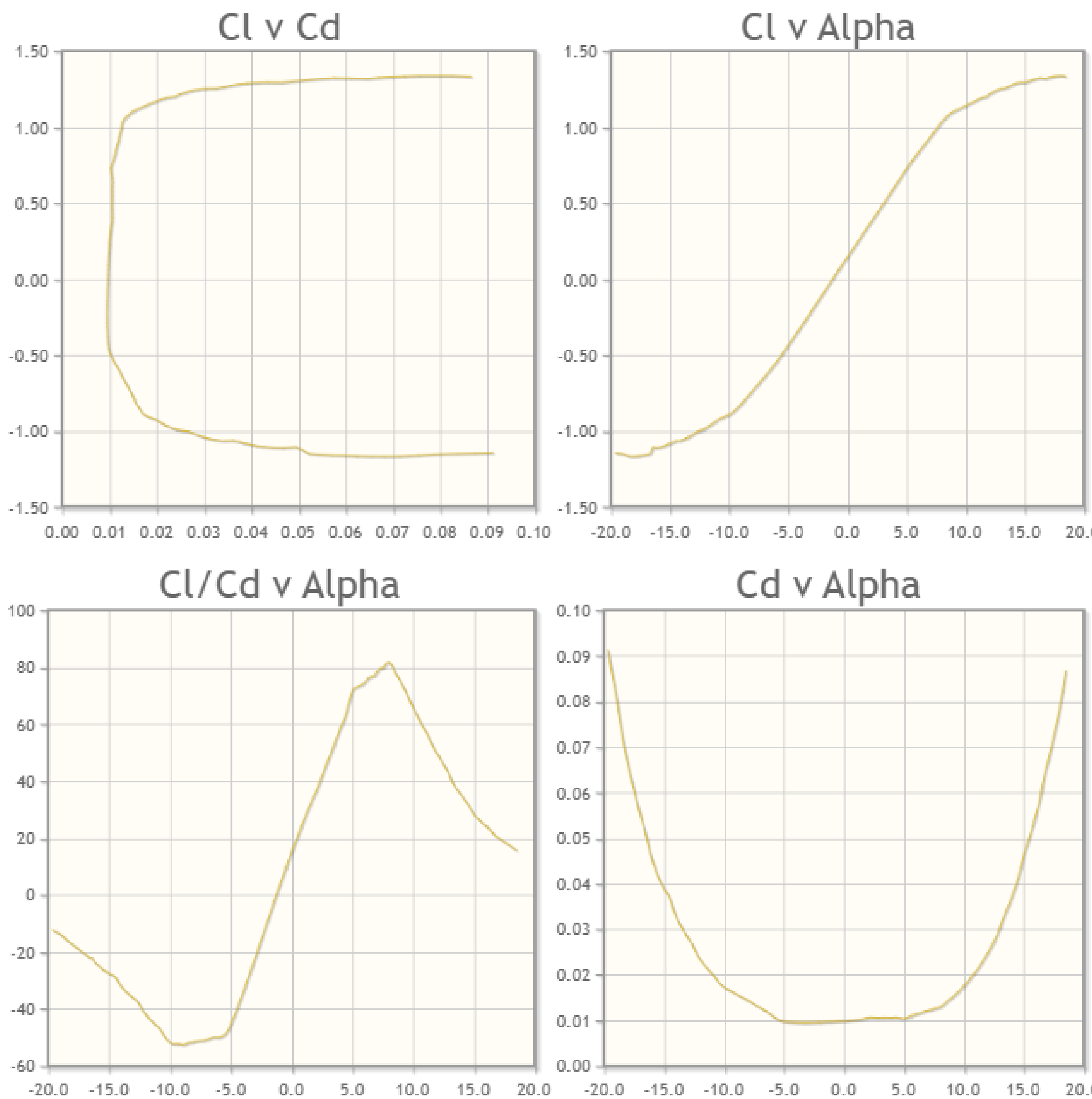

Figure: Aerodynamic Performance of NACA 63-218 airfoil (AirfoilTools.com, 2024))

A-2 ANSYS Fluent Lift and Drag Coefficient Result Plot

For baseline model

Lift coefficient

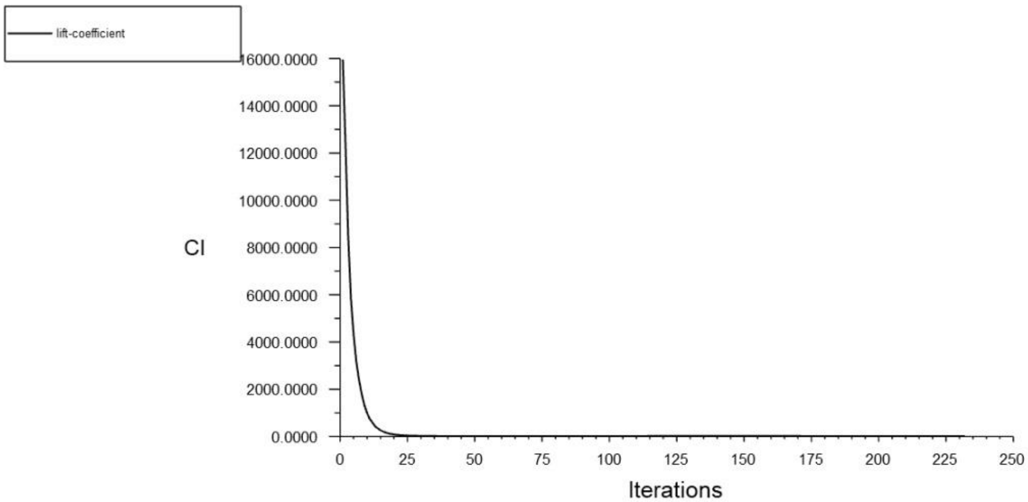

Fig Baseline lift coefficient at α= 0^0

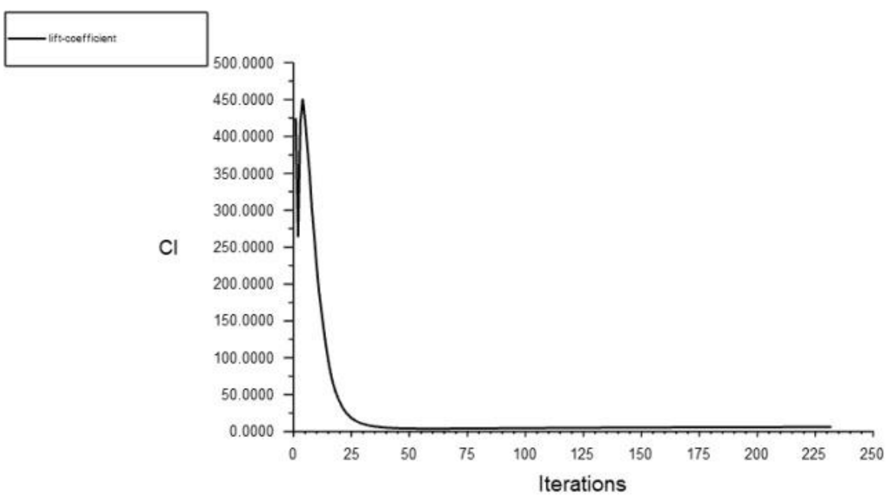

Fig Baseline lift coefficient at α= -5^0

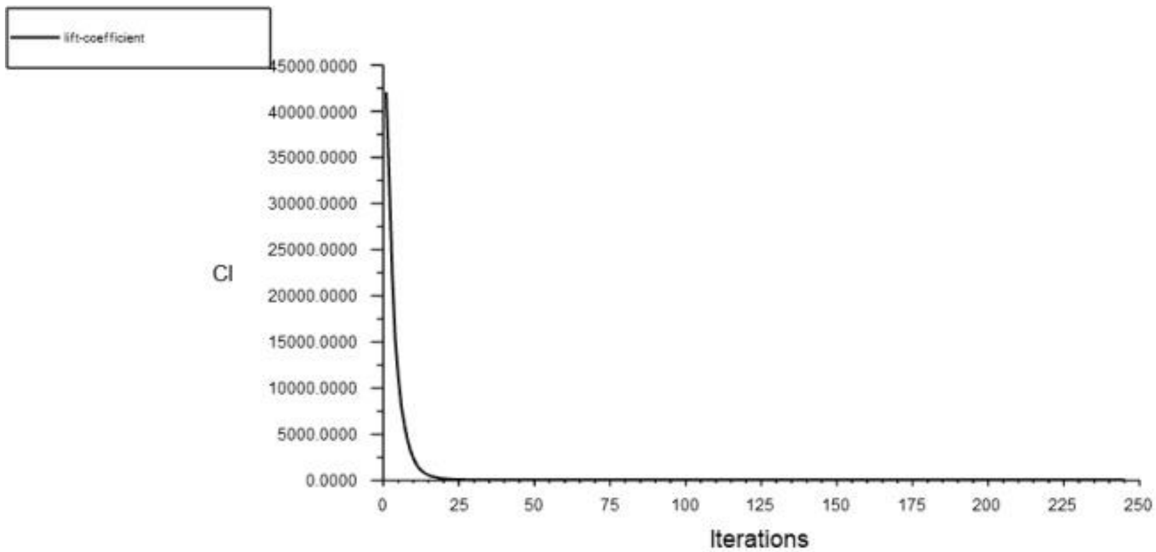

Fig Baseline lift coefficient at α= 10^0

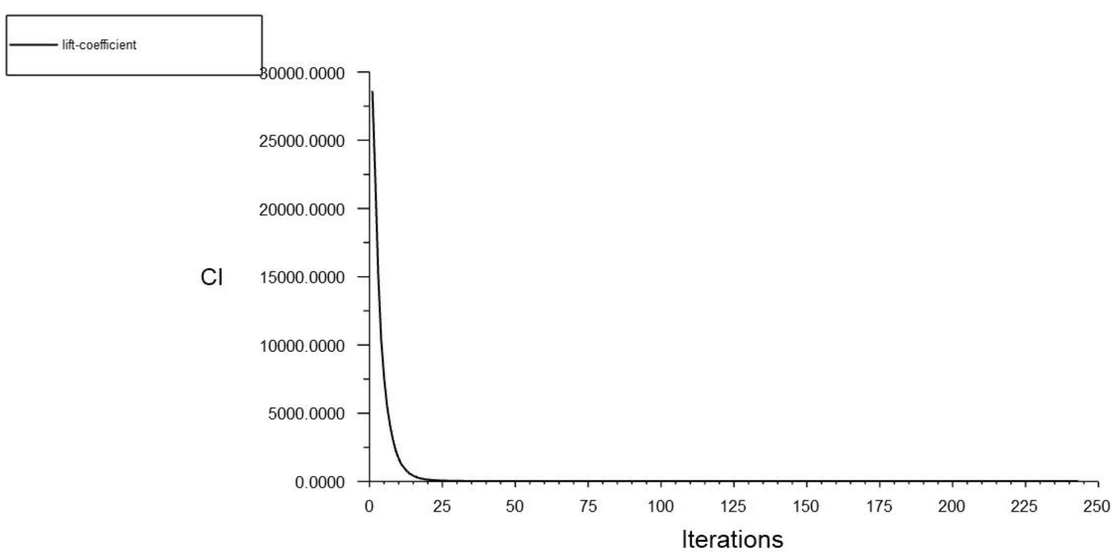

Fig Baseline lift coefficient at α= 5^0

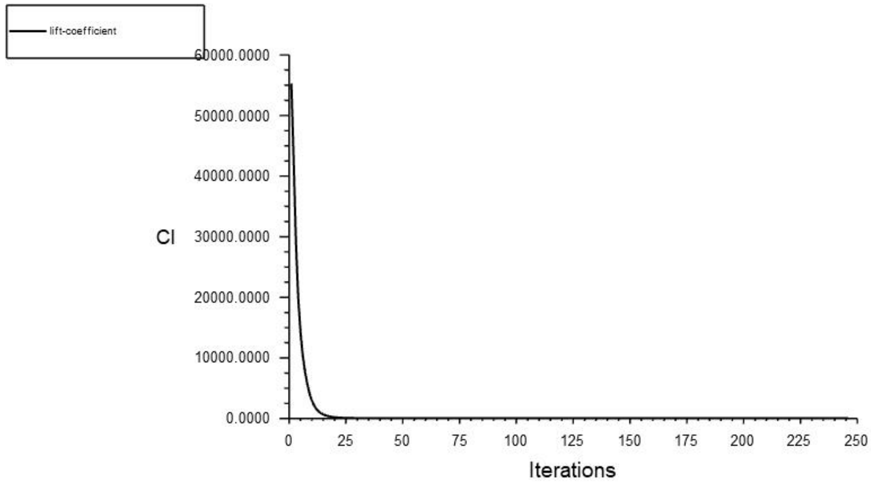

Fig Baseline lift coefficient at α= 15^0

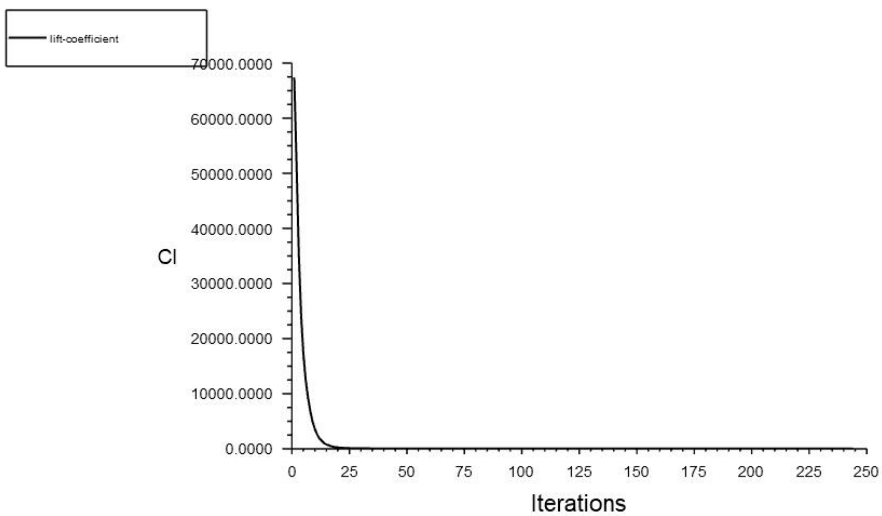

Fig Baseline lift coefficient at α= 20^0

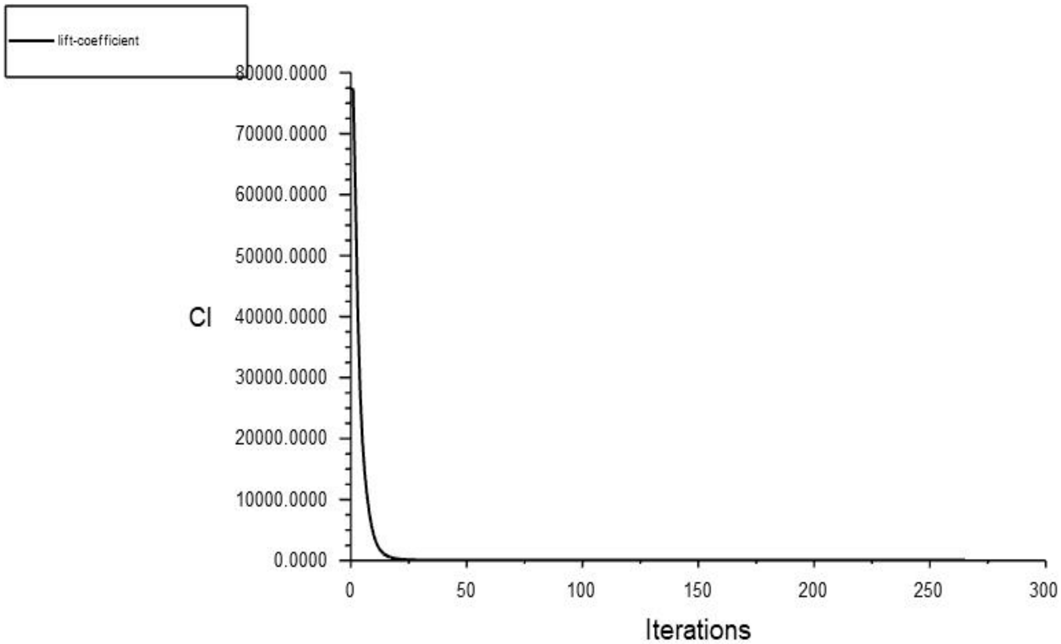

Fig Baseline lift coefficient at α= 25^0

Drag coefficient

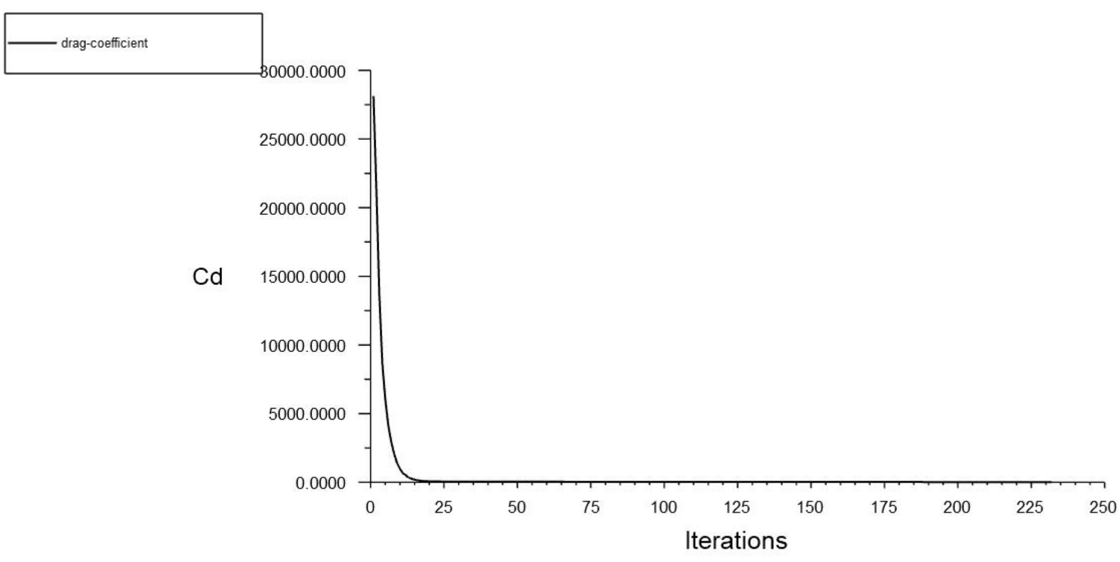

Baseline drag coefficient at α= 0^0

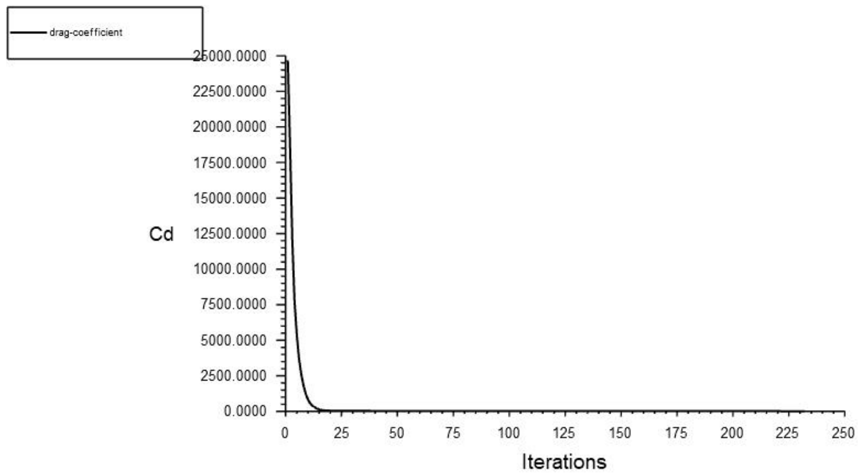

Fig Baseline drag coefficient at $\alpha = -5^0$

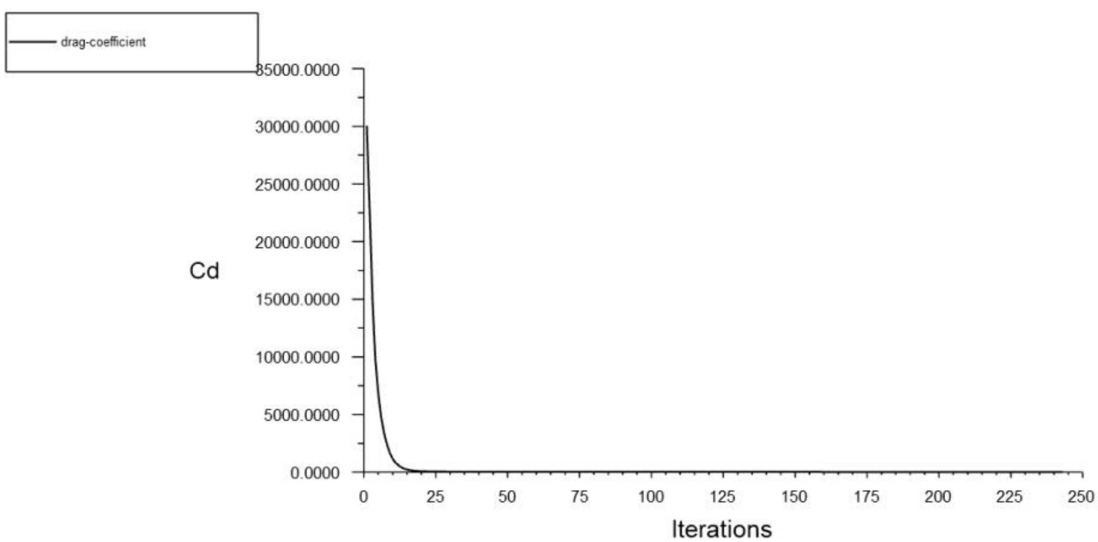

Fig Baseline drag coefficient at $\alpha = 5^0$

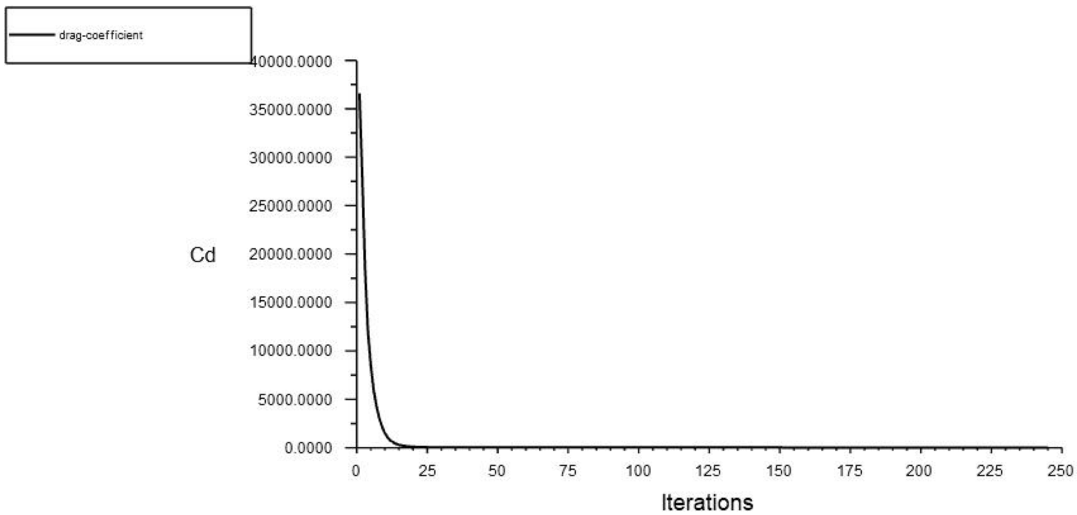

Fig Baseline drag coefficient at $\alpha = 10^0$

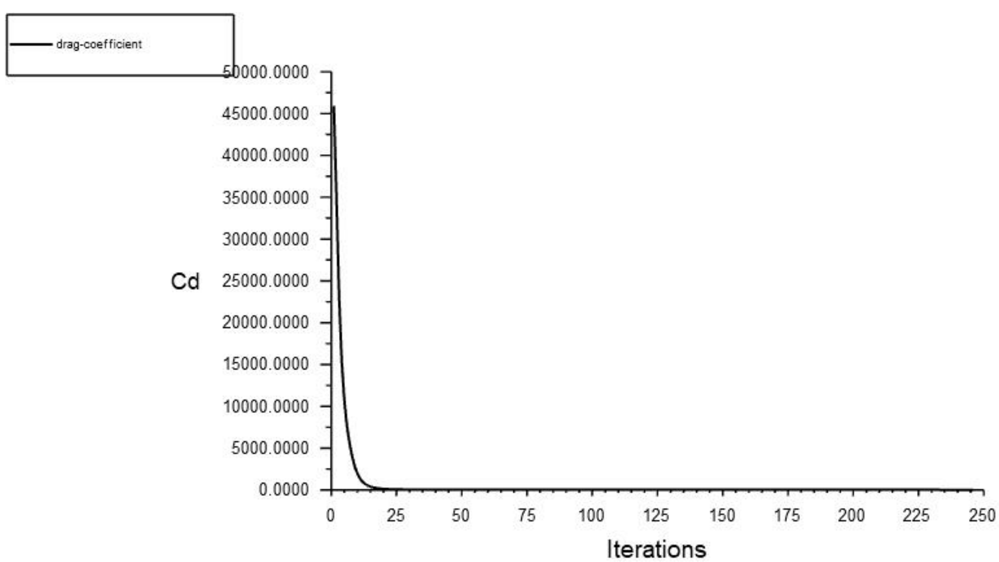

Fig Baseline drag coefficient at $\alpha = 15^0$

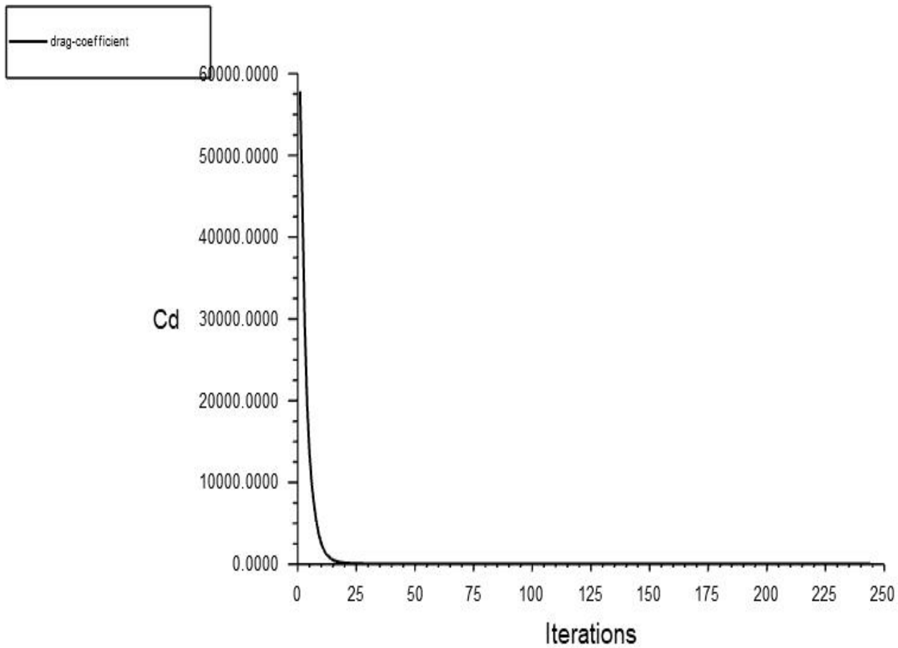

Fig Baseline drag coefficient at α= 20^0

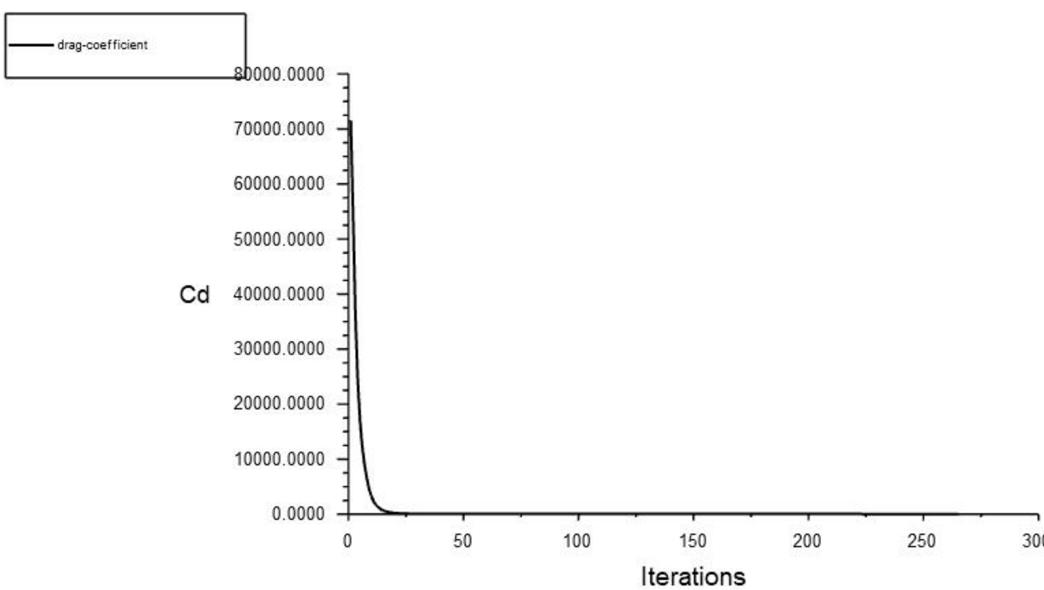

Fig Baseline drag coefficient at α= 25^0

Blade with vortex generator

Blade Lift Coefficient

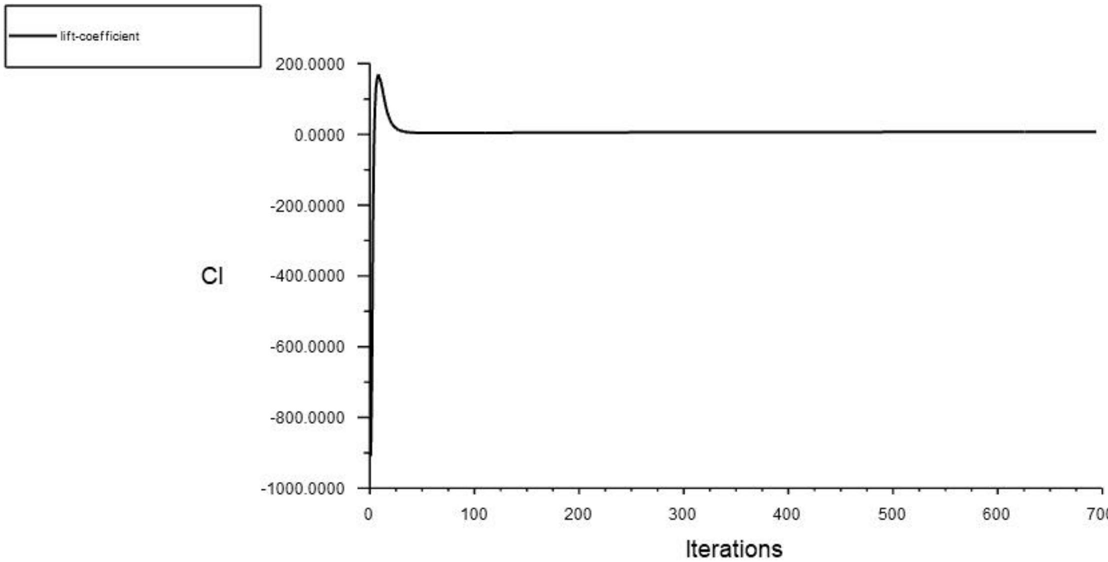

Fig VG orientation one α= -5^0

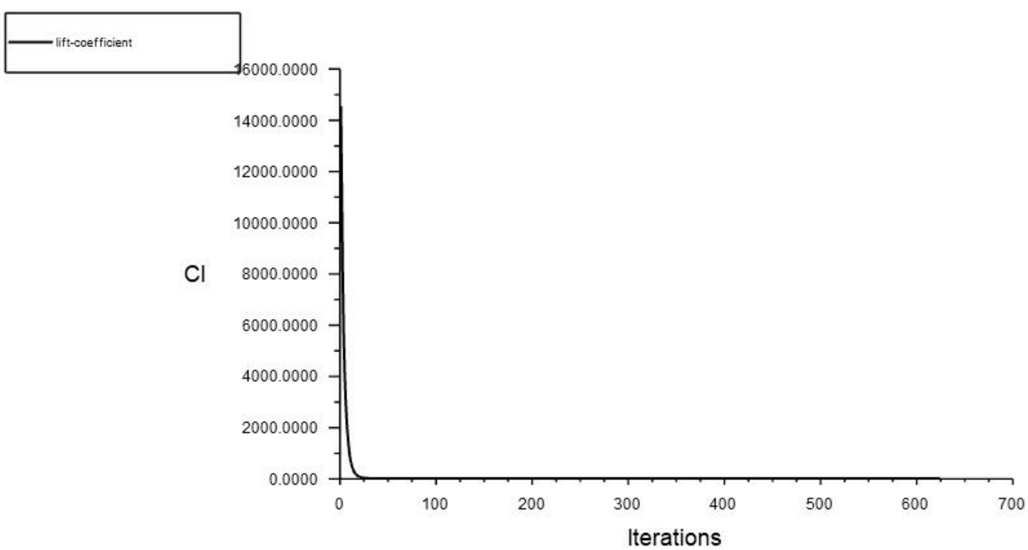

Fig VG orientation one α= 0^0

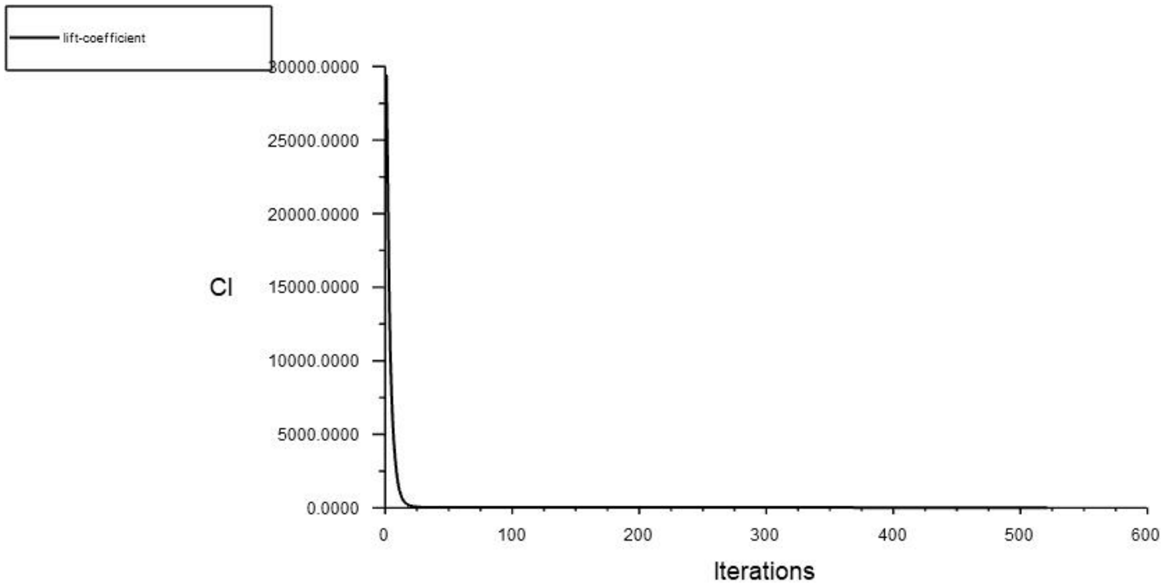

Fig VG orientation one α= 5^0

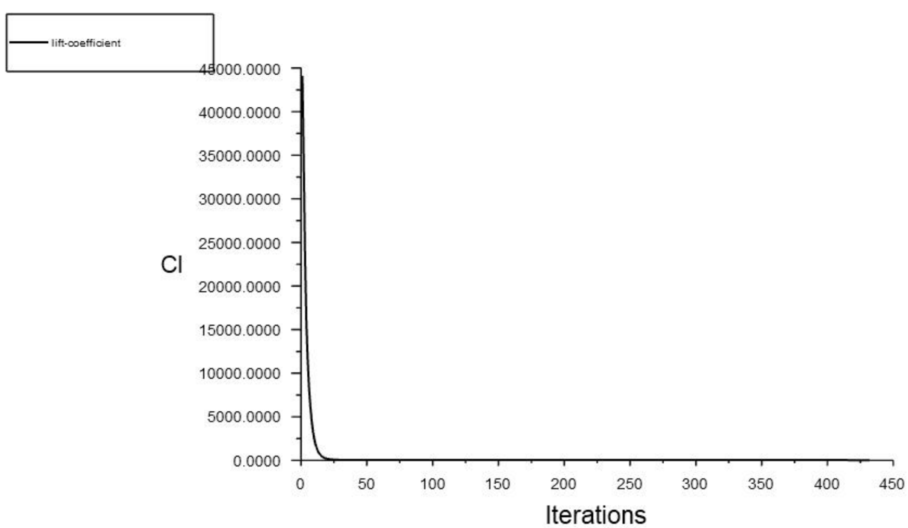

Fig VG orientation one α= 10^0

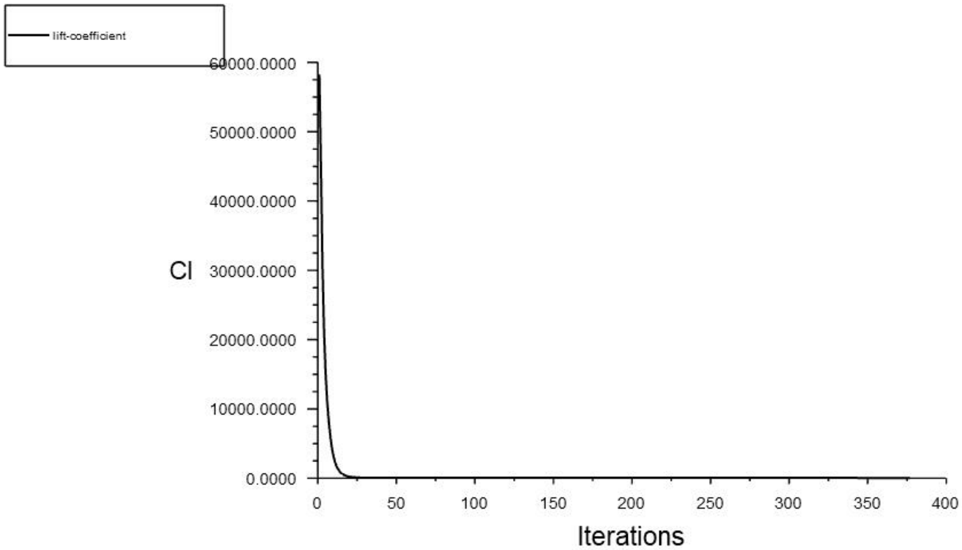

Fig VG orientation one α= 15^0

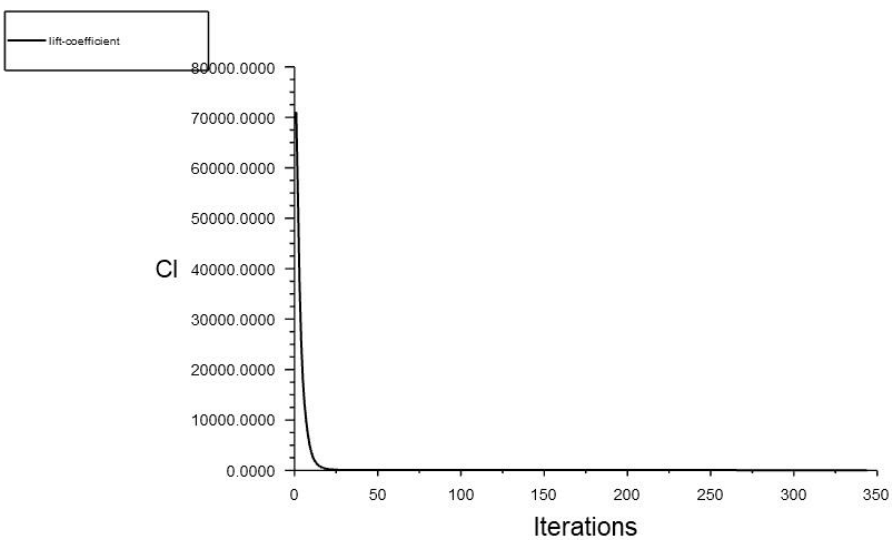

Fig VG orientation one α= 20^0

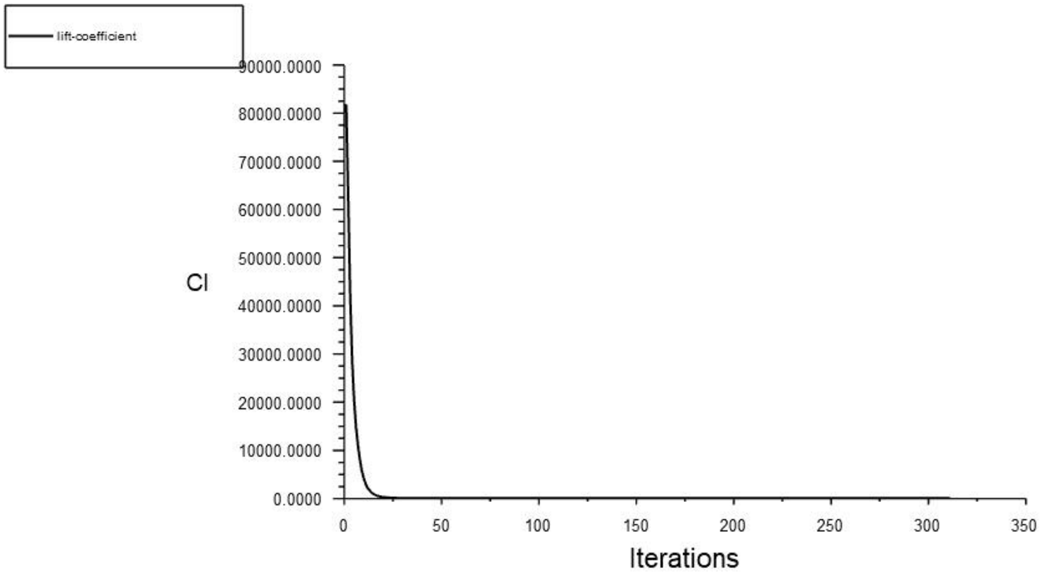

Fig VG orientation one α= 25^0

Blade drag coefficient

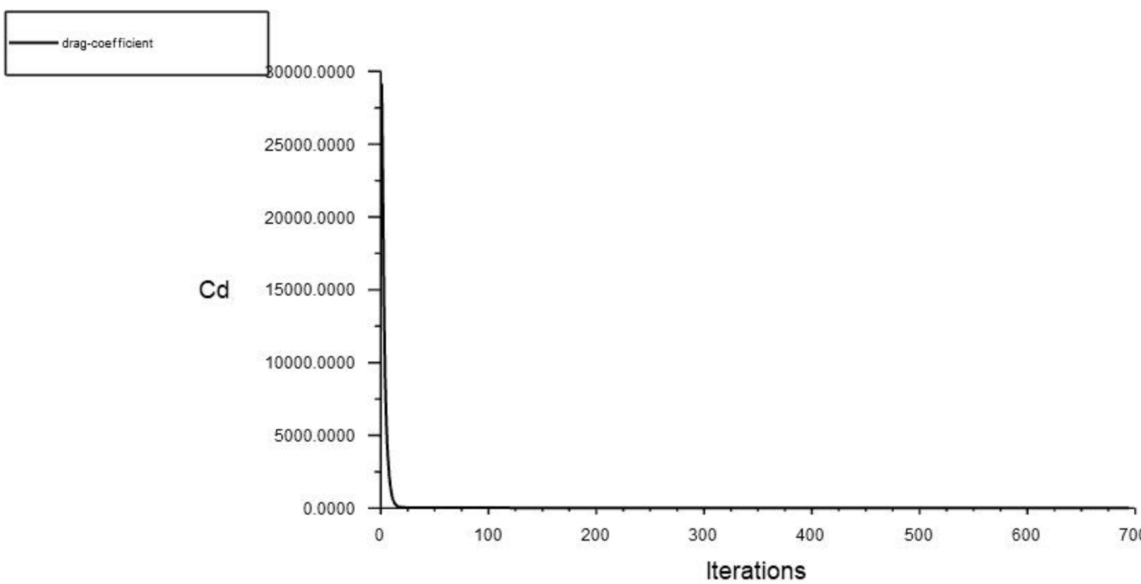

Fig VG orientation one α= -5^0

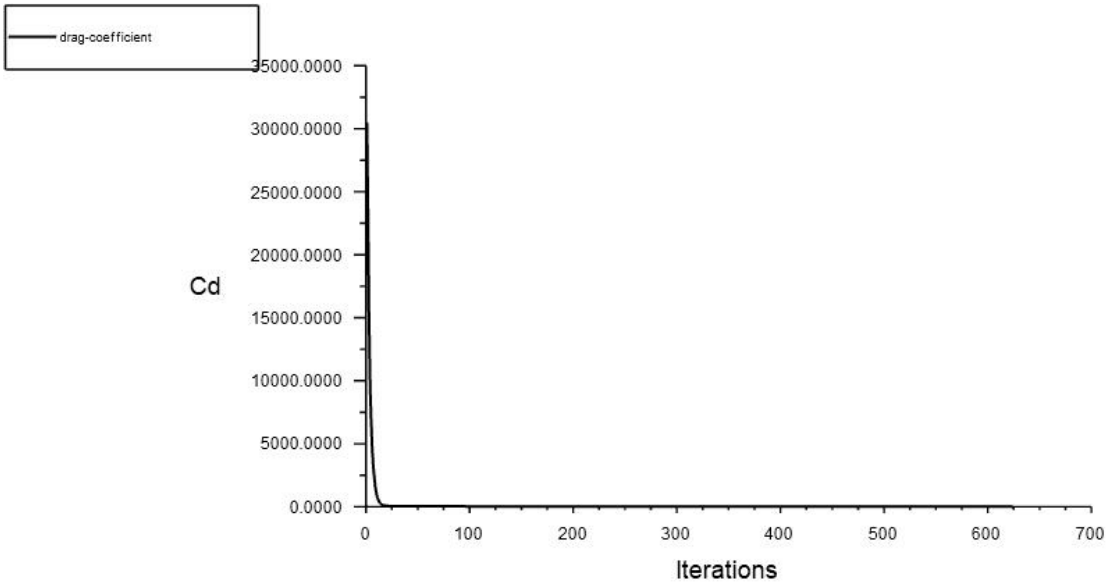

Fig VG orientation one α= 0^0

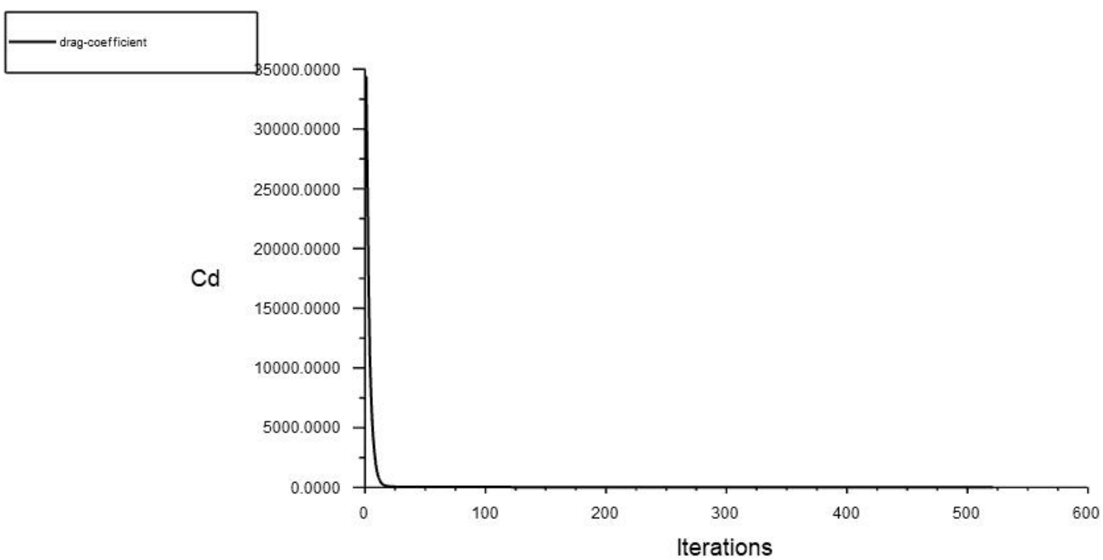

Fig VG orientation one α= 5^0

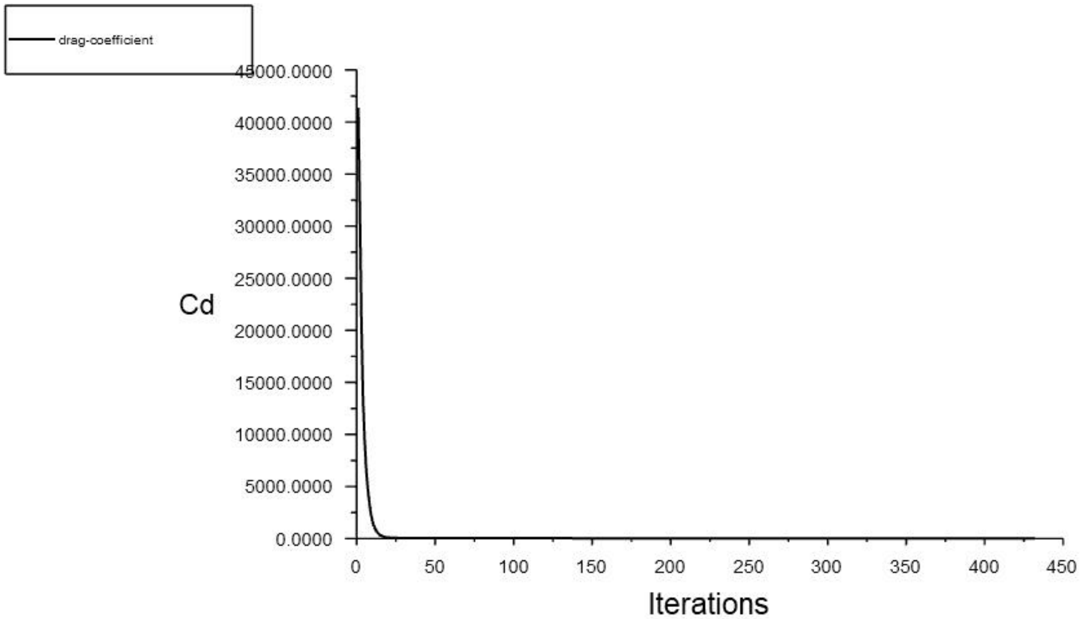

Fig VG orientation one α= 10^0

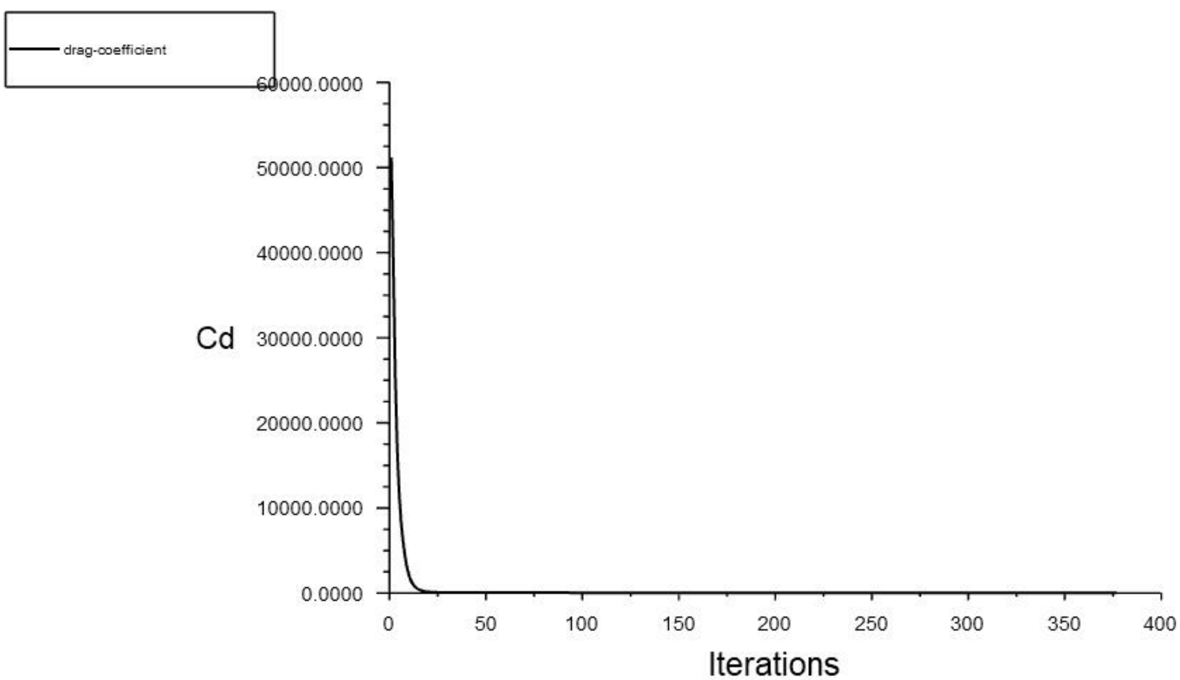

Fig VG orientation one α= 15^0

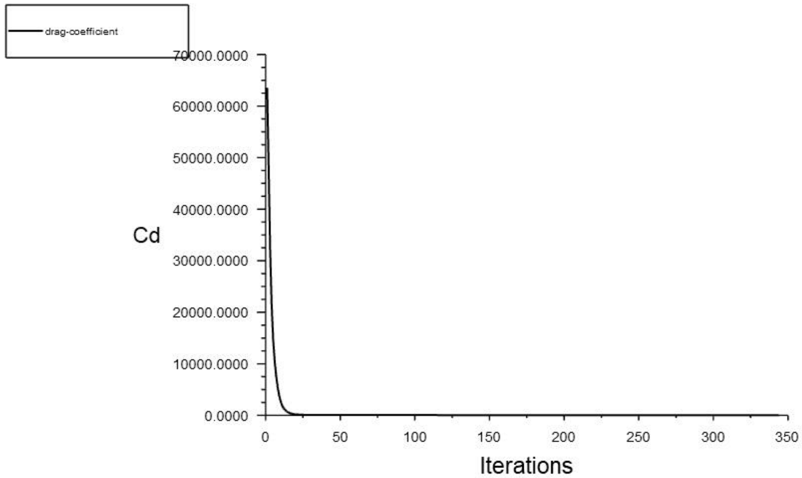

Fig VG orientation one α= 20^0

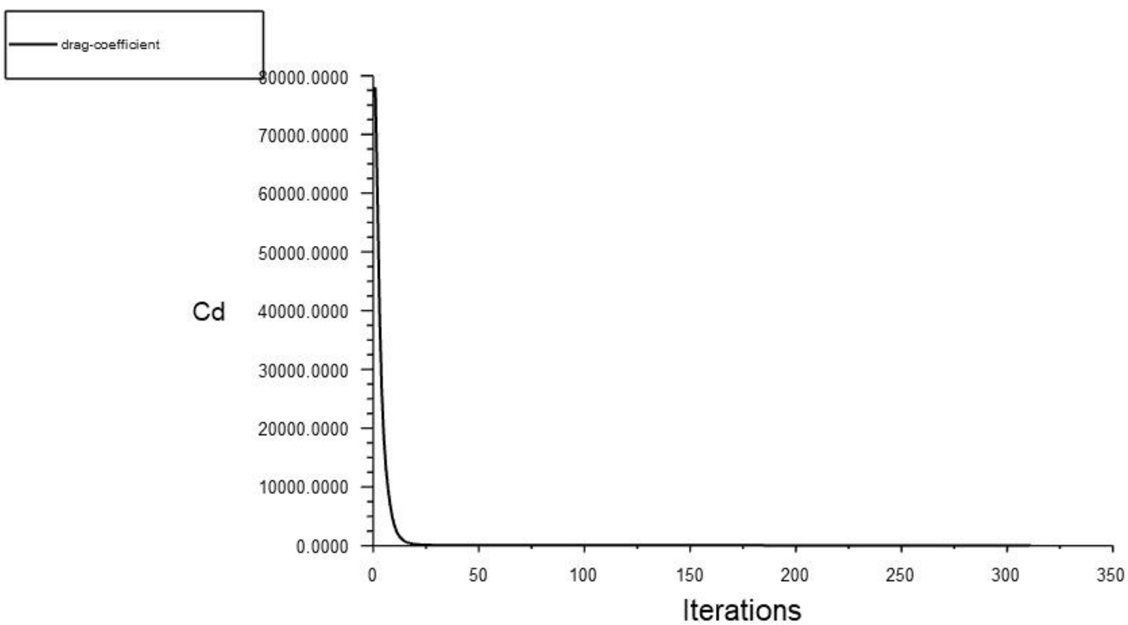

Fig VG orientation one α= 25^0

A-3 Grid Independent test setup

Details of "Mesh"

Display	
Display Style	Use Geometry Setting
Defaults	
Physics Preference	CFD
Solver Preference	Fluent
Element Order	Linear
Element Size	2.5 m
Export Format	Standard
Export Preview Surface Mesh	No
Sizing	
Quality	
Inflation	
Advanced	
Statistics	
Nodes	299730
Elements	984417

Figure: Mesh 1 setup

Details of "Mesh"

Display	
Display S...	Use Geometry Setting
Defaults	
Physics P...	CFD
Solver Pr...	Fluent
Element ...	Linear
Eleme...	2.5 m
Export F...	Standard
Export Pr...	No
Sizing	
Quality	
Inflation	
Advanced	
Statistics	
Nodes	104658
Eleme...	416840

Figure: Mesh 2 setup

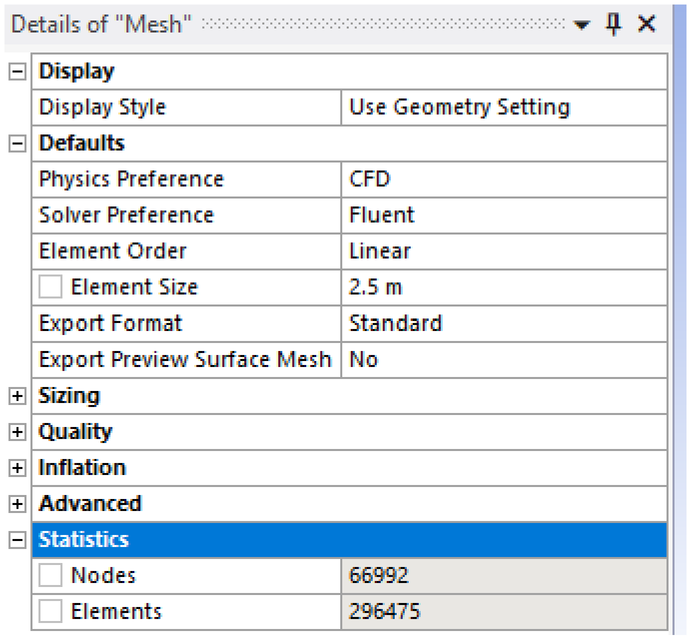

Figure: Mesh 3 setup

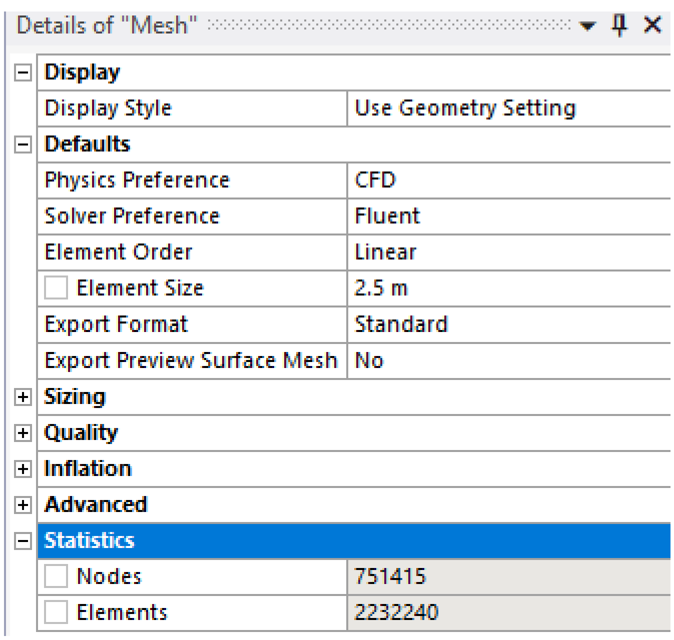

Figure: Mesh 4 setup

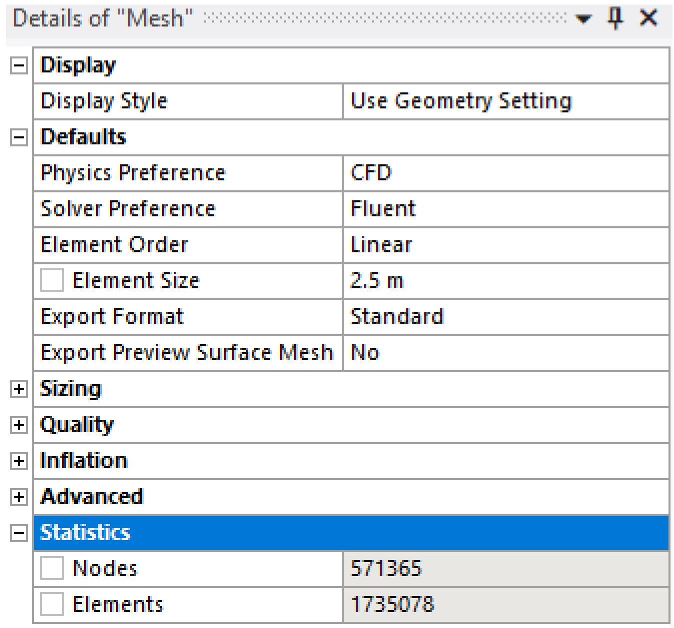

Figure: Mesh 5 setup

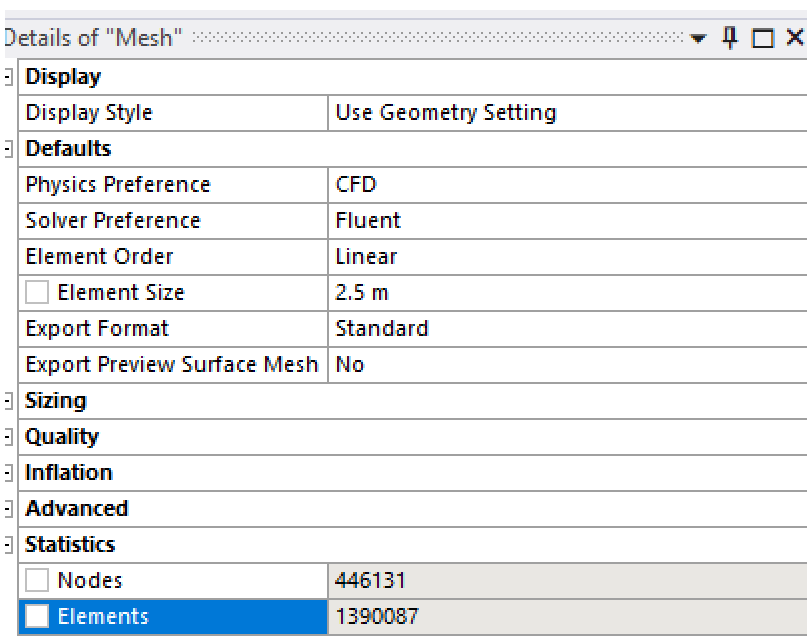

Figure: Mesh 6 setup